GSK3α/β IN ENDOTHELIAL ACTIVATION AND ATHEROSCLEROSIS

INVESTIGATING THE ROLE OF ENDOPLASMIC RETICULUM STRESS-GLYCOGEN SYNTHASE KINASE3α/β SIGNALLING ON ENDOTHELIAL ACTIVATION AND THE INITIATION AND PROGRESSION OF ATHEROSCLEROSIS

By LAUREN MASTROGIACOMO, B.SC(HONOURS), MSC

A Thesis Submitted to the School of Graduate Studies in Partial Fulfilment of the Requirements for the Degree Doctor of Philosophy

McMaster University © Copyright by Lauren Mastrogiacomo, 2022

DOCTOR OF PHILOSOPHY (2022)	McMaster University
(Medical Sciences)	Hamilton, Ontario, Canada
TITLE:	Investigating the role of endoplasmic reticulum stress-glycogen synthase kinase3α/β signalling on endothelial activation and the initiation and progression of atherosclerosis
AUTHOR:	Lauren Mastrogiacomo, B.Sc in Biomedical Science (Honours), University of Ottawa, Canada, MSc in Human Tissue Repair, University College London, United Kingdom
SUPERVISOR:	Geoff H. Werstuck, B.Sc, Ph.D
NUMBER OF PAGES:	xxi, 244

LAY ABSTRACT

The leading cause of death in the world is heart disease. The most common type of heart disease is caused by fatty plaque build-up in the artery wall. Certain risk factors put you at higher risk of developing heart disease, some risk factors are: high blood glucose levels, high blood cholesterol levels, obesity and smoking. However, we do not know how these risk factors increase the risk of heart disease. This thesis project uses mouse models that develop plaques in the heart. We examine how risk factors affect the heart and focus on a pathway that is involved in disease progression. This allows us to study how specific factors promote the fatty plaque build-up. The results of these studies are important as they will give us more information on how to protect individuals from heart disease.

ABSTRACT

Cardiovascular disease (CVD) is the leading cause of mortality worldwide. CVD risk factors include diabetes, dyslipidemia, hypertension, and obesity. Atherosclerosis is the major underlying cause of CVD. Endothelial cells (ECs) line the vasculature and function to maintain homeostasis and regulate blood vessel dynamics. Endothelial activation is thought to be an early predictor of atherosclerosis initiation.

Studies have concluded that CVD risk factors cause endoplasmic reticulum (ER) stress. More recently, from work in macrophage models, it was found that ER stress may signal through the glycogen synthase kinase (GSK)3α/β pathway to promote atherosclerosis. The aim of this thesis is to examine the role of ER stress-GSK3α/β signalling on endothelial activation and atherosclerosis initiation and progression.

This thesis contains three data chapters that each describe the results of a standalone study. Chapter 3 focuses on the role of hyperglycemia in EC activation. $ApoE^{-/-}Ins2^{+/akita}$ and $ApoE^{+/-}Ins2^{+/akita}$ mice were used to examine the effects of hyperglycemia on adhesion protein expression, monocyte/macrophage recruitment and atherosclerotic plaque development at the aortic sinus.

The fourth chapter investigates a potential mechanism by which hyperglycemia promotes EC activation in vitro using cultured human aortic endothelial cells (HAEC). 4-phenylbutyric acid (4-PBA), an ER stress attenuator and tideglusib, a GSK3α/β inhibitor, were added to cells cultured in elevated glucose media. Adhesion protein expression and monocyte attachment were assessed. The results of these experiments support a role for glucose-induced ER stress signalling through GSK3α/β in the activation of EC.

Chapter 5 describes the results of in vivo experiments examining adhesion protein expression, monocyte/macrophage recruitment and atherosclerotic progression in endothelium-selective GSK3α and GSK3β knockout mice. These experiments are the first to support a role for endothelial GSK3α, but not GSK3β, in the progression and development of atherosclerosis.

Together these data show that hyperglycemia, and perhaps other cardiovascular risk factors, promote early EC activation by a mechanism involving ER stress signalling through GSK3α. These findings further support the viability of a strategy to specifically target GSK3α as a way to block or impede atherosclerosis.

ACKNOWLEDGEMENTS

The completion of my Ph.D would not have been possible without the continual support and guidance of my family, friends, lab colleagues and most importantly, my supervisor. Dr. Geoff Werstuck, I am immensely thankful for your invaluable guidance and knowledge throughout my research. It is thanks to your mentorship that I completed this Ph.D. I would also like to extend my appreciation to my committee members, Dr. Bernardo Trigatti and Dr. Paul Kim. Without your time, contributions and support, this would not have been possible. Thank you for helping me pursue my research career.

To my lab colleagues/friends, you have all made this experience enjoyable and rewarding. I am so lucky to be part of a lab that prioritises teamwork and success. Dr. Yuanyuan (Peter) Shi, Dr. Daniel Venegas, Dr. Monica De Paoli, Dr. Sarvitat Patel, Alex Bruton, Rangana Talpe and Sophie Enright, thank you for your friendship and support throughout my Ph.D.

These acknowledgements cannot be complete without thanking my family, this degree was a team-effort and I will be forever grateful for you all.

To my dad, I am so lucky to have you to look up to. Thank you for all the sacrifices you have made for myself and the family and thank you for listening to me, guiding me and believing in me throughout my life and academic career. Without your constant love, patience and support, this would not have been possible.

To my mum, thank you. There are not enough words or gestures that I can say or do that would express how thankful I am to have you. Your constant support, not only for the past 4-5 years, but in whatever I choose to do, has gotten me to

where I am today. Your positive outlook on everything has always inspired me to keep moving forward. Without you I would not have gotten this far.

To my dear brother, Stefan, life is either a daring adventure, or nothing. This was definitely an adventure! I know you are watching me and supporting me from above, I could feel it, and oftentimes I needed it, thank you.

To my sister, and best friend, Elsa. Thank you for always being by my side when I needed you, and reassuring me when I needed it. Life has changed a lot in the past 4-5 years and I am so lucky that I had you to go through it with.

To my partner, Curtis, thank you for your constant and unconditional love and support. You didn’t sign up for this path, but I'm sure sometimes it felt like you were also pursuing this degree. Thank you for always believing in me and telling me to believe in myself.

Thank you! (times infinity)

TABLE OF CONTENTS

Chapter 1: General Introduction **1**

1.1 Introduction 1

1.2 CVD 1

Risk factors 1

Atherosclerosis 2

The pathogenesis of atherosclerosis 3

1.3 The endothelium 7

EC activation 7

P-selectin 9

E-selectin 10

Vascular cell adhesion molecule (VCAM-1) 11

Intracellular adhesion molecule (ICAM-1) 11

Platelet endothelial cell adhesion molecule (PECAM-1), and vascular endothelial cadherin (VE-cadherin) 12

CVD risk factors and EC activation 15

Obesity 15

Hypertension 15

Diabetes Mellitus (DM) 16

1.4 Endoplasmic reticulum (ER) stress 17

IRE1 21

ATF6 21

PERK 21

CVD risk factors and ER stress 22

ER stress and EC activation 23

1.5 Glycogen synthase kinase (GSK)3α/β 24
  GSK3α/β signalling pathways 29
    Insulin signalling pathway 29
    Wnt/ β-catenin signalling pathway 29
    MAPK signalling pathway 30
    ER stress signalling pathway 30
  GSK3α/β roles in atherosclerosis 34
  GSK3α/β role in ECs 35
1.6 Research goals 35

Chapter 2: General Hypothesis and Objectives **36**
2.1 General hypothesis 36
2.2 General objectives 36

Chapter 3: The Effects of Hyperglycemia on Early Endothelial Activation and the Initiation of Atherosclerosis **37**
3.1 Foreword 37
3.2 Abstract 38
3.3 Introduction 39
3.4 Material and methods 41
  HAEC culture treatment conditions and analysis 41
  Mice 44
  Empagliflozin treatment 46
  Analysis of plasma and urine 46
  Analysis of atherosclerosis – Masson's trichrome staining 46
  Immunofluorescence/immunohistochemistry staining 47
  Blood cell count 48

Statistical analysis 48

3.5 Results 49

Elevated concentrations of glucose promote adhesion protein expression in cultured ECs 49

Atherosclerotic plaque development in ApoE-/- and ApoE-/-Ins2+/akita mice 52

EC activation in hyperglycemic/dyslipidemic ApoE-/-Ins2+/akita mice 55

Hyperglycemia is insufficient to promote plaque development in the absence of dyslipidemia 61

Hyperglycemia promotes EC activation 63

SGLT2 inhibitor lowers glucose levels in ApoE+/-Ins2+/akita 68

3.6 Discussion 75

3.7 References for Chapter 3 80

3.8 Supplementary material for Chapter 3 85

Chapter 4: Investigating the effects of elevated glucose concentration on human aortic endothelial cell activation 93

4.1 Foreword 93

4.2 Abstract 94

4.3 Introduction 95

4.4 Material and methods 97

Cell lines and drug treatment 97

Human aortic endothelial cells 97

THP-1 Cells 98

Monocyte cell attachment assay 101

GSK3α/β expression 101

Statistical analysis 102

4.5 Results 102

Adhesion protein expression is induced in HAEC exposed to elevated glucose concentrations 102

4-PBA reduces adhesion protein expression 106

Tideglusib reduces the expression of adhesion proteins 110

The effect of elevated glucose concentration and the role of ER stress-GSK3α/β signalling on other markers of endothelial activation 114

ECs exposed to elevated glucose concentrations have increased monocyte adhesion 117

4.6 Discussion 120

4.7 References for Chapter 4 124

4.8 Supplementary material for Chapter 4 131

Chapter 5: Investigating the role of endothelial GSK3α/β in atherogenesis 135

5.1 Foreword 135

5.2 Abstract 136

5.3 Introduction 137

5.4 Material and methods 139

GSK3α/β knockout mouse strains 139

Bone marrow transplant 140

Experimental design 142

Tissue harvesting 142

EC isolation 143

Macrophage collection 143

Assessing tissue specific GSK3α and GSK3β gene expression 144

Analysis of blood and plasma 144

Atherosclerotic plaque analysis 145

Analysis of EC activation 145

Statistical analysis 146

5.5 Results 147

The Tie2Cre recombinase is not endothelial specific 147

Endothelial/macrophage knockout of GSK3α attenuates atherosclerosis 148

Endothelial activation is reduced in endothelial/macrophage knockout of GSK3α 153

Bone marrow transplant (BMT) replenished GSK3α and GSK3β expression in myeloid cells 159

Endothelial knockout of GSK3α attenuates atherosclerosis 160

Endothelial activation is reduced in endothelial GSK3α knockout mice 165

5.6 Discussion 171

5.7 References for Chapter 5 174

5.8 Supplementary material for Chapter 5 178

Chapter 6: General Discussion **194**

Limitations 212

Future Directions 213

Significance 214

6.1 References for introduction and general discussion 218

LIST OF FIGURES

Chapter 1: General Introduction

Figure 1.1 The artery wall 5

Figure 1.2 Monocyte recruitment 13

Figure 1.3 ER stress signalling 19

Figure 1.4 Glycogen synthase kinase3α/β 26

Figure 1.5 GSK3α/β signalling pathways 32

Chapter 3: The Effects of Hyperglycemia on Early Endothelial Activation and the Initiation of Atherosclerosis

Figure 3.1 Analysis of the effects of hyperglycemia on HAEC activation 50

Figure 3.2 Atherosclerotic progression in ApoE$^{-/-}$ and ApoE$^{-/-}$ Ins2$^{+/akita}$ mice 53

Figure 3.3 Endothelial P-selectin, E-selectin, VCAM-1 and ICAM-1 expression in male ApoE$^{-/-}$ and ApoE$^{-/-}$ Ins2$^{+/akita}$ mice 57

Figure 3.4 Endothelial monocyte/macrophage recruitment in ApoE$^{-/-}$ and ApoE$^{-/-}$Ins2$^{+/akita}$ mice 59

Figure 3.5 Endothelial P-selectin, E-selectin, ICAM-1 and VCAM-1 expression in ApoE$^{+/-}$ and ApoE$^{+/-}$ Ins2$^{+/akita}$ mice 64

Figure 3.6 Endothelial monocyte/macrophage recruitment in ApoE$^{+/-}$ and ApoE$^{+/-}$ Ins2$^{+/akita}$ mice 66

Figure 3.7 The effects of SGLT2 inhibitor, empagliflozin, on endothelial activation in ApoE$^{+/-}$ and ApoE$^{+/-}$ Ins2$^{+/akita}$ mice 71

Figure 3.8 Endothelial monocyte/macrophage recruitment in empagliflozin treated mice 73

Supplementary Figure 3.1 Negative controls for immunofluorescence and immunohistochemistry staining 87

Supplementary Figure 3.2 Analysis of the effects of hyperglycemia on HAEC gene expression of eNOS, iNOS, vWF and PECAM 89

Supplementary Figure 3.3 Atherosclerotic progression in ApoE$^{+/-}$ and ApoE$^{+/-}$ Ins2$^{+/akita}$ mice 91

Chapter 4: Investigating the effects of elevated glucose concentration on human aortic endothelial cell activation

Figure 4.1 Effects of elevated glucose concentration on HAEC 104

Figure 4.2 Effects of 4-PBA on glucose induced HAEC activation 108

Figure 4.3 Effects of tideglusib on glucose induced HAEC activation 112

Figure 4.4 eNOS, iNOS, vWF and PECAM-1 expression in HAEC 115

Figure 4.5 THP-1 cell attachment assay 118

Supplementary Figure 4.1 ER stress activation in HAEC cultured in elevated glucose concentration 131

Supplementary Figure 4.2 Western blot analysis of GSK3α/β expression in HEAC 133

Chapter 5: Investigating the role of endothelial GSK3α/β in atherogenesis

Figure 5.1 Atherosclerosis in endothelial/macrophage GSK3α/β knockout mice 151

Figure 5.2 Adhesion protein expression in endothelial/macrophage GSK3α/β knockout mice 154

Figure 5.3 Monocyte/macrophage recruitment in endothelial/macrophage GSK3α/β knockout mice 157

Figure 5.4 Atherosclerosis in BMT endothelial GSK3α/β knockout mice 163

Figure 5.5 Adhesion protein expression in BMT endothelial GSK3α/β knockout mice 166

Figure 5.6 Monocyte/macrophage recruitment in endothelial GSK3α/β knockout mice 169

Supplementary Figure 5.1: Characterizing the endothelial/macrophage GSK3α/β knockout mouse model 178

Supplementary Figure 5.2 Confirmation that BMT restored GSK3α and GSK3β in macrophages 180

Supplementary Figure 5.3 Experimental design 182

Supplementary Figure 5.4 Negative controls for immunofluorescence and immunohistochemistry staining 184

Supplementary Figure 5.5 Atherosclerosis in control mice from the endothelial/macrophage GSK3α/β knockout mouse model 186

Supplementary Figure 5.6 Co-staining of adhesion protein and vWF 188

Supplementary Figure 5.7 Atherosclerosis assessment comparison between non-BMT mice and BMT mice 190

Supplementary Figure 5.8 Atherosclerosis assessment in control mice from the BMT endothelial GSK3α/β knockout mouse model 192

Chapter 6: Discussion

Figure 6.1 Summary of findings from Chapter 3 197

Figure 6.2 Summary of findings from Chapter 4 203

Figure 6.3 Summary of findings from Chapter 5 208

Figure 6.4 Summary of findings from this thesis 216

LIST OF TABLES

Chapter 3: The Effects of Hyperglycemia on Early Endothelial Activation and the Initiation of Atherosclerosis

Table 3.1 Primer sequences 43
Table 3.2 Metabolic parameters of ApoE$^{-/-}$ and ApoE$^{-/-}$ Ins2$^{+/akita}$ mice 45
Table 3.3 Metabolic parameters of ApoE$^{+/-}$ and ApoE$^{+/-}$ Ins2$^{+/akita}$ mice 62
Table 3.4 Metabolic parameters of empagliflozin treated ApoE$^{+/-}$ and ApoE$^{+/-}$Ins2$^{+/akita}$ mice 70

Supplementary Table 3.1 Hematology Profile 85
Supplementary Table 3.2 Plasma lipid levels 86

Chapter 4: Investigating the effects of elevated glucose concentration on human aortic endothelial cell activation

Table 4.1 Primer sequences 100

Chapter 5: Investigating the role of endothelial GSK3α/β in atherogenesis

Table 5.1: Primer sequences 141
Table 5.2 Metabolic parameters for endothelial/macrophage knockout mice 149
Table 5.3 Metabolic parameters for BMT endothelial knockout mice 161

LIST OF ABBREVIATIONS

DAB	3,3' diaminobenzidine
4-PBA	4-phenylbutyric acid
ATF6	Activating transcription factor
ATF4	Activating transcription factor 4
APC	Adenomatous polyposis coli
BCE	Bovine capillary endothelial cells
CHOP	C/EBP homologous protein
CVD	Cardiovascular disease
CK1	Casein kinase 1
Mac-3	CD107b$^+$/Mac-3$^+$
CD44	Cluster of differentiation 44
DM	Diabetes mellitus
ER	Endoplasmic reticulum
ER stress	Endoplasmic reticulum stress
EC	Endothelial cell
eNOS	Endothelial nitric oxide synthase
ECL	Enhanced chemiluminescence system
eIF2α	Eukaryotic translation initiation factor -2α
GSK3α/β	Glycogen Synthase Kinase3α/β
GSK3α	Glycogen Synthase Kinase3α
GSK3β	Glycogen Synthase Kinase3β
GRP78	Glucose regulated protein
GFAT	Glutamine fructose-6-phosphate amino-transferase
gl-LDL	Glycated low-density lipoproteins
HBP	Hexamine biosynthesis pathway
HFD	High fat diet
HAEC	Human aortic endothelial cells

HLMEC	Human lung microvascular endothelial cells
HUVEC	Human umbilical vein endothelial cells
iNOS	Inducible nitric oxide synthase
IKK	Inhibitory κB kinase
IRE1	Inositol-requiring enzyme
IRS	Insulin receptor substrates
IL-1	Interleukin-1
ICAM-1	Intracellular adhesion molecule
IHD	Ischemic heart disease
LDL	Low-density lipoproteins
LDLR	Low-density lipoprotein receptor
MEF	Mouse embryonic fibroblasts
NO	Nitric oxide
NF-κB	Nuclear factor kappa B
ox-LDL	Oxidized low-density lipoproteins
PCC	Pancreatic cancer cell
PI3K	Phosphatidylinositol 3-kinase b
PECAM-1	Platelet endothelial cell adhesion molecule
PERK	Protein kinase R-like endoplasmic reticulum kinase
PKB/Akt	Protein kinase B
MAPK	P38 mitogen-activated protein kinase
PKC	Protein kinase C
PSGL-1	P-selectin glycoprotein ligand 1
RT-PCR	Reverse transcription-polymerase chain reaction
Ser9	Serine 9
Ser21	Serine 21
S1	Site-1 proteases
S2	Site-2 proteases
SGLT-2	Sodium-glucose cotransporter-2

sE-selectin	Soluble E-selectin
sICAM-1	Soluble ICAM-1
sP-selectin	Soluble P-selectin
sVCAM-1	Soluble VCAM-1
STZ	Streptozotocin
sXBP1	Spliced X-box-binding protein 1
TLR	Toll-like receptor
TNFα	Tumour necrosis factor alpha
Tyr216	Tyrosine 216
Tyr279	Tyrosine 279
UPR	Unfolded protein response
VCAM-1	Vascular Cell Adhesion Molecule
VE-Cadherin	Vascular endothelial cadherin

DECLARATION OF ACADEMIC ACHIEVEMENT

Lauren Mastrogiacomo started as a Ph.D student in the Medical Science graduate programme in 2018. This research project has been conducted between September 2018 and December 2022.

Publications:

Lauren Mastrogiacomo, Geoff Werstuck. Investigating the Role of Endothelial GSK3α/β in Atherogenesis in Low Density Lipoprotein Receptor Knockout Mice. *Int J Mol Sci*. 2022, 23(23):14780

Lauren Mastrogiacomo, Robert Ballagh, Daniel E Venegas-Pino, Hargun Kaur, Peter Shi and Geoff H Werstuck. The Effects of Hyperglycemia on Early Endothelial Activation and the Initiation of Atherosclerosis. *Am. J. Pathol*. 2022, 193(1):121-133

Sarvatit Patel, **Lauren Mastrogiacomo,** Madison Fulmer, Yuanyuan Shi, Geoff Werstuck. Deletion of myeloid GSK3α promotes atherosclerotic regression in LDLR -/- mice. *Front. Cardiovasc. Med.* 2022, 23(16):9293

Lauren Mastrogiacomo, Geoff Werstuck. The potential of Cannabidol in the Treatment of Cardiovascular Disease. *Int J Cardiovasc Dis Diagn.* 2021, 6(1):013-016

Awards:

Medical Science Internal Thesis Fellowship, 2021-2022

CSTAVB Travel Award. Canadian vascular and lipid biology conference, 2019

McMaster Graduate Scholarship 2018-2022

CHAPTER 1: General Introduction

1.1 INTRODUCTION

Cardiovascular disease (CVD) is the leading cause of mortality worldwide[1,2,3]. In 2019 it is estimated that 32% of global deaths were due to CVD[1]. Over 75% of CVD death occurs in low-middle income areas[1,4]. Due to the global rise in obesity and diabetes, mortality associated with CVD is predicted to continually rise in years to come[1,5]. In Canada, CVD is the second leading contributor to healthcare costs, with an estimated annual cost of 22 billion dollars per year[6,7].

1.2 CVD

Risk factors

CVD describes a complex heterogeneous group of conditions that affect the circulatory system (heart and/or blood vessels)[8]. There are five major risk factors associated with the development of CVD including high body mass index (>25kg/m^2), high blood pressure (>130mg/dL systolic, >80 diastolic), diabetes (fasting glucose levels >7mM), elevated plasma cholesterol (>200mg/dL total cholesterol and >130 mg/dL low-density lipoproteins (LDL) cholesterol) and elevated triglycerides (>150mg/dL)[9,10,11,12]. If a patient is diagnosed with three or more of these risk factors, they are considered to suffer from the metabolic syndrome, and their risk for CVD increases 50-60%[10,13,14]. In addition to these metabolic risk factors for CVD, lifestyle factors including smoking, diet, and physical inactivity can also significantly contribute to cardiovascular risk[8,15]. The mechanism(s) by which these risk factors promote CVD are not fully understood. An understanding of these mechanisms will facilitate the development of future therapeutic strategies to reduce the burden of CVD.

Atherosclerosis

Atherosclerosis is an inflammatory disease and a major underlying cause of CVDs[16]. In humans, the progression of atherosclerosis usually spans decades, and patients are typically asymptomatic for years before signs of clinical manifestation[16]. Atherosclerosis is a progressive inflammatory disease characterised by plaque accumulation in the arterial wall, causing narrowing of the artery, and thus altering blood flow[16]. Atherosclerosis initiates in focal areas of the artery wall that are predisposed to disrupted laminar blood flow, including bifurcations, branches and/or inner curvatures[16]. The major symptoms of atherosclerotic CVD include chest pain, shortness of breath and edema due to plaque build-up in the arterial wall causing insufficient blood flow[17]. The obstruction of major blood vessels can ultimately lead to heart attacks, strokes and peripheral vascular disease[18].

Atherosclerotic CVD can be classified into two main diseases, ischemic heart disease (heart attack) and cerebrovascular disease (stroke). Ischemic heart disease (IHD) (also called coronary heart disease or coronary artery disease) is caused by a build-up of atherosclerotic plaque in the artery wall compromising blood flow resulting in inadequate delivery of blood and oxygen to the heart[19]. An inadequate supply of blood and nutrients can lead to cardiomyocyte death (myocardial infarction) resulting in a heart attack[19]. IHD is often asymptomatic and events are likely to occur during exercise or stress when the heart's demand for oxygen is increased[19]. Cerebrovascular disease refers to a group of conditions that ultimately present as plaque build-up in the artery wall (atherosclerosis) affecting the blood supply to the brain. The most common cerebrovascular event is a stroke[20]. Atherosclerotic CVD accounts for 84.5% of cardiovascular deaths, with the largest number of deaths involving ischemic heart disease (followed by cerebrovascular disease)[20].

The pathogenesis of atherosclerosis

Atherogenesis is the development of plaque in the arterial wall causing a narrowing of the artery[21]. The artery wall is composed of three layers, the inner layer being the intima that consists of a single layer of endothelial cells (ECs), a middle layer composed of multiple layers of vascular smooth muscle cells called the tunica media, and the outer layer, the tunica adventitia (Figure 1.1)[22]. Atherosclerosis is believed to initiate at sites of endothelial injury/activation. Circulating monocytes are attracted to the site of injury and infiltrate the endothelium[23]. In the intima, monocytes differentiate to macrophages, which uptake oxidized low-density lipoproteins particles (ox-LDL) and glycated LDL (gl-LDL) and efferocytose cellular debris[24]. As the macrophages become engorged with lipids they become foam cells[24]. Foam cells can undergo apoptosis, and their lipid-filled contents contribute to the acellular, lipid-rich necrotic core that can grow in size and destabilize the plaque[25]. Major acute cardiovascular events, such as heart attacks and strokes, usually occur when an atherosclerotic plaque ruptures and the resulting thrombus occludes the vessel[26]. ECs play a pivotal role in the initiation of atherogenesis. Therefore, further understanding of how CVD risk factors affect ECs will advance our knowledge of how risk factors, such as diabetes and dyslipidemia, promote CVD.

Figure 1.1: The artery wall. The artery wall is composed of three layers. The innermost layer is referred to as the tunica intima, which consists of ECs that are in direct contact with circulating blood. The tunica media is composed mainly of vascular smooth muscle cells. The outermost layer of the vessel is composed of connective tissue and provides structural support. *Figure created using Biorender.com 2022.*

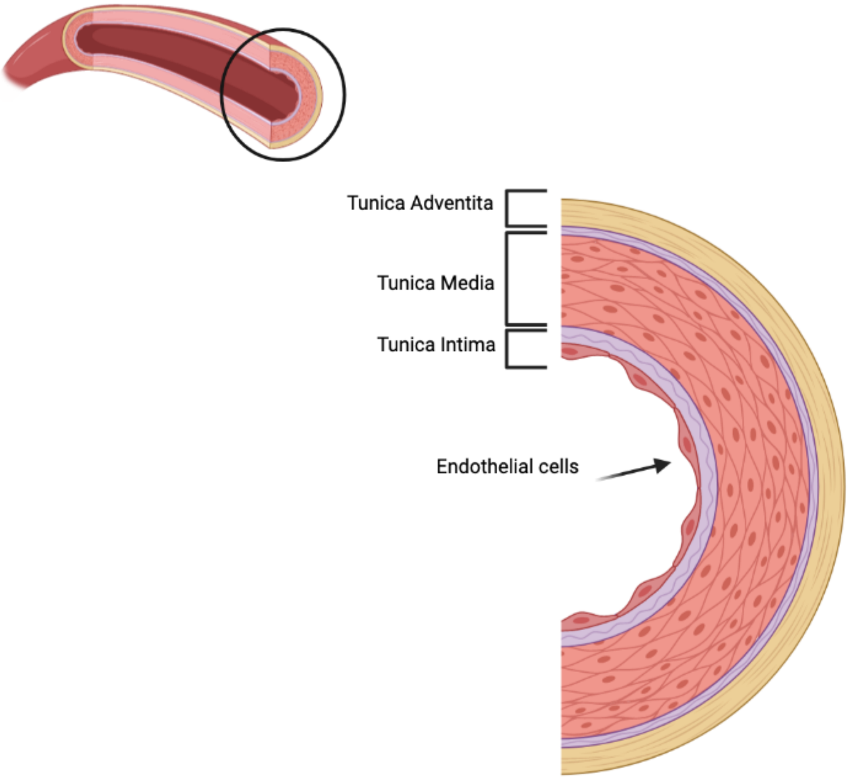
Tunica Adventita
Tunica Media
Tunica Intima
Endothelial cells

1.3 THE ENDOTHELIUM

ECs form a single semi-permeable layer of cells that line the vasculature acting as a barrier between circulating blood and the vessel wall[27]. They are critical for maintaining vascular homeostasis[28]. ECs are responsible for vessel wall maintenance, regulating inflammatory responses and providing barrier functions[29]. Healthy ECs regulate blood flow via vasodilation and vasoconstriction by signalling the vascular smooth muscle cells in the medial layer to relax or constrict[30].

EC activation

EC activation in lesion-prone areas is an important stage in the initiation of atherosclerosis[31]. ECs are subjected to hemodynamic forces[32]. Branches and bends in the vasculature are susceptible to disturbed blood flow and alterations in shear stress[32]. This causes a change in EC morphology, which alters the barrier function, promotes low-level inflammation, and increases permeability[32]. Atherosclerotic prone areas of the artery have lower levels of endothelial nitric oxide synthase (eNOS) expression[33] and elevated expression of p65, an inflammatory marker associated with nuclear factor kappa B (NF-κB) activity[34]. The NF-κB pathway mediates inflammatory processes and contributes to atherogenesis[35].

NF-κB is a transcription factor involved in the regulation of inflammatory genes, cell proliferation and apoptosis[34]. NF-κB can be activated through extracellular stimuli, including cytokines, tumour necrosis factor alpha (TNFα) and Interleukin-1 (IL-1)[34]. In an inactive state, NF-κB is bound to the inhibitory κB kinase (IKK) complex, upon activation IKK is phosphorylated, allowing NF-κB to migrate to the nucleus and upregulate the transcription of target genes. NF-κB activation increases the transcription of many genes that contribute to the pathogenesis of atherosclerosis[34]. In endothelial cells, activation of NF-κB causes induction of inflammatory cytokines and upregulation of adhesion proteins, which promote monocyte recruitment and atherosclerosis initiation[35].

EC activation has been associated with specific cardiovascular risk factors. Diabetes mellitus (DM)[36], hypertension[37], dyslipidemia [38], and obesity[39] have all been linked to an activated endothelium. In addition, it is known that pro-inflammatory cytokines, such as TNFα can promote EC activation[40,41]. TNFα is an inflammatory and immune regulator. Exposure to inflammatory stimuli causes macrophages and other cells of the myeloid lineage to produce TNFα[42]. TNFα has been linked to impaired vasodilation[43]. In particular, TNFα inhibits eNOS activity, thereby altering vascular functions[43]. TNFα also promotes leukocyte adhesion through the activation of the NF-κB pathway, increasing gene transcription of adhesion proteins[43,44].

EC activation and enhanced adhesion protein expression is thought to be one of the earliest stages in the initiation of atherogenesis[45]. Although the adhesion proteins work in a coordinated fashion to assist in monocyte recruitment, they have distinct roles and are regulated in different ways.

P-selectin

P-selectin is an inflammatory transmembrane adhesion molecule that is expressed on activated ECs and platelets[46]. P-selectin is stored in Weibel Palade bodies that are specific to EC[47]. Upon inflammatory stimulation, the Weibel Palade bodies move to the endothelial membrane allowing rapid translocation of P-selectin to the endothelial surface[48]. P-selectin, in concert with other adhesion molecules, plays a role in inflammation and atherogenesis by assisting in leukocyte/monocyte recruitment[49]. Endothelial P-selectin mediates adhesion and rolling of monocytes to the endothelial layer via interaction with the P-selectin glycoprotein ligand 1 (PSGL-1) on monocytes[50]. A study done by *Johnson RC et al* genetically eliminated P-selectin in an atherosclerotic prone mouse model (LDL Receptor knockout (LDLR$^{-/-}$)) and showed that these mice had a reduced plaque size as well as reduced monocyte rolling across the endothelial layer[51]. In vitro studies explore the role of TNFα and P-selectin regulation. Human umbilical vein endothelial cells (HUVEC)[52] and bovine capillary endothelial cells (BCE)[53] exposed to TNFα had elevated levels of P-selectin gene expression. This suggests that TNFα promotes EC activation.

E-selectin

E-selectin is a glycoprotein adhesion molecule that is primarily expressed on activated endothelium, and like P-selectin, aids in the initial recruitment of leukocytes to the vessel wall[54]. E-selectin can bind to the PSGL-1 and cluster of differentiation 44 (CD44) present on monocytes[55]. In rodents, both P/E-selectin are upregulated in the presence of inflammatory cytokines, however, in HUVEC the response is mainly upregulated E-selectin[56]. In mice it has been shown that deficiency of E-selectin results in a reduction in atherosclerotic lesion size[57]. A combined P/E-selectin deficiency was associated with a far greater reduction in lesion size, suggesting synergistic roles of these selectins in leukocyte recruitment and atherosclerotic initiation[58]. An in vitro study exposed HUVEC to TNFα or Interleukin- 1 (IL-1) and found that E-selectin was upregulated within 2-4 hours of exposure to an inflammatory cytokine. In this same study they stimulated the cells with TNFα and an NF-κB inhibitor and found a reduction in soluble E-selectin (sE-selectin)[59]. This suggests that TNFα promotes E-selectin expression by activating NF-κB.

Vascular cell adhesion molecule (VCAM-1)

VCAM-1 is a cell surface glycoprotein that is present in mice and humans and plays a role in leukocyte/monocyte recruitment[55,60]**.** VCAM-1 is upregulated in response to inflammatory stimuli, including TNFα[61]**.** After P/E-selectin slow monocyte rolling on the endothelium, VCAM-1 and intracellular adhesion molecule (ICAM-1) arrest monocytes on the endothelium[62]. Very late antigen 4 (VLA4/α4β1) and α4β7 are the two leukocyte binding integrin's that bind to the endothelial VCAM-1 receptor[63,64]. VCAM-1 plays an active role in leukocyte recruitment as well as in leukocyte translocation across the endothelium and into the vessel wall[64]. An in vitro study exposed HUVEC to TNFα and assessed VCAM-1 expression. VCAM-1 levels were significantly elevated in TNFα stimulated cells compared to untreated cells. In this study expression of ICAM-1 was also induced[65].

Intracellular adhesion molecule (ICAM-1)

ICAM-1 is a cell surface glycoprotein expressed on ECs[66,67]. ICAM-1 is constitutively active on resting/healthy ECs, however its expression can be induced by inflammatory cytokines[66,67]. ICAM-1 binds to integrin's CD11a/CD18 (Lymphocyte function associated antigen-1 (LFA-1)) present on leukocytes and thus is thought to play an active role in leukocyte recruitment[68]. Like VCAM-1, ICAM-1 aids in the transmigration of leukocytes across the EC layer into the wall of the vessel. Studies by *Cybulsky et al.* showed that VCAM-1, but not ICAM-1 plays a role in early atherosclerosis development[64]. Human lung microvascular endothelial cells (HLMEC) exposed to increasing concentration of TNFα had a dose-dependent increase in ICAM-1 expression[69].

Platelet endothelial cell adhesion molecule (PECAM-1), and vascular endothelial cadherin (VE-cadherin)

PECAM-1 and VE-cadherin are present at EC junctions and assist primarily in leukocyte transmigration through the vascular EC layer[70]. PECAM-1 is highly and constitutively expressed at ECs junctions, it is also expressed on platelets and circulating leukocytes[71]. PECAM-1 assists in regulation of vascular permeability[71]. Inhibition of PECAM-1 in HUVEC blocked transmigration of monocytes, however did not alter monocyte adhesion to the endothelial layer[70,72]. VE-cadherin is an endothelial specific adhesion molecule also located between EC junctions and assists in vascular permeability[73].

Cardiovascular risk factors, including hyperglycemia, are believed to promote EC injury, thereby contributing to the progression of atherosclerosis[74]. Insults to lesion prone areas of arterial vasculature, cause EC activation and the expression and/or presentation of cell adhesion molecules (P selectin, E selectin, ICAM-1 and VCAM-1) that promote monocyte recruitment making these areas prone to the initiation of atherosclerosis (Figure 1.2)[75].

Figure 1.2: Monocyte recruitment. EC activation involves the induction of adhesion protein expression. P-selectin captures the circulating monocytes, P/E-selectin, ICAM-1 and VCAM-1 assist in the slow rolling of the monocyte across the endothelial layer. PECAM-1 and VE-Cadherin facilitate the transmigration of the monocyte into the subendothelial layer.

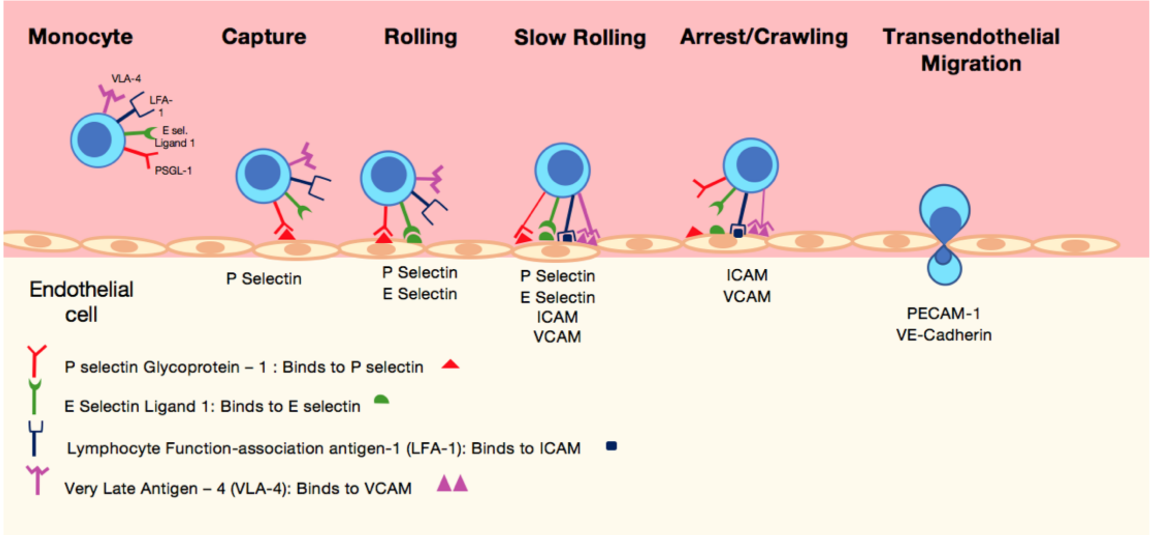
Monocyte
Capture
Rolling
Slow Rolling
Arrest/Crawling
Transendothelial Migration
VLA-4
LFA-1
E sel. Ligand 1
PSGL-1
Endothelial cell
P Selectin
P Selectin
E Selectin
P Selectin
E Selectin
ICAM
VCAM
ICAM
VCAM
PECAM-1
VE-Cadherin
P selectin Glycoprotein – 1 : Binds to P selectin
E Selectin Ligand 1: Binds to E selectin
Lymphocyte Function-association antigen-1 (LFA-1): Binds to ICAM
Very Late Antigen – 4 (VLA-4): Binds to VCAM

CVD risk factors and EC activation

Cardiovascular risk factors, including obesity, hypertension, and diabetes induce vascular changes and EC activation[76]. Although these risk factors are fundamentally different, they are thought to activate common pathways to initiate and promote EC activation and the development of atherosclerosis[77].

Obesity

A study comparing obese subjects to healthy subjects found that obese patients had elevated serum concentrations of soluble ICAM-1 (sICAM-1), sE-selectin and soluble P-selectin (sP-selectin)[78]. This suggests that obesity can activate ECs and could explain why these patients have increased risk of CVD development.

Hypertension

Hypertension is a CVD risk factor characterized by elevations in blood pressure[79]. VCAM-1 was found to be significantly elevated in the aorta, and soluble VCAM-1 (sVCAM-1) was elevated in serum from hypertensive mice, compared to normotensive controls[79]. Blockade of VCAM-1 via VCAM-1 neutralizing antibody, resulted in reduced blood pressure, improved vascular function, as well as reduced adhesion and infiltration of monocytes in the hypertensive mouse model[79]. Although other adhesion protein markers were not assessed, these results are consistent with a role for VCAM-1 in endothelial activation and potentially atherogenesis initiation.

Diabetes Mellitus (DM)

DM/hyperglycemia is a well-established risk factor for CVD[80,81]. In HUVEC, ICAM-1 and P-selectin expressions were increased when exposed to intermittent high glucose (12 hours elevated glucose followed by 12 hours normal glucose)[80]. ICAM-1 expression was significantly increased in human aortic endothelial cells (HAEC) exposed to elevated glucose concentrations[81]. HAEC treated in elevated glucose conditions for 7 days had increased monocyte binding compared to normal glucose control[82]. A clinical study showed that serum levels of soluble VCAM-1 (sVCAM-1), sICAM-1 and sE-selectin were higher in diabetic patients, compared to healthy controls[83]. This thesis will use diabetes/hyperglycemia as a CVD risk factor to start to delineate a mechanism by which CVD risk factors lead to EC activation.

The molecular mechanisms that link CVD risk factors to the initiation and progression of atherosclerosis are not fully understood. Specifically, it is not known how conditions of CVD risk factors may affect adhesion protein expression and/or monocyte recruitment to the growing plaque. Previous work, in our lab and others, has implicated hyperglycemic-induced ER stress as a potentially important pathway in atherogenesis[84,85,86,87,88].

1.4 ENDOPLASMIC RETICULUM (ER) STRESS

The ER is a tubular network of membranes that facilitates protein biosynthesis, folding and modification[89]. There are two distinct forms of the ER, smooth ER and rough ER[90]. The rough ER contains ribosomes and is important for protein synthesis and processing, whilst the smooth ER does not contain ribosomes and is involved in lipid biosynthesis and intracellular calcium homeostasis[90]. When ER functionality is disrupted, aberrant unfolded/misfolded proteins accumulate and cause ER stress[91]. Cardiovascular risk factors including obesity, hypertension, elevated cholesterol, and diabetes/hyperglycemia have all been associated with increased ER stress[92,93]. Interestingly, these are the cardiovascular risk factors associated with the metabolic syndrome.

The adaptive unfolded protein response (UPR) is a protective mechanism, initiated by conditions of ER stress, that functions to restore ER homeostasis[94]. The UPR involves the activation of signal transduction pathways leading to the inhibition of protein translation, upregulation of ER resident chaperone expression and degradation of misfolded proteins[94,95]. Persistent ER stress can promote inflammation and induce the apoptotic UPR, resulting in cell death[94,95,96]. UPR activation has been detected in all stages of lesion development and therefore provides insight into a potential role of ER stress in the initiation and progression of atherosclerosis[97].

The UPR is comprised of three signalling cascades that are initiated by three ER membrane bound ER stress sensors; 1) inositol-requiring enzyme (IRE1), 2) activating transcription factor (ATF6) and 3) protein kinase R-like endoplasmic reticulum kinase (PERK)[98]. Under normal conditions, these three sensors are inactive and bound to a chaperone protein, glucose-regulated protein (GRP78). When misfolded proteins accumulate in the ER, GRP78 dissociates from IRE1, ATF6 and PERK leading to their activation[99] (Figure 1.3).

Figure 1.3: ER stress signalling. CVD risk factors cause ER stress and activation of the UPR response. The 3 signalling pathways that make up the UPR response are initiated by IRE1, ATF6 and PERK. IRE1 autophosphorylates and splices X-box-binding protein 1 (XBP1) to make sXBP1, allowing it to translocate to the nucleus and transcribe UPR associated genes. ATF6 translocates to the Golgi where it is cleaved, cleaved ATF6 relocates to the nucleus and transcribes UPR associated genes. PERK autophosphorylates and phosphorylates/inhibits eIF2. Phosphorylation of eIF2 results in activation of ATF4 which translocates to the nucleus and promotes an upregulation of apoptotic UPR associated genes. *Figure created using Biorender.com 2022.*

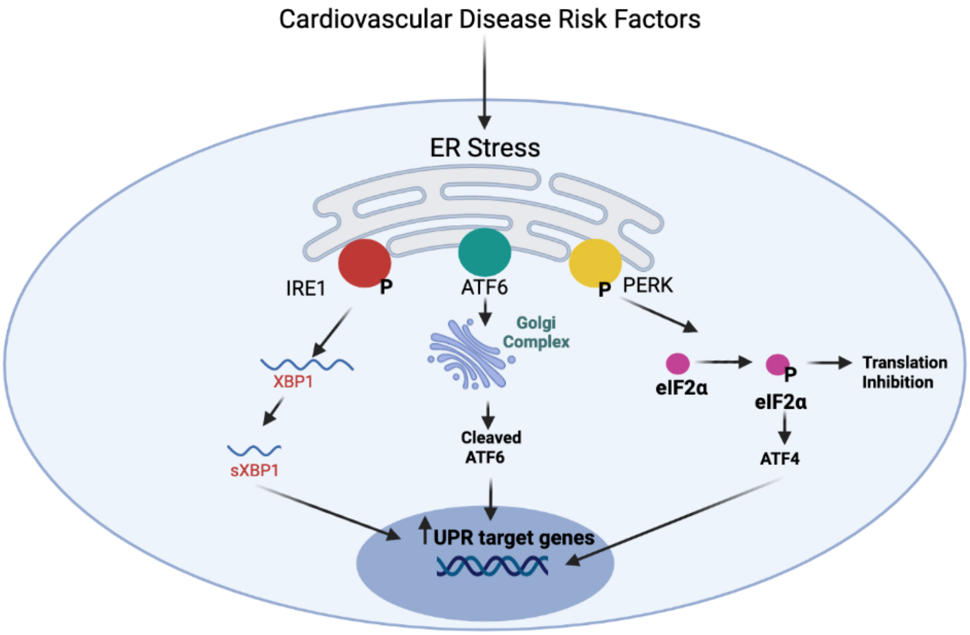
Cardiovascular Disease Risk Factors
ER Stress
IRE1
P
ATF6
P
PERK
Golgi Complex
XBP1
sXBP1
Cleaved ATF6
eIF2α
P
eIF2α
Translation Inhibition
ATF4
↑UPR target genes

IRE1

IRE1 is an ER transmembrane protein that is non-covalently associated with GRP78[100,101]. When GRP78 disassociates in response to ER stress, IRE1 auto-phosphorylates and its RNase domain is activated. Activated IRE1 splices the X-box-binding protein 1 (sXBP1) mRNA in such a way as a coding frame shift allows its translation[101]. sXBP1 translocates to the nucleus and enhances the transcription of UPR associated genes, including GRP78 and genes involved in ER-associated degradation (ERAD)[102,103]. sXBP1 activity enhances the folding capacity, but also facilitates the elimination of misfolded proteins as a means to reduce ER stress[104].

ATF6

Activated ATF6 translocates to the Golgi complex. In the Golgi, ATF6 is cleaved by site-1 proteases (S1) and site-2 proteases (S2)[105]. The cleaved ATF6 relocates to the nucleus where it binds to the ER stress response elements causing an upregulation in the expression of ER resident chaperone proteins[105].

PERK

PERK is a transmembrane protein kinase. When activated, PERK auto-phosphorylates and also phosphorylates/inhibits eukaryotic translation initiation factor -2α (eIF2α)[106]. eIF2α mediates translation initiation, therefore the inhibition of eIF2α results in a general reduction in protein synthesis[106]. The phosphorylation of eIF2α also causes activation of activating transcription factor 4 (ATF4), which translocates to the nucleus and promotes the expression of C/EBP homologous protein (CHOP), an apoptotic factor[107].

CVD risk factors and ER stress

CVD risk factors have been associated with increased ER stress suggesting a common pathway by which risk factors promote the development of atherosclerosis. Dyslipidemia involves elevated levels of circulating lipids, and It is well documented that dyslipidemia can cause ER stress[108]. Free cholesterol and specific fatty acids can cause ER stress by disrupting the ER membrane[109,110,111,112]. Human mesenchymal stem cells exposed to palmitate (a fatty acid) had elevated ER stress and apoptosis assessed by western blot of ER stress markers[113].

Individuals with DM have a 2-4 fold increased risk of developing CVD[114], however the mechanism underlying this pathway is presently not well defined. The hexamine biosynthesis pathway (HBP) is responsible for production of precursors required for N-linked glycosylation[115]. Glycosylation is important as it ensures proper protein folding in the ER[116]. HBP converts glucose-6-phosphate to fructose-6-phosphate to glucosamine-6-phosphate. The rate limiting enzyme responsible for this conversion is glutamine fructose-6-phosphate amino-transferase (GFAT)[116]. Mouse embryonic fibroblasts (MEF) exposed to elevated levels of glucosamine had elevated expression of ER stress markers[117]. Additionally, overexpression of GFAT in HepG2 cells promotes ER stress and inflammation[118]. In human and rat myotubes, glucosamine treatments increased ER stress markers[119]. Another study added high levels of glucosamine to HUVEC which promoted ER stress and increased pro-inflammatory markers, suggesting a role of hyperglycemia and the HBP impairing ER function[120]. Thus, increased flux through the HBP could be the mechanism by which elevated glucose levels accelerate atherosclerosis.

ER stress and EC activation

Atherosclerosis is associated with inflammation, ER stress, and vascular dysfunction[121]. CVD risk factors have been shown to cause ER stress, and therefore it is possible that there is a downstream mechanism of ER stress that causes EC activation and adhesion protein expression, thus initiating early atherogenesis.

HUVEC treated with TNFα (inflammatory cytokine associated with increased gene transcription of adhesion proteins) had elevated levels of ER stress markers, as well as increased monocyte adhesion[122]. Another study in which HUVECs were treated with glucosamine, ER stress markers as well as adhesion protein expression were elevated[123]. HUVEC exposed to LDL showed activation of the UPR response, adhesion protein expression was not assessed[124,125]. In a separate study, HUVEC exposed to LDL showed a decrease in eNOS and nitric oxide (NO) production[125,126].

Studies support the possibility that ER stress may be a unifying mechanism between CVD risk factors and accelerated atherogenesis, however further research and understanding of this process is needed. In particular, the downstream signalling associated with ER stress is not fully understood. Our lab has identified an important role for ER stress signalling through glycogen synthase kinase (GSK)3α/β in myeloid cells in the accelerated development of atherosclerosis[127].

1.5 GLYCOGEN SYNTHASE KINASE (GSK)3α/β

GSK3α/β is a serine/threonine protein kinase enzyme that is present in two main isoforms; GSK3α and GSK3β. They are 98% identical in the kinase domain, however only share 36% similarities in their C-terminal amino acid residues[128]. GSK3α and GSK3β are encoded by different genes. In mice, GSK3α is located on chromosome 7 and GSK3β is located on chromosome 16[129]. In humans, GSK3α is located on chromosome 19 and GSK3β is located on chromosome 3 (Figure 1.4)[129]. There is more than 90% sequence similarity in the kinase domains across species[129]. GSK3α (51kDa) has an N-terminus glycine-rich extension which makes the protein larger than GSK3β (47kDa)[129]. GSK3α and GSK3β have structural similarities, however they also have unique functional roles[130]. The strongest evidence for functional differences between GSK3α and GSK3β is that whole-body GSK3β knockout mice die during embryogenesis due to heart defects and liver degeneration related to hepatic apoptosis[131], whereas whole-body GSK3α knockout mice are viable and have no overt phenotype[132].

Figure 1.4: Glycogen synthase kinase3α/β. Figure adapted from Doble B.W and Woodget J.R.[128]. In humans, GSK3α (51kDa) is located on chromosome 19 and GSK3β (47kDa) is located on chromosome 3. They both contain a kinase domain highlighted in red, which are 98% identical between the two isoforms. Phosphorylation of Tyrosine 279 or Tyrosine 216 activates GSK3α and GSK3β, respectively. Phosphorylation on Serine 21 or Serine 9 phosphorylation inactivates GSK3α and GSK3β, respectively. GSK3α has a glycine rich N-terminal domain highlighted in blue, making the protein larger. *Figure created using Biorender.com 2022.*

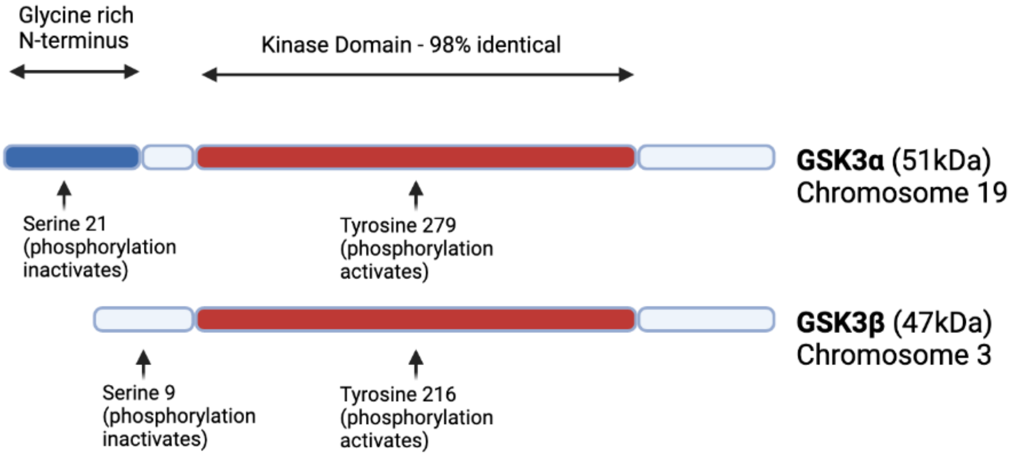
Glycine rich
N-terminus
Kinase Domain - 98% identical
GSK3α (51kDa)
Chromosome 19
Serine 21
(phosphorylation
inactivates)
Tyrosine 279
(phosphorylation
activates)
GSK3β (47kDa)
Chromosome 3
Serine 9
(phosphorylation
inactivates)
Tyrosine 216
(phosphorylation
activates)

GSK3α/β are constitutively active kinases that are involved in many cellular processes including regulation of gene expression, apoptosis[133,134] and cellular proliferation[135,136]. GSK3α/β were first identified as kinases involved in the phosphorylation/regulation of glycogen synthase. GSK3α/β now have over 100 known biological substrates[134]. They are unusual kinases as they are constitutively active in resting cells, and therefore can be both inhibited and induced. In addition, GSK3α/β activity often requires that substrates are pre-phosphorylated/primed by other kinases. The consensus sequence for GSK3α/β substrates is serine/threonine-x-x-x- serine/threonine-P. The first serine/threonine is the target residue for GSK3α/β, whereas the last serine/threonine-P is the priming residue. Although not always needed, primed substrates tend to increase the kinases activity[137].

GSK3α/β activity can be regulated by phosphorylation of serine residues. Inhibition of GSK3α is achieved by phosphorylation of serine 21(Ser21), and GSK3β inhibition by serine 9 (Ser9). Phosphorylation of Ser21/9 residues on GSK3α/β inactivates the kinase and blocks its ability to phosphorylate substrates. Some substrates known to phosphorylate GSK3α/β serine 21/9 residues include protein kinase B (PKB/Akt) (insulin signalling pathway), p38 mitogen-activated protein kinase (MAPK)[138] and protein kinase C (PKC)[139]. Conversely, autophosphorylation of tyrosine mediates upregulation and activation of GSK3α/β activity (tyrosine 279 (Tyr279)/tyrosine 216 (Tyr216) respectively)[140]. GSK3α/β has been detected in the mitochondria and nucleus, as well as the cytosol. Very little is known about mitochondria GSK3α/β activity. Nuclear GSK3α/β activity has been associated with regulation of gene expression[141,142].

Dysregulation of GSK3α/β has been associated with diseases including DM[143], atherosclerosis[144], Alzheimer's[145] and mood disorders[146]. GSK3α/β is involved in many signalling pathways and diseases, therefore more research is needed to better understand its roles and regulation in different cellular pathways.

GSK3α/β signalling pathways

Insulin signalling pathway

GSK3α/β was initially discovered as a regulatory kinase for glycogen synthase[147](Figure 1.5). Insulin binds to the insulin receptor and activates the phosphatidylinositol 3-kinase (PI3K)-PKB/Akt pathways via phosphorylation of insulin receptor substrates (IRS)[148]. PKB/Akt phosphorylates the serine residues on GSK3α/β resulting in inhibition of GSK3α/β activity[148]. This allows glycogen synthase activity and facilitates glucose storage as glycogen.

Wnt/ β-catenin signalling pathway

Wnt/β-catenin signalling is involved in aspects of cell proliferation, cell migration and cell polarity[149]. It is an important pathway in embryonic development[149, 150]. Wnt ligands bind to the frizzled receptor forming a complex of proteins consisting of axin, casein kinase 1 (CK1), adenomatous polyposis coli (APC) and Dishevelled kinase[148,149,151]. This complex inhibits GSK3α/β activity by phosphorylation of Ser21/Ser9. This allows β-catenin accumulation and migration to the nucleus triggering transcription of Wnt-specific genes[151,152].

MAPK signalling pathway

MAPK signalling cascades play an important role in embryonic development, cell division, proliferation, apoptosis and differentiation[153]. GSK3α/β regulates some of the transcription factors in the MAPK signalling cascade. Myc proteins regulate cell growth and division. GSK3α/β phosphorylates c-Myc labelling it for degregation[154]. GSK3α/β also phosphorylates c-Jun thereby blocking its ability to transcribe genes[155]**.** MAPK has been shown to inactivate GSK3α/β[156].

ER stress signalling pathway

More recently there has been a proposed mechanism of GSK3α/β signalling in the ER stress pathway. ER stress has been implicated in many diseases such as DM, neurodegenerative disorders and CVD[131,132,157,158,159]. Under conditions of ER stress, there is activation of the UPR. The UPR has 3 distinct pathways (mentioned earlier), IRE-1, PERK and ATF6. Our lab has shown that ER stress/UPR activation promotes GSK3α/β activity through the PERK signalling branch of the UPR[129].

Figure 1.5: GSK3α/β signalling pathways. Insulin binds to the insulin receptor phosphorylating insulin receptor substrates. This causes activation of the PI3K-PKB/Akt pathway which results in inactivation of GSK3α/β (phosphorylation of serine residue). Another pathway is Wnt binding to the frizzled receptor causing a complex of proteins. This protein complex inhibits GSK3α/β via serine phosphorylation, which allows an accumulation of β-catenin. CVD risk factors cause ER stress, upregulating the UPR response, GSK3α/β activity is upregulated through the PERK pathway. Finally, growth factors cause activation of MAPK, which inactivates GSK3α/β via serine phosphorylation. *Figure created using Biorender.com 2022.*

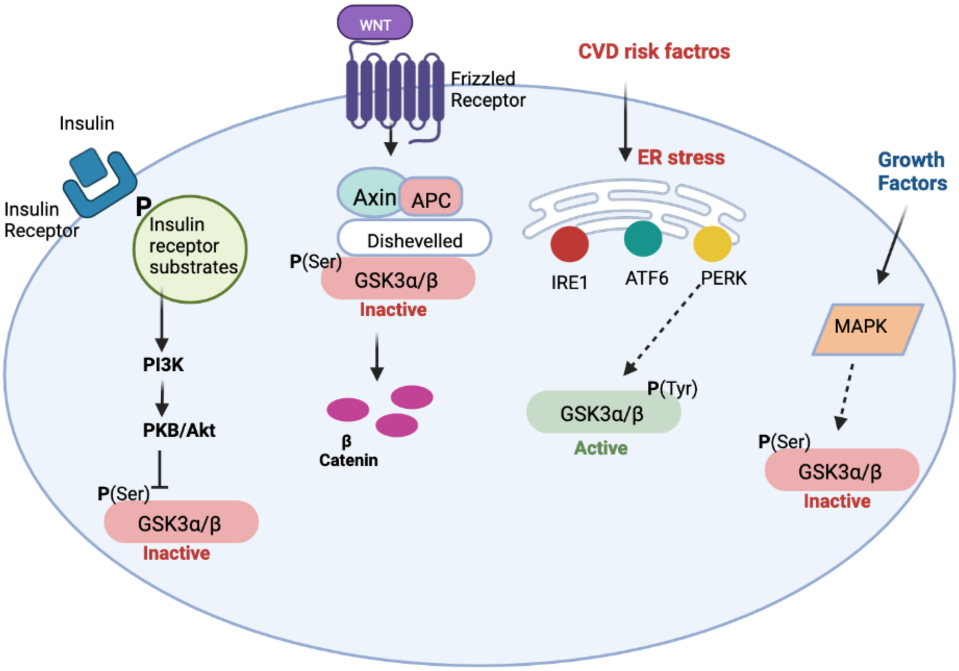
WNT
Frizzled Receptor
CVD risk factros
Insulin
Insulin Receptor
P
Insulin receptor substrates
Axin
APC
Dishevelled
P(Ser)
GSK3α/β
Inactive
ER stress
IRE1
ATF6
PERK
Growth Factors
MAPK
PI3K
PKB/Akt
β Catenin
P(Tyr)
GSK3α/β
Active
P(Ser)
GSK3α/β
Inactive
P(Ser)
GSK3α/β
Inactive

GSK3α/β roles in atherosclerosis

GSK3α/β has been implicated in signalling pathways involved in atherosclerosis. Toll-like receptors (TLR) are signal transducers that regulate the immune response through NF-κB gene transcription signalling and are reported to be upregulated in atherosclerosis[160]. It has been shown that human monocytes subjected to TLR agonists in the presence of a GSK3α/β inhibitor have reduced pro-inflammatory cytokine production[161]. GSK3α/β has been implicated in the regulation of NF-κB, and therefore alters inflammatory gene transcription[161,162,163]. Additionally, a whole body knockout of GSK3α in an atherosclerotic mouse model significantly reduced plaque volume[144]. Further analysis of cell specific roles of GSK3α/β showed that a myeloid knockout of GSK3α in an atherosclerosis-prone mouse model resulted in reduced plaque volume[127]. Others have shown that pharmacological inhibition of GSK3α/β using lithium chloride alleviated atherosclerotic plaque progression as well as VCAM-1 expression, suggesting that GSK3α/β could be involved in endothelial activation and therefore atherosclerosis initiation[164]. More recently, inhibition of myeloid GSK3α has been associated with atherosclerotic plaque regression[165]. These studies all support a causative role of GSK3α/β, in particular GSK3α, in the progression and initiation of atherosclerosis.

GSK3α/β role in ECs

To date, few studies have focussed on the role of GSK3α/β in ECs, especially with respect to the development and progression of atherosclerosis. GSK3β inhibition in primary human lung ECs has been shown to increase cell proliferation and migration[166]. GSK3β inhibition reduced monocyte adhesion in an inflammatory mouse model[167]. GSK3β concentrations were increased in HAEC exposed to elevated glucose concentrations[168]. Research to date largely focuses on the effects of GSK3β inhibition in ECs. Further research is needed to fully understand the specific roles of GSK3α/β isoforms in EC activation and its potential relation to atherogenesis initiation.

1.6 RESEARCH GOALS

CVD has been a major burden on global healthcare systems. Therapies available are focused on reducing CVD risk factors and thereby reducing the risk and severity of CVD. However, even with the availability of therapies, CVD remains the leading cause of mortality worldwide. Further understanding of cellular and molecular mechanisms involved in atherosclerosis initiation will allow for the identification of new targeted therapies for CVD. The objective of the research described in this thesis is to investigate if and how CVD risk factors cause EC activation, and to determine the potential roles that GSK3α/β may have in EC activation and the initiation of atherogenesis.

CHAPTER 2: General Hypothesis and Objectives

2.1 GENERAL HYPOTHESIS

The molecular mechanisms that link cardiovascular risk factors, including dyslipidemia and hyperglycemia, to the accelerated development of atherosclerosis are not clear. A better understanding of the mechanisms which drive the initiation of atherosclerosis will facilitate the development of more effective treatment strategies.

We hypothesize that risk factors for CVD promote EC activation leading to atherosclerotic initiation by signalling through the ER stress-GSK3α/β pathway.

2.2 GENERAL OBJECTIVES

The objectives of these studies is as follows:

1) To investigate the effects of hyperglycemia (a CVD risk factor) on EC activation and the initiation of atherosclerosis.
2) Delineate the molecular mechanism by which elevated glucose concentrations activate ECs, with specific focus on the ER stress-GSK3α/β pathway.
3) Investigate the role of endothelial GSK3α and GSK3β in the initiation and progression of atherosclerosis.

CHAPTER 3: The Effects of Hyperglycemia on Early Endothelial Activation and the Initiation of Atherosclerosis

Lauren Mastrogiacomo[1,2], Robert Ballagh[1], Daniel E Venegas-Pino[1], Hargun Kaur[1], Peter Shi[1], Geoff H Werstuck[1,2]

[1]Thrombosis and Atherosclerosis Research Institute, Hamilton, ON, Canada.

[2]Department of Medicine, McMaster University, Hamilton, ON, Canada.

3.1 FOREWORD

This study investigates the effects of hyperglycemia on endothelial cell (EC) activation and initiation of atherosclerosis. Results suggest that elevated glucose levels increase plaque volume and adhesion protein expression in dyslipidemia and hyperglycemic mice. In a hyperglycemic mouse model (in the absence of dyslipidemia) there was no plaque accumulation, however, hyperglycemic mice had an increased expression of adhesion proteins in the aortic sinus. The use of an SGLT2 inhibitor was able to reduce adhesion protein expression suggesting that regulating/normalizing glucose may be beneficial for EC health.

The experiments in this study were conducted by Lauren Mastrogiacomo with assistance from co-authors; Robert Ballagh, Dr. Daniel E Venegas-Pino, Hargun Kaur and Peter Shi. The manuscript was written by Lauren Mastrogiacomo in collaboration with Dr. Geoff Werstuck. This paper has been accepted for publication in the American Journal of Pathology 2022.

3.2 ABSTRACT

It is well established that patients with diabetes have an increased risk of developing atherosclerotic cardiovascular disease (CVD). The earliest detectable sign of atherosclerosis initiation is EC activation. Activated ECs express adhesion proteins, P-selectin, E-selectin, vascular cell adhesion molecule-1, and intercellular adhesion molecule-1, which function to recruit monocytes to the subendothelial layer. This study examines the effect of hyperglycemia on EC activation and the initiation and progression of atherosclerosis. In vitro studies revealed that exposure of human aortic ECs to elevated (30mM) glucose concentrations significantly increased the expression of P-selectin, E-selectin and vascular cell adhesion molecule-1. In vivo studies showed that, before lesion development, 5-week-old hyperglycemic ApoE$^{-/-}$Ins2$^{+/akita}$ mice had significantly increased expression of these adhesion proteins in the aortic sinus and increased macrophage infiltration, compared with normoglycemic ApoE$^{-/-}$ controls. At 25 weeks of age, ApoE$^{-/-}$Ins2$^{+/akita}$ mice had significantly larger atherosclerotic plaques than ApoE$^{-/-}$ controls (0.022 mm^3± 0.004 vs 0.007 mm^3± 0.001, $P<0.05$). Similar endothelial activation was observed in heterozygous ApoE$^{+/-}$Ins2$^{+/akita}$ mice; however, detectable atherosclerotic lesions did not develop in the absence of dyslipidemia. Lowering blood glucose levels (by 55%) using a sodium-glucose cotransporter 2 inhibitor did reduce endothelial activation. These findings support a causative role for hyperglycemia in atherogenesis and

highlight the importance of blood glucose regulation to prevent atherosclerotic CVD.

3.3 INTRODUCTION

Diabetes mellitus (DM) is a heterogenous group of diseases that are characterized by hyperglycemia[1]. The global prevalence of adults diagnosed with diabetes is estimated to be 463 million (in 2019) and this is projected to continually increase over the coming years[2,3]**.** Despite advances in care, patients with diabetes have a 2-4 fold increased risk for developing CVD compared to individuals that do not have diabetes[4,5,6,7]. Although a great deal of work has been done, and several potential mechanisms have been proposed[8], a definitive underlying pathway linking diabetes to the pathogenesis of CVD has not yet been identified.

Atherosclerosis is an inflammatory disease that is the underlying cause of most CVD[9,10]. Atherosclerosis typically appears at sites of endothelial injury, in regions of the artery that contain bifurcations, branches, or inner curvatures, which tend to disrupt laminar blood flow[11,12]. The endothelium is composed of a single layer of semi-permeable cells that line the inner vasculature[13]. ECs assist in regulation of vascular wall permeability, blood fluidity, vascular tone (contraction and relaxation) and monocyte/leukocyte attachment[14,15,16]. Therefore, ECs are critical components and regulators of the cardiovascular system, and play a large role in the maintenance of vascular homeostasis and cardiovascular health[15]. The endothelium is adaptive to many inflammatory and metabolic environments; however persistent stressors can activate/damage ECs[17]. Endothelial activation is one of the earliest signs of atherosclerosis initiation[18,19].

Activated ECs are characterized by increased expression of cell surface proteins, including cell adhesion molecules, P-selectin, E-selectin, intercellular adhesion molecule (ICAM)-1 and vascular cell adhesion molecule (VCAM)-1[19,20,21,22]. These surface proteins function in the attachment and infiltration of monocytes into the subendothelial space of the artery wall[23]. Here, infiltrating monocytes differentiate into macrophages that efferocytose modified lipoproteins and cell debris[23,24]. These lipid engorged macrophages, called foam cells, are the predominant cell type in a growing atherosclerotic plaque[24]. They also play an important role in plaque stability and potential plaque rupture. Thus, regulation of the endothelial activation and monocyte infiltration is a potential strategy to protect against the development and progression of CVD.

Preclinical studies have clearly shown that the presence of diabetes/hyperglycemia can accelerate the development of atherosclerosis in rodent models[25,26]. However, the molecular mechanisms by which elevated concentrations of glucose promote processes that result in enhanced disease progression are not well understood. In this study we examine the effect of hyperglycemia on the endothelium. We hypothesize that hyperglycemia promotes the earliest events in atherogenesis – the activation of ECs. A better understanding of how diabetes promotes atherosclerosis CVD will give us insight on how to prevent CVD in this growing population.

3.4 MATERIALS AND METHODS

HAEC culture treatment conditions and analysis

Human aortic endothelial cells (HAEC) (ATCC, Manassas, VA) were cultured in EGM™-2 Endothelial Cell Growth Medium-2 BulletKit (Lonza, Basel, Switzerland) supplemented with 1% penicillin-streptomycin at 37°C in 5% CO_2. Cells from passage 4-10 were used for experiments. Cells were grown to confluency and split into a 12 well plate at a seeding density of $5x10^5$ cells/well. Cells were cultured in regular media (5mM glucose), high mannitol (media (5mM glucose) + 25mM mannitol) or high glucose (media (5mM glucose) + 25mM glucose for a total of 30mM glucose)[27,28] for 24 hours and collected using the TRIzol Reagent method (Thermo Fisher Scientific, Waltham, MA). Total RNA was isolated from the cells and cDNA was synthesized using the High-Capacity cDNA Reverse Transcription Kit (Thermo Fisher Scientific, Waltham, MA). The expression of P-selectin, E-selectin, ICAM-1, VCAM-1, iNOS, eNOS, vWF, and PECAM, were quantified using the SYBR Green (with ROX) method (Thermo Fisher Scientific, Waltham, MA) and the StepOnePlus Real-Time PCR System (Thermo Fisher Scientific, Waltham, MA)(see Table 3.1). Samples were run in technical triplicates and the comparative threshold cycle method was used to determine gene expression. Expression levels were normalised to a β-actin control.

Table 3.1: Primer Sequences

Transcript	**Primer Sequence**
Human P-selectin	F: 5’- TGAGCACTGCTTGAAGAAAAAGC -3’ R: 5’- CACGTATTCACATTCTGGCCC -3’
Human E-selectin	F: 5’- AGAGGTTCCTTCCTGCCAAG -3’ R: 5’- CAGAGCCATTGAGGGTCCAT-3’
Human VCAM-1	F: 5’- CCCTTGACCGGCTGGAGATT –3’ R: 5’- CTGGGGGCAACATTGACATAAAGTG -3’
Human ICAM-1	F: 5’- GCAGACAGTGACCATCTACAGCTT -3’ R: 5’- CTTCTGAGACCTCTGGCTTCGT – 3’
Human eNOS	F: 5′- TGG ACC TGG ATA CCC GGA C-3′ R: 5′- TGG TGA CTT TGG CTA GCT GGT 3′
Human iNOS	F: 5′- GTT TCT GGC AGC AGC GGC TC-3′ R: 5′- GCT CCT CGC TCA AGT TCA GC-3′
Human vWF	F: 5’- TAA GAG GGC AAC ACA AAC G – 3’ R: 5’- ATC TTC ACC TGC CCA CTC C – 3’
Human PECAM	F: 5’- CCA GTG TCC CCA GAA GCA AA – 3’ R: 5’- TGA TAA CCA CTG CAA TAA GTC CTT TC– 3’
Human β-actin	F: 5’ - ACC GAG CGC GGC TAC AG – 3’ R: 5’ - CTT AAT GTG ACG CAC GAT TTC – 3’

F – forward primer, R- reverse primer

Mice

All animal studies were pre-approved by the McMaster University Animal Research Ethics Board. Male $ApoE^{-/-}Ins2^{+/akita}$ mice were mated with female $ApoE^{-/-}$ to obtain $ApoE^{-/-}Ins2^{+/akita}$ and $ApoE^{-/-}$ littermates (Jackson Laboratory, Bar Harbor, ME). All mice are in a C57BL/6 genetic background. Previous studies have shown that male, but not female, $ApoE^{-/-}Ins2^{+/akita}$ mice present with chronic hyperglycemia[25]. Therefore only male mice were used in this study. Fasting blood glucose levels were determined at 5 weeks of age. Male $ApoE^{-/-}Ins2^{+/akita}$ mice with fasting blood glucose levels above 15mM were included in the study. Male $ApoE^{-/-}$ littermates had blood glucose levels <10mM (Table 3.2). To obtain heterozygous $ApoE^{+/-}$ mice, male $ApoE^{-/-}Ins2^{+/akita}$ mice were mated with female C57BL/6 to produce $ApoE^{+/-}Ins2^{+/akita}$ and $ApoE^{+/-}$ littermates. Fasting blood glucose levels were determined at 5 weeks of age and similar blood glucose inclusion criteria were used. All mice had free access to a regular chow diet (2018 Teklad Global 18% Protein Diet, Harlan Teklad, 2918, Madison, WI) with 18% of the calories are derived from fat. Mice were euthanized at 5, 7, 10, 15, or 25 weeks of age. Blood was collected and the vasculature was flushed with PBS and then fixed with 10% formalin. Heart/aorta, adipose and liver tissue were collected for analysis.

Table 3.2: Metabolic parameters of ApoE$^{-/-}$ and ApoE$^{-/-}$Ins2$^{+/akita}$ mice

Genotype	**Age, weeks**	**Blood glucose, mM**	**Plasma triglyceride, mM**	**Plasma cholesterol, mM**	**Body weight, g**	**Liver weight, g**	**Adipose weight, g**
ApoE$^{-/-}$	5	8.70 ±0.39	1.10 ±0.13	6.44 ±0.60	14.48 ±0.31	1.06 ±0.05	0.07 ±0.02
	25	7.77 ±0.63	1.21 ±0.04	9.40 ±0.47	30.11 ±0.65	1.33 ±0.05	0.31 ±0.06
ApoE$^{-/-}$ Ins2$^{+/akita}$	5	20.43 ±1.13 ****	1.46 ±0.12	8.15 ±0.34	15.56 ±0.29	1.38 ±0.10 *	0.03 ±0.02
	25	25.08 ±0.91 ††††	1.04 ±0.08	20.40 ±0.92 ††††	24.86 ±0.73 †	1.31 ±0.07	0.02 ±0.01 ††

*P<0.05 and ****P<0.00005 compared to 5 week old ApoE$^{-/-}$ mice,

†P<0.05, ††P<0.005 and ††††P<0.00005 compared to 25 week old ApoE$^{-/-}$ mice,

n=5

Empagliflozin treatment

Five-week-old ApoE$^{+/-}$ and ApoE$^{+/-}$Ins2$^{+/akita}$ were provided with regular drinking water or water supplemented with 35mg/kg body weight empagliflozin (MedChem Express, Monmouth Junction, NJ), as previously described[29]. After 2 weeks, mice were sacrificed and urine, blood and heart/aorta tissue were collected.

Analysis of plasma and urine

Fasting blood glucose levels were measured using the OneTouch Verio Flex Meter (Lifescan, Inc., Milpitas, CA). Fasting plasma total cholesterol and triglyceride levels were determined using the colormetric infinity cholesterol/triglyceride kit (Thermo Fisher Scientific, Waltham, MA). Urine glucose levels were measured using the colormetic infinity glucose kit (Thermo Fisher Scientific, Waltham, MA).

Analysis of atherosclerosis – Masson's trichrome staining

The heart was removed and embedded in paraffin and 5 um serial sections of the aortic sinus were collected on glass slides as previously described[30]. Sections were deparaffinised and then stained with Weigert's Hematoxylin (Sigma-Aldrich, St. Louis, MI). The slides were further stained with Biebrich scarlet-acid fuchsin solution and alanine blue (Sigma-Aldrich, St. Louis, MI). Coverslips were attached using DPX mounting media and images were captured using the Olympus DP71 digital camera (Olympus Imaging, Center Valley, PA) mounted on a Leitz Laborlux S bright-field microscope (Leica Microsystems, Concord, ON). Atherosclerotic plaque areas were determined from 10 serial sections per mouse. The atherosclerotic volumes were calculated manually using Image J software (Version1.15j8, https://imagej.nih.gov/ij/index.html, Date of last access: 23rd August 2021) as previously described[30].

Immunofluorescence/immunohistochemistry staining

Immunofluorescence and immunohistochemistry were used to quantify markers of EC activation in cross sections of the aortic sinus. Six sections at 50 um intervals were immunostained with antibodies against P-selectin (Novus Biologicals, Littleton, CO, NB100-65392 1:50 dilution), E-selectin (Novus Biologicals, Littleton, CO, NBP1-45545 1:100 dilution), VCAM-1 (Abcam, Cambridge, UK, ab134047 1:50 dilution), vWF (Agilent Dako, Santa Clara, CA, A008202 1:50 dilution) and CD107b$^+$/Mac3 (BD Biosciences, Franklin Lakes, NJ, 550292 1:50 dilution). Primary antibodies were detected with appropriate conjugated secondary antibodies (Alexa Fluor 488 anti-mouse, Alexa Fluor 488 anti-rabbit or Alexa Fluor 488 anti-rat – all from Thermo Fisher Scientific, Waltham, MA) and the percentage of the endothelium stained in each case was determined by immunofluorescence. ICAM-1 was assessed using immunohistochemistry using a primary antibody (R&D Systems, Minneapolis, MN, BAF796 1:50 dilution) and biotinylated anti-goat secondary antibody

(Thermo Fisher Scientific, Waltham, MA). Immunohistochemical staining was detected with horseradish peroxidase and 3,3' diaminobenzidine (DAB) (Agilent, Santa Clara, CA). Negative controls for staining were performed using pre-immune IgG in place of the primary antibody (Supplementary Figure 3.1).

Blood cell count

Whole blood cell counts were assessed in 5 week-old male ApoE$^{-/-}$ and ApoE$^{-/-}$Ins2$^{+/akita}$ mice using a DREW scientific HEMAvet HV950 multispecies haematology instrument, according to manufactures instructions (Drew Scientific Inc, Miami Lakes, FL).

Statistical analysis

Data was analysed using t-test, one or two-way ANOVA test followed by a multiple comparison test using Graph-Pad Prism 9 (GraphPad Software, San Diego, CA), and expressed as +/- SEM. For all experiments a P value of <0.05 was considered to be statistically significant. *P<0.05, **P <0.005, ***P<0.0005 and ****P<0.00005.

3.5 RESULTS

Elevated concentrations of glucose promote adhesion protein expression in cultured ECs

To assess the effects of glucose on endothelial activation, HAECs were cultured in standard media containing 5mM glucose, or elevated concentrations of glucose (total 30mM) for 24 hours. As an osmotic control for the high glucose treatment, HAECs were exposed to an equimolar concentration of mannitol (25mM mannitol and 5mM glucose). The expression of genes encoding adhesion proteins and other endothelial markers were determined by reverse transcription-polymerase chain reaction (RT-PCR) and results were normalized to β-actin expression. Treatment with elevated concentrations of glucose significantly increased expression of adhesion proteins P-selectin, E-selectin and VCAM-1 genes, compared to the 5mM glucose control and mannitol controls (Figure 3.1). Inducible nitric oxide synthase (iNOS), vWF and PECAM expression was also significantly elevated, (Supplementary Figure 3.2). No significant difference was detected in ICAM-1 expression between experimental groups. Mannitol did not significantly affect the expression of any of the genes examined. These results suggest that hyperglycemia may play a direct role in activation of ECs and thus contribute to early initiation of atherosclerosis.

Figure 3.1: Analysis of the effects of hyperglycemia on HAEC activation. HAEC cultured in 5mM glucose were exposed to an additional 25mM glucose or 25mM mannitol for 24 hours. The expression of adhesion proteins P-selectin, E-selectin, ICAM-1 and VCAM-1 was quantified by RT-PCR and normalized to β-actin expression. n= 4-6, $^{*}P<0.05$, $^{**}P < 0.005$.

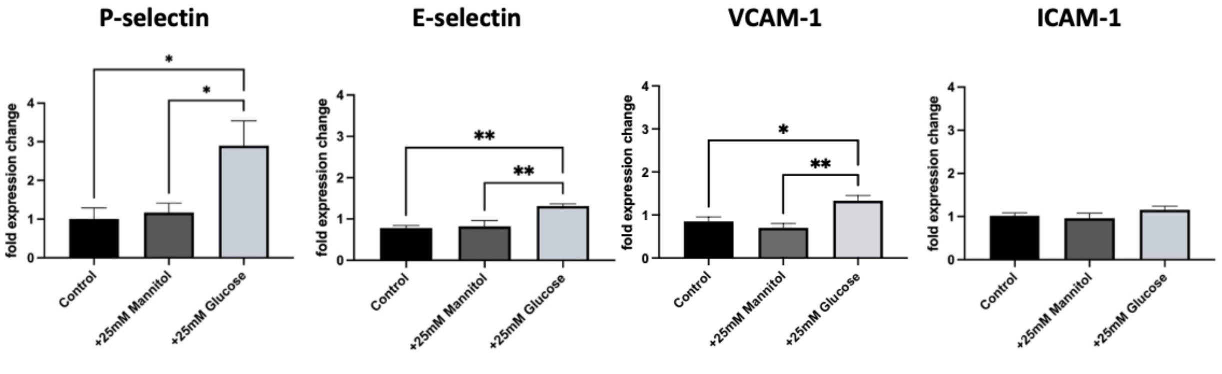
P-selectin
E-selectin
VCAM-1
ICAM-1
fold expression change
0
1
2
3
4
*
**
Control
+25mM Mannitol
+25mM Glucose

Atherosclerotic plaque development in ApoE$^{-/-}$ and ApoE$^{-/-}$Ins2$^{+/akita}$ mice

ApoE$^{-/-}$ and ApoE$^{-/-}$Ins2$^{+/akita}$ mice were used to investigate the effects of hyperglycemia on adhesion protein expression in vivo. All mice were fed a standard chow diet ad libitum. Subsets of mice were sacrificed at 5, 10, 15 and 25 weeks of age and metabolic parameters were assessed (Table 3.2). ApoE$^{-/-}$Ins2$^{+/akita}$ mice presented with hyperglycemia and dyslipidemia at 5 and 25 weeks of age, relative to age matched ApoE$^{-/-}$ mice. Plasma total cholesterol was significantly elevated in 25 week-old ApoE$^{-/-}$Ins2$^{+/akita}$, relative to 25 week-old ApoE$^{-/-}$ mice. Body weight and adipose weight was significantly lower in 25 week-old ApoE$^{-/-}$Ins2$^{+/akita}$, compared to ApoE$^{-/-}$ (Table 3.2).

Atherosclerotic plaque volume was quantified from the aortic sinus into the ascending aorta of 5, 10, 15 and 25 week-old mice (Figure 3.2A-B). Plaques were not detected in 5 week-old ApoE$^{-/-}$ or ApoE$^{-/-}$Ins2$^{+/akita}$ mice. Plaques were identified in both mouse models at ≥10 weeks of age. Atherosclerotic plaques were significantly larger in 25 week-old hyperglycemic ApoE$^{-/-}$Ins2$^{+/akita}$, compared to age matched normoglycemic ApoE$^{-/-}$ mice (0.022 mm^3± 0.004 vs 0.007 mm^3± 0.001, $P<0.05$). Necrotic cores were 70% larger ($p<0.05$) in 25 week-old ApoE$^{-/-}$Ins2$^{+/akita}$ mice, compared to aged matched ApoE$^{-/-}$ (Figure 3.2C). This is consistent with previous findings[25,26] and indicates that hyperglycemia accelerates plaque development in this dyslipidemic mouse model.

Figure 3.2: Atherosclerotic progression in ApoE$^{-/-}$ and ApoE$^{-/-}$Ins2$^{+/akita}$ mice. **A**. Representative images of cross sections of aortic sinus stained with Masson's trichrome from 5 and 25 week-old mice. Plaques are indicated by blue outlines. **B** Quantification of the plaque volume in the aortic sinus at 5, 10, 15, and 25 weeks of age. **C** Quantification of necrotic core area at the aortic sinus of 25 week-old mice. n=5-6 (**A-C**), *P < 0.05.Scale bar equals 100µm (**A**).

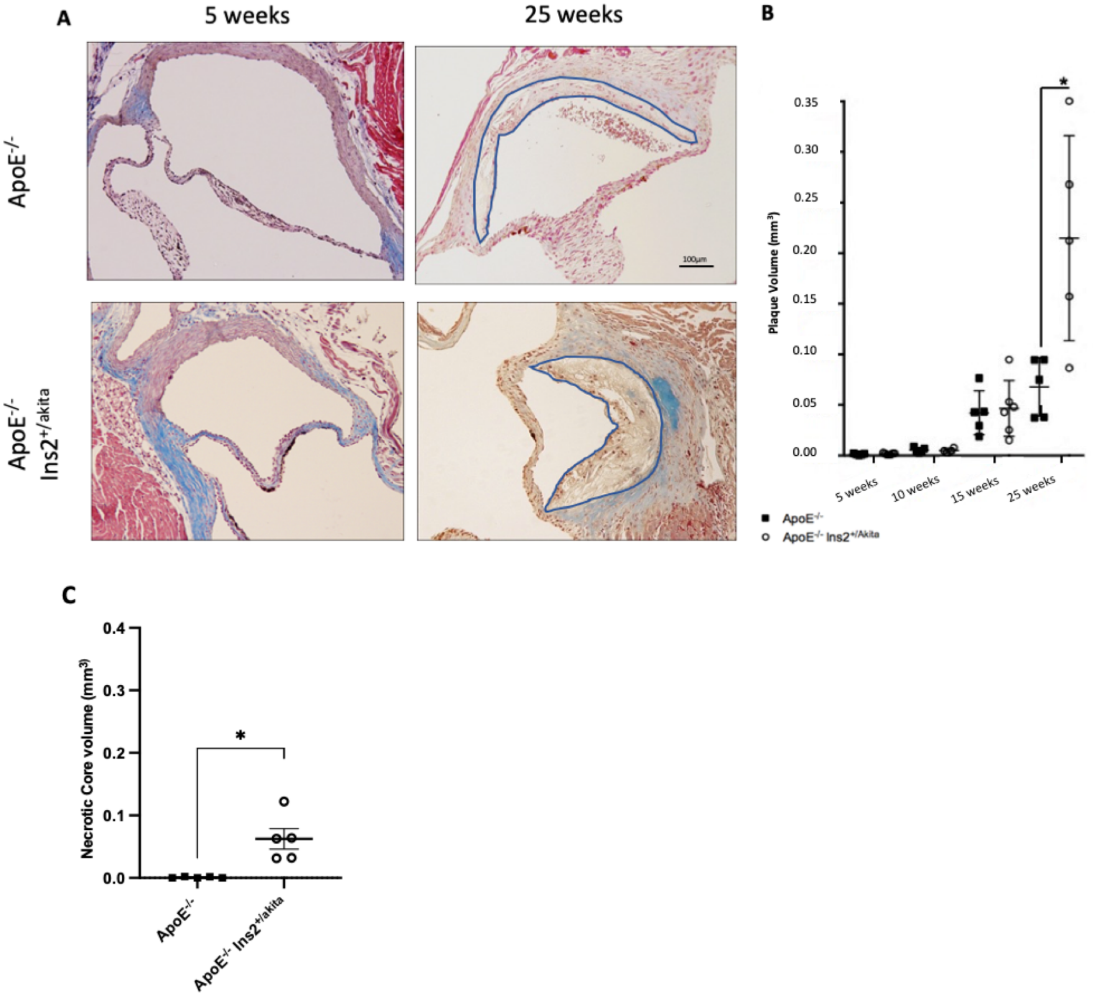
A
5 weeks
25 weeks
ApoE-/-
ApoE-/- Ins2+/akita
100μm
B
Plaque Volume (mm³)
0.35
0.30
0.25
0.20
0.15
0.10
0.05
0.00
5 weeks
10 weeks
15 weeks
25 weeks
*
ApoE-/-
ApoE-/- Ins2+/Akita
C
Necrotic Core volume (mm³)
0.4
0.3
0.2
0.1
0.0
*
ApoE-/-
ApoE-/- Ins2+/akita

EC activation in hyperglycemic/dyslipidemic ApoE$^{-/-}$Ins2$^{+/akita}$ mice

To assess endothelial activation, adhesion factors P-selectin, E-selectin, ICAM-1, and VCAM-1 were quantified by immunostaining of cross sections of aortic sinus from 5 and 25 week-old ApoE$^{-/-}$ and ApoE$^{-/-}$Ins2$^{+/akita}$ mice (Figure 3.3A). P-selectin, E-selectin and VCAM-1 expression was significantly elevated in 5 week-old hyperglycemic ApoE$^{-/-}$Ins2$^{+/akita}$ (52% increase $P<0.05$, 69% increase $P<0.005$ and 47% increase $P<0.005$, respectively), compared to age matched ApoE$^{-/-}$ (Figure 3.3B-D). There was no significant difference in ICAM-1 staining between mouse models at 5 weeks of age (Figure 3.3E). At 25 weeks of age, expression of all endothelial activation markers was elevated, relative to 5 week-old controls, however no significant difference in expression was detected between 25 week-old ApoE$^{-/-}$ and ApoE$^{-/-}$Ins2$^{+/akita}$ mice for any of the markers. The specificity of the immunostaining is supported by slides stained with pre-immune IgG (Supplementary Figure 3.1).

Endothelial adhesion proteins bind to circulating monocytes, which can be recruited into the artery walls where they differentiate into macrophages[31]. Monocyte/macrophage recruitment was assessed at 5 weeks of age in both mouse models by immunofluorescence staining. Significantly more monocyte/macrophage (CD107b^{+}/Mac-3^{+}) staining was detected in 5 week-old ApoE$^{-/-}$Ins2$^{+/akita}$ mice, compared to 5 week-old ApoE$^{-/-}$ controls (Figure 3.4). A hematology profile of 5 week-old ApoE$^{-/-}$ and ApoE$^{-/-}$Ins2$^{+/akita}$ mice showed that hyperglycemia does not affect circulating blood cell counts in this model (Supplementary Table 3.1). Together, these findings suggest that the observed increase in adhesion protein expression in ApoE$^{-/-}$Ins2$^{+/akita}$ mice results in a significant increase in monocyte recruitment.

Figure 3.3: **Endothelial P-selectin, E-selectin, VCAM-1 and ICAM-1 expression in male ApoE$^{-/-}$ and ApoE$^{-/-}$Ins2$^{+/akita}$ mice**. **A** Representative images of cross sections of aortic sinus from 5 and 25 week-old ApoE$^{-/-}$ and ApoE$^{-/-}$Ins2$^{+/akita}$ mice immunostained for P-selectin, E-selectin, VCAM-1 or ICAM-1. White and red boxes indicate more highly magnified sections of the image. Quantification of percent of endothelium showing immunofluorescence staining for P-selectin (**B**), E-selectin (**C**) and VCAM-1 (**D**) in 5 and 25 week-old ApoE$^{-/-}$ and ApoE$^{-/-}$ Ins2$^{+/akita}$ mice, as indicated. **E** Quantification of percent of endothelium stained by immunohistochemistry for ICAM-1 expression in 5 and 25-week old ApoE$^{-/-}$ and ApoE$^{-/-}$Ins2$^{+/akita}$ mice, as indicated. n=5-9 (**A-E**), *P<0.05, **P<0.005. Scale bar equals 100μm (**A**, main images); 50 μm (**A**, boxed areas).

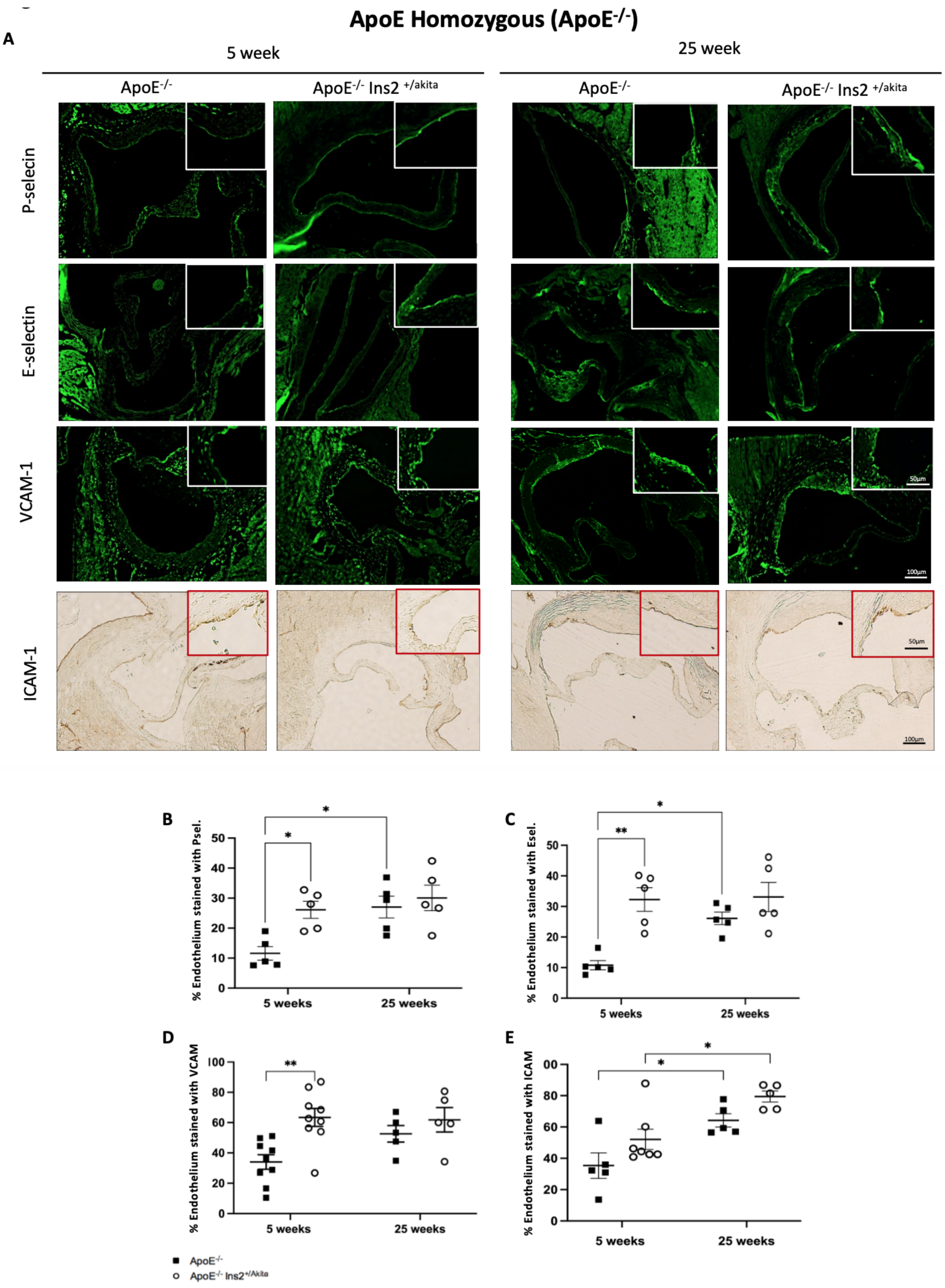
ApoE Homozygous (ApoE-/-)
A
5 week
25 week
ApoE-/-
ApoE-/- Ins2 +/akita
ApoE-/-
ApoE-/- Ins2 +/akita
P-selecin
E-selectin
VCAM-1
ICAM-1
50µm
100µm
50µm
100µm
B
% Endothelium stained with Psel.
0
10
20
30
40
50
*
*
5 weeks
25 weeks
C
% Endothelium stained with Esel.
0
10
20
30
40
50
**
*
5 weeks
25 weeks
D
% Endothelium stained with VCAM
0
20
40
60
80
100
**
5 weeks
25 weeks
E
% Endothelium stained with ICAM
0
20
40
60
80
00
*
*
5 weeks
25 weeks
ApoE-/-
ApoE-/- Ins2+/Akita

Figure 3.4: Endothelial monocyte/macrophage recruitment in ApoE$^{-/-}$ and ApoE$^{-/-}$Ins2$^{+/akita}$ mice. **A** Representative images of cross sections of aortic sinus from 5 week-old ApoE$^{-/-}$ and ApoE$^{-/-}$Ins2$^{+/akita}$ mice immunostained with an antibody against CD107b^{+}/Mac3. White box indicates a more highly magnified sections of the image. **B** Quantification of CD107b^{+}/Mac3 positive immunostained area. n=7-9 (**A-B**), **P < 0.005.Scale bar equals 50μm (**A**, main image); Scale bar equals 25 μm (**A**, boxed area).

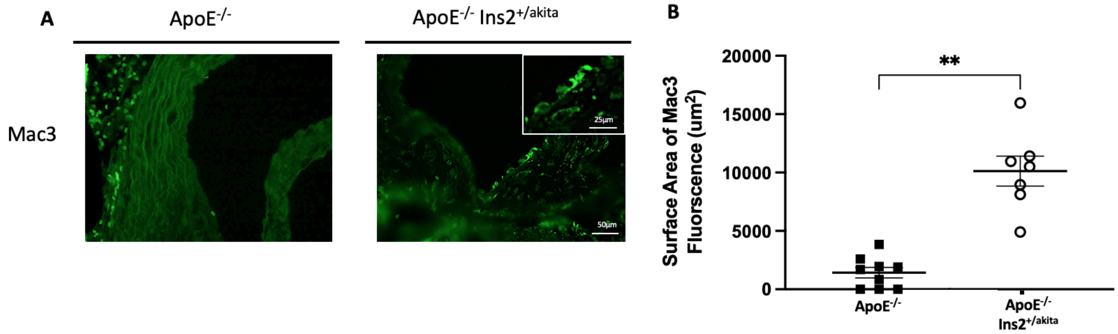
A
ApoE-/-
ApoE-/- Ins2+/akita
Mac3
25µm
50µm
B
**
Surface Area of Mac3 Fluorscence (um2)
20000
15000
10000
5000
0
ApoE-/-
ApoE-/- Ins2+/akita

Hyperglycemia is insufficient to promote plaque development in the absence of dyslipidemia

To determine if hyperglycemia could enhance adhesion protein expression and accelerate atherogenesis independent of dyslipidemia, ApoE$^{-/-}$ and ApoE$^{-/-}$Ins2$^{+/akita}$ mice were crossed with C57Bl/6 mice to create heterozygous ApoE$^{+/-}$ and ApoE$^{+/-}$Ins2$^{+/akita}$ mice. The ApoE$^{+/-}$ mice are normolipidemic and normoglycemic and ApoE$^{+/-}$Ins2$^{+/akita}$ mice are normolipidemic and hyperglycemic (Table 3, Supplementary Table 3.2). Mice were fed a standard chow diet ad libitum and sacrificed at 5 or 25 weeks of age. No differences were detected in triglyceride and cholesterol levels between mouse models at 5 or 25 weeks of age (Table 3.3). Blood glucose levels were significantly elevated in both 5 and 25 week-old ApoE$^{+/-}$Ins2$^{+/akita}$, compared to age matched ApoE$^{+/-}$ controls. Body weight and adipose weight were significantly reduced in 25 week-old ApoE$^{+/-}$Ins2$^{+/akita}$ mice, compared to 25 week-old ApoE$^{+/-}$ controls. Atherosclerotic plaques were not detected at 5 or 25 weeks of age in either mouse strain (Supplementary Figure 3.3). This finding suggests that hyperglycemia alone is not sufficient to initiate detectable plaque development in the absence of dyslipidemia in this mouse model.

Table 3.3: Metabolic parameters of ApoE$^{+/-}$ and ApoE$^{+/-}$Ins2$^{+/akita}$ mice

Genotype	**Age, weeks**	**Blood glucose, mM**	**Plasma triglyceride, mM**	**Plasma cholesterol, mM**	**Body Weight, g**	**Liver weight, g**	**Adipose weight , g**
ApoE$^{+/-}$	5	10.22 ±0.48	0.36 ±0.04	2.48 ±0.17	19.04 ±0.65	0.86 ±0.07	0.13 ±0.03
	25	11.7 ±0.57	0.77 ±0.03	2.85 ±0.20	31.98 ±0.66	1.31 ±0.09	0.50 ±0.13
ApoE$^{+/-}$ Ins2$^{+/akita}$	5	20.48 ±1.89 ***	0.58 ±0.08	2.83 ±0.16	21.1 ±1.58	1.04 ±0.05	0.11 ±0.01
	25	23.78 ±2.42 ††††	0.62 ±0.20	2.61 ±0.31	22.27 ±1.17 ††††	1.21 ±0.11	0.01 ±0.01 †††

***P<0.0005 compared to 5 week-old ApoE$^{+/-}$ mice,

†††P<0.0005 and ††††P<0.00005 compared to 25 week-old ApoE$^{+/-}$ mice

n=5

Hyperglycemia promotes EC activation

To determine if hyperglycemia, in the absence of dyslipidemia, can promote EC activation, aortic cross sections from 5 and 25 week-old ApoE$^{+/-}$ and ApoE$^{+/-}$Ins2$^{+/akita}$ mice were assessed for adhesion protein expression using immunofluorescence staining (Figure 3.5A). ApoE$^{+/-}$Ins2$^{+/akita}$ mice (normolipidemic and hyperglycemic) had elevated P-selectin, E-selectin, and VCAM-1 at 5 and 25 weeks of age, compared to age matched normolipidemic and normoglycemic ApoE$^{+/-}$ controls (Figure 3.5B-D). Expression of ICAM-1 was elevated in 25 week-old ApoE$^{+/-}$ and ApoE$^{+/-}$Ins2$^{+/akita}$ mice relative to 5 week-old mice. However, there was no significant difference in ICAM-1 expression between age-matched ApoE$^{+/-}$ and ApoE$^{+/-}$Ins2$^{+/akita}$ mice (Figure 3.5E).

To determine if adhesion protein expression was associated with increased monocyte/macrophage recruitment, CD107b^{+} (Mac-3^{+}) staining was assessed on the aortic sinus arterial wall of 5 week-old ApoE$^{+/-}$ and ApoE$^{+/-}$Ins2$^{+/akita}$ mice. Five week-old ApoE$^{+/-}$Ins2$^{+/akita}$ mice showed a significant increase in CD107b^{+} (Mac-3^{+}) staining compared to 5 week-old ApoE$^{+/-}$ controls (Figure 3.6). Overall, monocyte/macrophage staining was much lower in ApoE$^{+/-}$ and ApoE$^{+/-}$Ins2$^{+/akita}$ mice compared to age matched ApoE$^{-/-}$ and ApoE$^{-/-}$Ins2$^{+/akita}$ mice (Figure 3.4).

Figure 3.5: **Endothelial P-selectin, E-selectin, ICAM-1 and VCAM-1 expression in ApoE$^{+/-}$ and ApoE$^{+/-}$ Ins2$^{+/akita}$ mice**. **A** Representative images of cross sections of aortic sinus from 5 and 25 week-old ApoE$^{+/-}$ and ApoE$^{+/-}$Ins2$^{+/akita}$ mice immunostained for P-selectin, E-selectin, ICAM-1 or VCAM-1. White and red boxes indicate a more highly magnified sections of the image. Quantification of percent of endothelium showing immunofluorescence staining for P-selectin (**B**), E-selectin (**C**), and VCAM-1 (**D**) in 5 and 25-week old ApoE$^{+/-}$ and ApoE$^{+/-}$Ins2$^{+/akita}$ mice, as indicated. **E** Quantification of percent of endothelium stained by immunohistochemistry for ICAM-1 expression in 5 and 25 week-old ApoE$^{+/-}$ and ApoE$^{+/-}$Ins2$^{+/akita}$ mice, as indicated. n=5 (**A-E**), ***P<0.0005 and ****P<0.00005. Scale bar equals 100μm (**A**, main images); 50 μm (**A**, boxed areas).

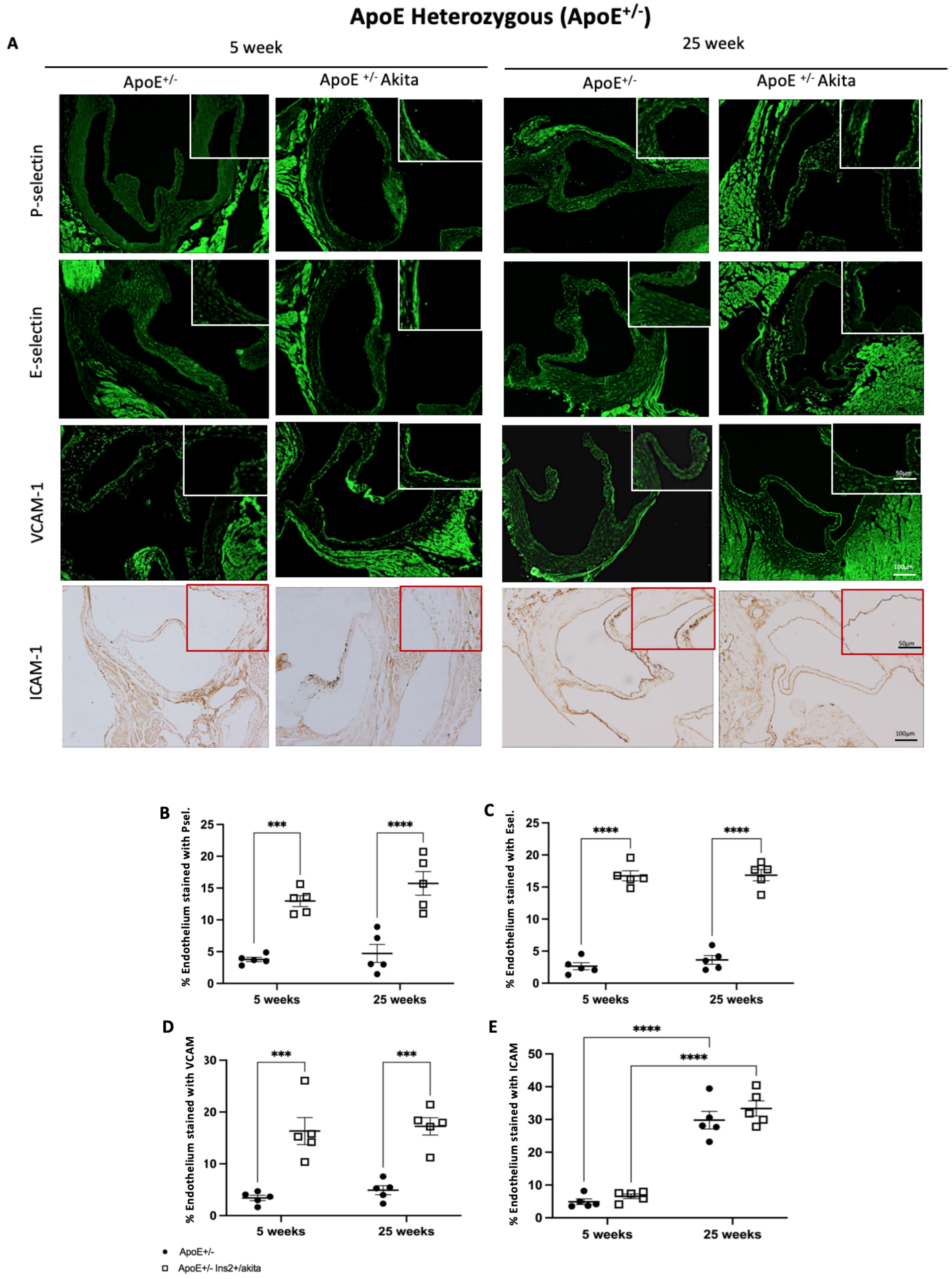
ApoE Heterozygous (ApoE+/-)
A
5 week
25 week
ApoE+/-
ApoE +/- Akita
ApoE+/-
ApoE +/- Akita
P-selectin
E-selectin
VCAM-1
ICAM-1
50μm
100μm
50μm
100μm
B
% Endothelium stained with Psel.
***
****
5 weeks
25 weeks
C
% Endothelium stained with Esel.
****
****
5 weeks
25 weeks
D
% Endothelium stained with VCAM
***
***
5 weeks
25 weeks
E
% Endothelium stained with ICAM
****
****
5 weeks
25 weeks
ApoE+/-
ApoE+/- Ins2+/akita

Figure 3.6: Endothelial monocyte/macrophage recruitment in ApoE$^{+/-}$ and ApoE$^{+/-}$Ins2$^{+/akita}$ mice. **A** Representative images of cross sections of aortic sinus from 5 week-old ApoE$^{+/-}$ and ApoE$^{+/-}$Ins2$^{+/akita}$ mice immunostained with an antibody against CD107b^{+}/Mac3. White box indicates a more highly magnified section of the image. **B** Quantification of CD107b^{+}/Mac3 positive immunostained area. n=5, *P<0.05 (**A-B**). Scale bar equals 100μm(**A**, main images); 50 μm (**A**, boxed area).

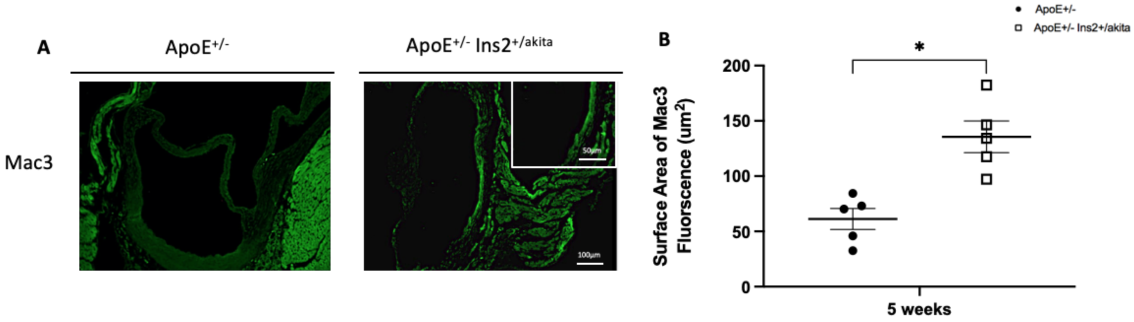
A
ApoE+/-
ApoE+/- Ins2+/akita
Mac3
50µm
100µm
B
● ApoE+/-
□ ApoE+/- Ins2+/akita
*
Surface Area of Mac3 Fluorscence (um2)
200
150
100
50
0
5 weeks

SGLT2 inhibitor lowers glucose levels in ApoE$^{+/-}$Ins2$^{+/akita}$

It is possible that the effects on adhesion protein expression associated with mice carrying the Ins2$^{+/akita}$ mutation are a result of deficiencies in functional insulin rather than hyperglycemia. To determine if lowering glucose levels would normalize adhesion protein expression, mice were treated with the SGLT2 inhibitor empagliflozin for 2 weeks. Treatments with empagliflozin significantly reduced fasting blood glucose in ApoE$^{+/-}$Ins2$^{+/akita}$ mice (55% reduction in blood glucose levels compared to age matched drinking water control ApoE$^{+/-}$Ins2$^{+/akita}$ mice, $P<0.00005$) and significantly increased urinary glucose output in both the ApoE$^{+/-}$ and ApoE$^{+/-}$Ins2$^{+/akita}$ mice, compared to controls (Table 3.4).

To determine the impact of empagliflozin on endothelial activation, P-selectin, E-selectin, ICAM-1, and VCAM-1 expression was assessed in the aortic sinus, as previously described[29]. As observed above, hyperglycemic ApoE$^{+/-}$Ins2$^{+/akita}$ mice showed elevated expression of P-selectin, E-selectin, and VCAM-1 aortic sinus, relative to controls (Figure 3.7). P-selectin, E-selectin and VCAM-1 expression was significantly lower in ApoE$^{+/-}$Ins2$^{+/akita}$ mice treated with empagliflozin. There was no significant difference seen in ICAM-1 in empagliflozin treated ApoE$^{+/-}$Ins2$^{+/akita}$, compared to untreated ApoE$^{+/-}$Ins2$^{+/akita}$ mice. Blood glucose reduction with empagliflozin also significantly reduced monocyte infiltration as assessed by CD107b^{+} (Mac-3^{+}) staining (Figure 3.8).

These results are consistent with hyperglycemia, and not hypoinsulinemia, being responsible for the observed modulation of adhesion protein expression/function.

Table 3.4: Metabolic parameters of empagliflozin treated ApoE$^{+/-}$ and ApoE$^{+/-}$Ins2$^{+/akita}$ mice

Genotype	Empagliflozin	Blood glucose before treatment, mM	Blood glucose after treatment, mM	Urine glucose, mM	Plasma triglyceride, mM	Plasma cholesterol, mM	Body weight, g	Liver weight, g	Adipose weight, g
ApoE$^{+/-}$	-	9.78 ±0.71	10.6 ±0.03	15.18 ±1.63	0.31 ±0.01	2.11 ±0.10	21.36 ±3.18	1.32 ±0.13	0.23 ±0.04
	+	10.64 ±0.74	7.68 ±0.40	799.85 ±40.39 ****/‡‡	0.32 ±0.03	2.41 ±0.26	20.9 ±0.38	1.03 ±0.07	0.17 ±0.02
ApoE$^{+/-}$ Ins2$^{+/akita}$	-	23.82 ±1.32 ****/††††	26.26 ±1.22 ****/††††	490.21 ±100.54 **	0.43 ±0.41	1.95 ±0.04	20.70 ±0.19	1.35 ± 0.05	0.13 ±0.01
	+	18.41 ±1.83 **/††	11.93 ±1.09 †/‡‡‡‡	674.42 ±37.57 ****/‡	0.34 ±0.03	1.70 ±0.34	21.37 ±0.48	1.11 ± 0.15	0.12 ±0.02

**P<0.005 and ****P<0.00005 compared to ApoE$^{+/-}$ regular drinking water,

†P<0.05, ††P<0.005, ††††<0.00005 compared to ApoE $^{+/-}$ Empagliflozin,

‡ P<0.05, ‡‡ P<0.005 ‡‡‡‡P<0.00005 compared to ApoE $^{+/-}$ Ins2$^{+/akita}$ regular drinking water,

n=5

Figure 3.7: **The effects of SGLT2 inhibitor, empagliflozin, on endothelial activation in ApoE$^{+/-}$ and ApoE$^{+/-}$Ins2$^{+/akita}$ mice.** Five week-old ApoE$^{+/-}$ and ApoE$^{+/-}$Ins2$^{+/akita}$ mice were given regular drinking water or water supplemented with 35mg/kg body weight empagliflozin for 2 weeks. All mice were sacrificed at 7 weeks of age and tissues were analyzed. **A** Representative images of cross sections of aortic sinus from 7 week-old ApoE$^{+/-}$ and ApoE$^{+/-}$Ins2$^{+/akita}$ control and empagliflozin treated mice immunostained with antibodies against P-selectin, E-selectin, VCAM-1, or ICAM-1. White and red boxes indicate more highly magnified sections of the image. **B** Quantification of percentage of the endothelium stained for P-selectin, E-selectin, VCAM-1 and VCAM-1, as indicated. n=5 (**A-B**), *P<0.05, ***P<0.0005 and ****P<0.00005. Scale bar equals 100µm (**A**, main images); 50 µm (**A**, boxed areas).

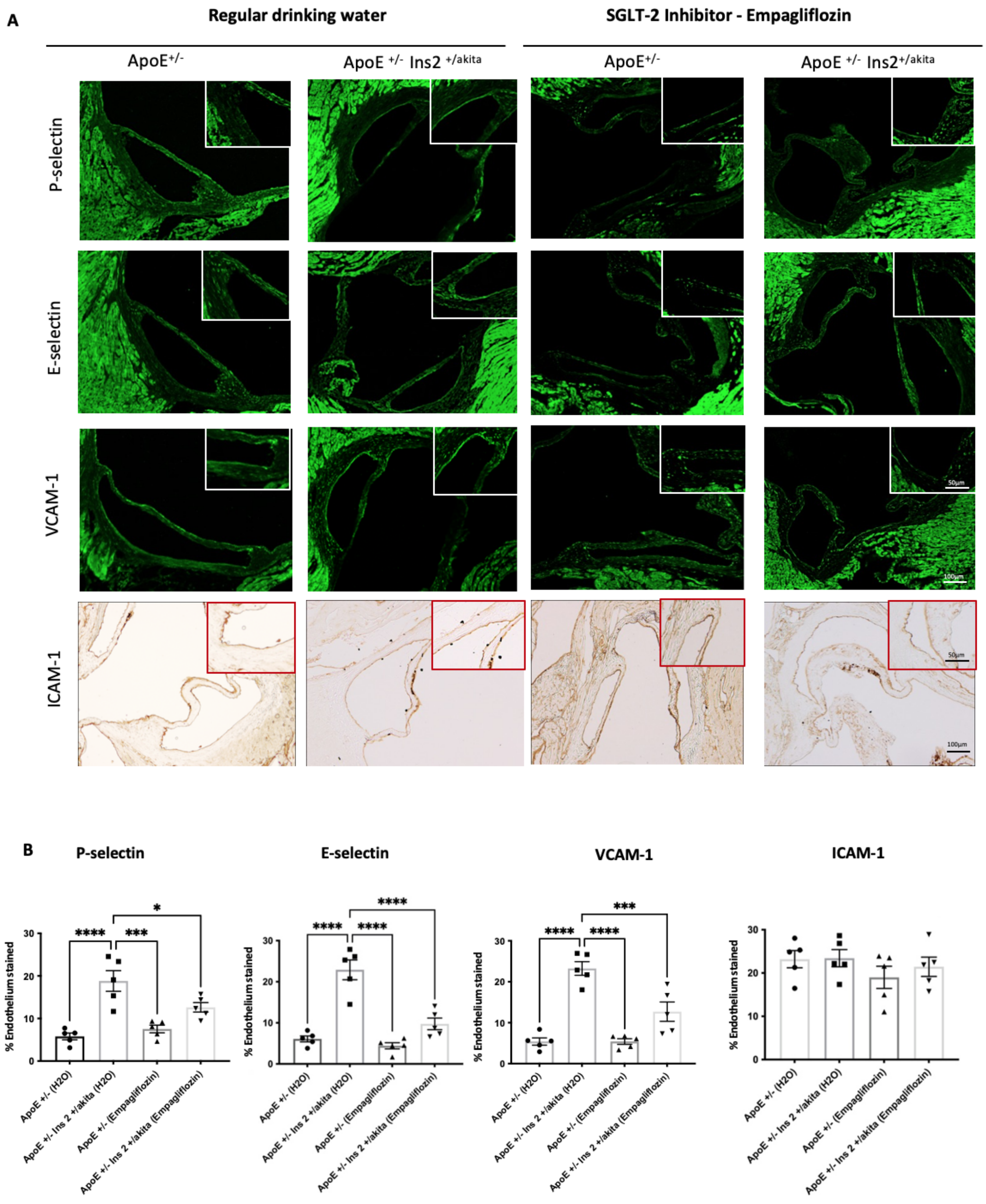
A
Regular drinking water
SGLT-2 Inhibitor - Empagliflozin
ApoE+/-
ApoE +/- Ins2 +/akita
ApoE+/-
ApoE +/- Ins2+/akita
P-selectin
E-selectin
VCAM-1
ICAM-1
50µm
100µm
50µm
100µm
B
P-selectin
E-selectin
VCAM-1
ICAM-1
% Endothelium stained
0
10
20
30
****
***
*
****
****
****
****
****
***
ApoE +/- (H2O)
ApoE +/- Ins 2 +/akita (H2O)
ApoE +/- (Empagliflozin)
ApoE +/- Ins 2 +/akita (Empagliflozin)

Figure 3.8: Endothelial monocyte/macrophage recruitment in empagliflozin treated mice. A Representative images of cross sections of aortic sinus from 7 week-old ApoE$^{+/-}$ and ApoE$^{+/-}$Ins2$^{+/akita}$ mice treated with empagliflozin (35mg/kg body weight) and immunostained with an antibody against CD107b^{+}/Mac3. Scale bar equals 100µm. **B** Quantification of CD107b^{+}/Mac3 positive immunostained area. n=5 (**A-B**), **** P<0.00005.

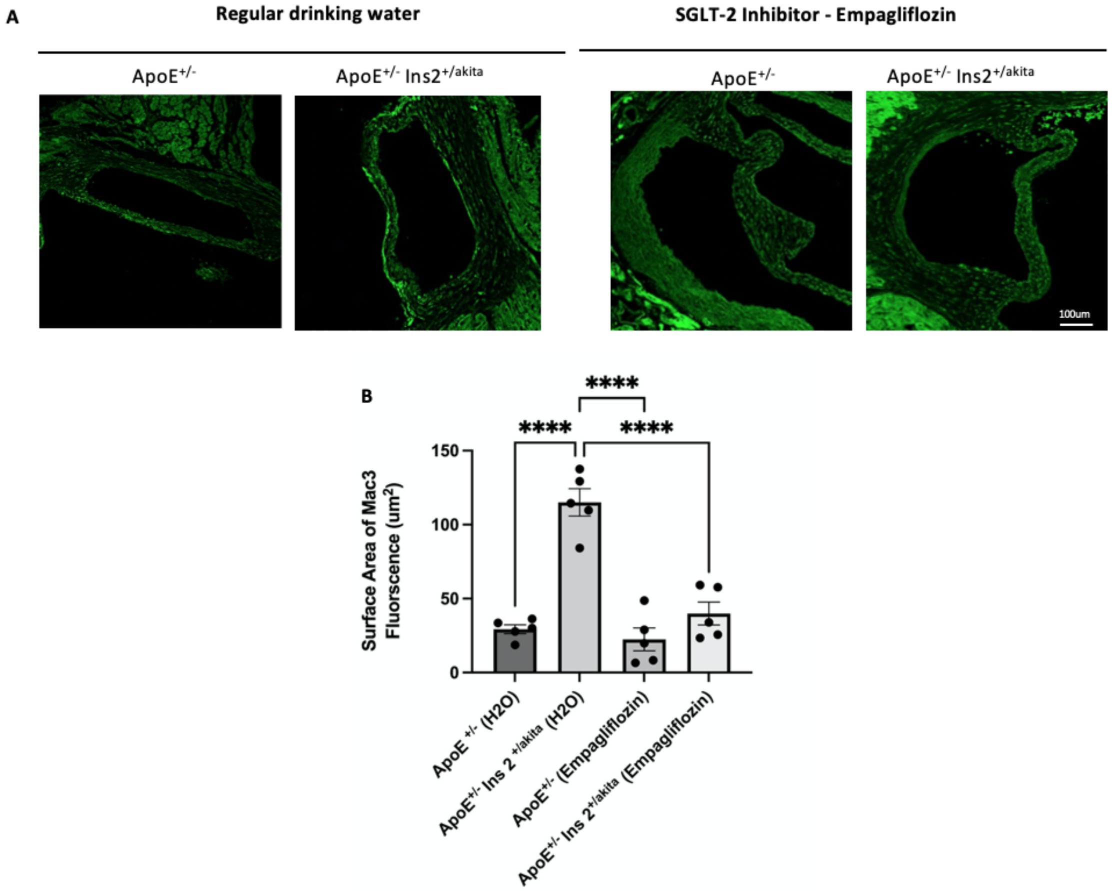
A
Regular drinking water
SGLT-2 Inhibitor - Empagliflozin
ApoE+/-
ApoE+/- Ins2+/akita
ApoE+/-
ApoE+/- Ins2+/akita
100um
B
****
****
****
Surface Area of Mac3 Fluorscence (um2)
150
100
50
0
ApoE +/- (H2O)
ApoE+/- Ins 2 +/akita (H2O)
ApoE+/- (Empagliflozin)
ApoE+/- Ins 2+/akita (Empagliflozin)

3.6 DISCUSSION

It is well established that individuals with DM have an increased risk of developing atherosclerotic CVD[32], however the molecular mechanisms underlying how DM promotes the pathogenesis of atherosclerosis are not well understood. The process of atherogenesis is believed to initiate at the EC layer when ECs are injured and activated[33]. In this study we directly investigated the effects of elevated glucose levels on endothelial activation both in vitro and in a mouse model of hyperglycemia-accelerated atherogenesis.

In cultured HAECs, we found that exposure to 30mM glucose for 24 hours caused an elevation in the expression of genes encoding P-selectin, E-selectin and VCAM-1. These findings suggest that hyperglycemia instigates EC activation, which could potentially contribute to early initiation and progression of atherosclerosis. ICAM-1 expression was unaffected by elevated glucose concentrations.

The results in HAECs encouraged us to investigate the association of hyperglycemia and atherosclerosis in the $ApoE^{-/-}Ins2^{+/akita}$ mouse model. The introduction of the $Ins2^{+/akita}$ mutation into atherosclerosis-prone $ApoE^{-/-}$ mice causes spontaneous hyperglycemia[34,35,36]. We have previously shown that $ApoE^{-/-}Ins2^{+/akita}$ mice present with larger plaques, compared to age matched $ApoE^{-/-}$ mice[25,26]. We assessed endothelial activation in $ApoE^{-/-}Ins2^{+/akita}$ and

ApoE$^{-/-}$ mice at 5 weeks of age, which corresponds to a time prior to the establishment of detectable atherosclerotic lesions, and at 25 weeks of age, when advanced atherosclerotic plaques can be easily detected/quantified. We found that the expression of P-selectin, E-selectin and VCAM-1 was significantly elevated in the 5 week-old ApoE$^{-/-}$Ins2$^{+/akita}$ mice, compared to age-matched ApoE$^{-/-}$ mice. This result suggests that hyperglycemia promotes endothelial activation of P-selectin, E-selectin and VCAM-1 before atherogenesis initiates. ICAM-1 levels were similar for both mouse models. Interestingly, it has previously been demonstrated that the genetic ablation of ICAM-1 had no effect on atherosclerotic lesion size in a mouse model of atherosclerosis[37]. The functionality of the upregulated adhesion factors was supported by the observation that monocyte recruitment was also elevated in the ApoE$^{-/-}$Ins2$^{+/akita}$ mouse model. Together these findings suggest that hyperglycemia-induced early endothelial activation contributes to the accelerated development of atherosclerotic plaques, which was detectable at 25 weeks of age. By 25 weeks of age, when advanced plaques were established in the aortic sinus, the expression of each of the measured adhesion proteins was similar, in the presence or absence of hyperglycemia.

The previously described experiments were performed in a mouse model that is severely dyslipidaemic. To determine if hyperglycemia was sufficient to induce endothelial activation and atherosclerosis, in the absence of dyslipidemia, we examined mice that were heterozygous for the ApoE gene (ApoE$^{+/-}$ and ApoE$^{+/-}$Ins2$^{+/akita}$). Neither ApoE$^{+/-}$ nor ApoE$^{+/-}$ Ins2$^{+/akita}$ mice developed detectable plaques by 25 weeks of age. However, protein markers of endothelial activation, P-selectin, E-selectin, and VCAM-1, were elevated in the ApoE$^{+/-}$Ins2$^{+/akita}$ at 5 and 25 weeks of age compared to age-matched ApoE$^{+/-}$ mice. This finding suggests that hyperglycemia is sufficient to activate ECs, but not sufficient to promote atherogenesis in the absence of dyslipidemia. ICAM-1 expression was not affected by hyperglycemia but was elevated in both strains at 25 weeks of age, relative to 5 weeks of age. These findings suggest that ICAM-1 expression is regulated independently of the other adhesion proteins. Monocyte recruitment was elevated in 5 week-old ApoE$^{+/-}$Ins2$^{+/akita}$ mice, compared to ApoE$^{+/-}$ mice however, it should be noted that monocyte recruitment was much lower in the ApoE$^{+/-}$Ins2$^{+/akita}$ mice compared to ApoE$^{-/-}$ mice. Thus, dyslipidemia plays a role in monocyte recruitment which likely drives early atherogenesis.

It is possible that the deficiency of functional insulin, in Ins2$^{+/akita}$ mice, could also be a factor in endothelial activation. To examine this possibility, ApoE$^{+/-}$Ins2$^{+/akita}$ mice were treated with the SGLT2 inhibitor, empagliflozin, to determine if lowering blood glucose levels would affect the expression of markers of endothelial activation. Mice treated with empagliflozin presented with significantly reduced blood glucose levels and elevated urine glucose levels, compared to controls. The reduction in blood glucose levels was associated with reduced expression of activation markers P–selectin, E-selectin and VCAM-1 in the empagliflozin treated ApoE$^{+/-}$Ins2$^{+/akita}$ when compared to ApoE$^{+/-}$Ins2$^{+/akita}$ mice given normal drinking water. Additionally, monocyte recruitment was significantly reduced in empagliflozin treated mice. These findings suggest that hypoinsulinemia does not significantly alter adhesion protein expression in the Ins2$^{+/akita}$ mouse model. In addition, it appears that early endothelial activation and monocyte recruitment can be reversed by regulating/normalizing blood glucose levels.

Our overall objective was to determine the effects of hyperglycemia on early endothelial activation and the initiation of atherosclerosis. Our results show that hyperglycemia is sufficient to induce the expression of functional adhesion proteins on the endothelial layer but that this is insufficient to induce atherogenesis in this mouse model. In the context of dyslipidemia, hyperglycemia can activate the endothelium, promote the early initiation of plaque progression, resulting in significantly advanced atherosclerotic plaques, compared to age-matched controls. Together these findings support a causative role of hyperglycemia in the early initiation of atherogenesis and highlight the importance of blood glucose regulation as a strategy to prevent, and perhaps reverse, atherosclerotic CVD.

Acknowledgements

GHW holds the ISTH-McMaster Chair in Thrombosis and Haemostasis Research and is supported by a HSFC Ontario Mid-Career Investigator Award.

3.7 REFERENCES FOR CHAPTER 3

1) Pietropaolo M, Barinas-Mitchell E, Kuller L.H. (2007). The Heterogeneity of Diabetes: Unraveling a Dispute: Is Systemic Inflammation Related to Islet Autoimmunity?. *Diabetes*, 56(5):1189-1197

2) Saeedi P, Petersohn I, Salpea P, Malanda B, Karuranga S, Unwin N, Colagiuri S, Guariguata L, Motala A.A, Ogurtsova K, Shaw J.E, Bright D, Williams R. (2019). Global and regional diabetes prevalence estimates for 2019 and projections for 2030 and 2045: Results from the International Diabetes Federation Diabetes Atlas, 9th edition. *Diabetes Res. Clin. Pract.*, 157:107843

3) Lin X, Xu Y, Pan X, Xu J, Ding Y, Sun X, Song X, Ren Y, Shan P.F. (2020). Global, regional, and national burden and trend of diabetes in 195 countries and territories: an analysis from 1990 to 2025. *Scientific Reports.*, 10(1):14790

4) Mahmood S.S, Levy D, Vasan R.S, Wang T.J. (2014) The Framingham Heart Study and the Epidemiology of Cardiovascular Diseases: A Historical Perspective. *Lancet.*, 383(9921): 999-1108

5) Hudspeth B. (2018). The burden of cardiovascular disease in patients with diabetes. *Am J Manag Care.*, 24(13 Suppl): S268-S272

6) Lehto S, Rönnemaa T, Pyörälä K, Laakso M. (2000). Cardiovascular risk factors clustering with endogenous hyperinsulinemia predict death from coronary heart disease in patients with type II diabetes. *Diabetologia.*, 43(2):148-155

7) Avogaro A, Albiero M, Menegazzo L, de Kreutzenberg S, Fadini GP. (2011). Endothelial Dysfunction in Diabetes: The role of reparatory mechanisms. *Diabetes Care.*, 34(Suppl 2): S285-S290

8) Shah M, Brownlee M. (2016) Molecular and Cellular Mechanisms of Cardiovascular Disorders in Diabetes. *Circ Res.*, 118(11):1808-1829

9) Frostegård J. (2013). Immunity, atherosclerosis and cardiovascular disease. *BMC Med.*, 11:117

10) Willerson J.T, Ridker P.M. (2004). Inflammation as a Cardiovascular Risk Factor. *Circulation*, 109: II-2–II-10

11) Zmysłowski A, Szterk A. (2017). Current knowledge on the mechanism of atherosclerosis and pro-atherosclerotic properties of oxysterols. *Lipids Health Dis.*, 16:188

12) Berliner J.A, Navab M, Fogelman A.M, Frank J.S, Demer L.L, Edwards P.A, Watson A.D, Lusis A.J. (1995). Atherosclerosis: Basic Mechanisms. *Circulation*, 91:2488-2496

13) Aman J, Weijers E.M, van Nieuw Amerongen G.P, Malik A.B, van Hinsbergh V.W.M. (2016). Using cultured endothelial cells to study endothelial barrier dysfunction: Challenges and opportunities. *Am J Physiol Lung Cell Mol Physiol.*, 311(2):L453-L466

14) Mai J, Virtue A, Shen J, Wang H, Yang X-F. (2013) An evolving new paradigm: endothelial cells - conditional innate immune cells. *J Hematol Oncol.*, 6:61

15) Sun H-J, Wu Z-Y, Nie X-W, Bian J-S. (2020). Role of Endothelial Dysfunction in Cardiovascular Diseases: The Link Between Inflammation and Hydrogen Sulfide. *Front. Pharmacol.*, 10:1568

16) Pober J.S, Sessa W.C. (2007) Evolving functions of endothelial cells in inflammation. *Nat Rev Immunol*., 7(10):803-815

17) Bakker W, Eringa E.C, Sipkema P, van Hinsbergh V.W.M. (2009). Endothelial dysfunction and diabetes: roles of hyperglycemia, impaired insulin signaling and obesity. *Cell Tissue Res.*, 335(1):165-189

18) Deanfield J.E, Halcox J.P, Rabelink T.J. (2007). Endothelial Function and Dysfunction. *Circulation*, 115:1285-1295

19) Gimbrone M.A, García-Cardeña G. (2016). Endothelial Cell Dysfunction and the Pathobiology of Atherosclerosis. *Circ Res.*, 118(4):620-636

20) Liao J.K. (2013). Linking endothelial dysfunction with endothelial cell activation. *J Clin Invest.*, 123(2):540-1

21) Hwang S.J, Ballantyne C.M, Sharrett A.R, Smith L.C, Davis C.E, Gotto Jr A.M, Boerwinkle E. (1997). Circulating adhesion Molecules VCAM-1, ICAM-1, and E-selectin in Carotid Atherosclerosis and Incident Coronary Heart Disease Cases: The Atherosclerosis Risk In Communities (ARIC) study. *Circulation.*, 96(12):4219-25

22) Muller W.A. (2002). Leukocyte-Endothelial Cell Interactions in the Inflammatory Response. *Lab. Invest.*, 82:521-534

23) Markin A.M, Sobenin I.A, Grechko A.V, Zhang D, Orekhov A.N. (2020). Cellular Mechanisms of Human Atherogenesis: Focus on Chronification of Inflammation and Mitochondrial Mutations. *Front. Pharmacol.*, 11:642

24) Moore K.J, Sheedy F.J, Fisher E.A. (2013). Macrophages in atherosclerosis: a dynamic balance. *Nat Rev Immunol.*, 13(10):709-721

25) Venegas-Pino D.E, Wang P-W, Stoute H.K, Singh-Pickersgill N.A, Hong B.Y, Khan M.I, Shi Y, Werstuck G.H. (2016). Sex-Specific Differences in an ApoE$^{-/-}$: Ins2$^{+/Akita}$ Mouse Model of Accelerated Atherosclerosis. *Am J Pathol.*, 186(1):67-77

26) Venegas-Pino D.E, Lagrotteria, Wang P-E, Morphet J, Clapdorp C, Shi Y, Werstuck G.H. (2018). Evidence of extensive atherosclerosis, coronary artery disease and myocardial infraction in the ApoE-/-:Ins2+/Akita mouse fed a western diet. *Atherosclerosis*, 275:88-96

27) Hamuro M, Polan J, Natarajan M, Mohan S. (2002). High glucose induced nuclear factor kappa B mediated inhibition of endothelial cell migration. *Atherosclerosis*, 162(2): 277-87

28) Sage A, Holtby-Ottenhof S, Shi Y, Damjanovic S, Sharma A, Werstuck G. (2012). Metabolic syndrome and acute hyperglycemia are associated with

endoplasmic reticulum stress in human mononuclear cells. *Obesity*, 20(4):748-55

29) Pennig J, Scherrer P, Gissler M.C, Anto-Michel N, Hoppe N, Füner L, Härdtner C, Stachon P, Wolf D, Hilgendorf I, Mullick A, Bode C, Zirlik A, Goldberg I.J, Willecke F. (2019). Glucose lowering by SGLT2-inhibitor empagliflozin accelerates atherosclerosis regression in hyperglycemic STZ-diabetic mice. *Scientific Reports.* 9(1):17937

30) Venegas-Pino D.E, Banko N, Khan M.I, Shi Y, Werstuck G.H. (2013). Quantitative analysis and characterization of atherosclerotic lesions in the murine aortic sinus. *J Vis Exp*., 82:50933

31) Mestas J, Ley K. (2008) Monocyte-endothelial cell interactions in the development of atherosclerosis. *Trends Cardiovasc Med*., 18(6):228-32

32) Martín-Timón I, Sevillano-Collantes C, Segura-Galindo A, Del Cañizo-Gómez F.J. (2014). Type 2 diabetes and cardiovascular disease: Have all risk factors the same strength?. *World J Diabetes*., 5(4):444-470

33) Crowther M.A. (2005). Pathogenesis of atherosclerosis. *Hematology Am Soc Hematol Educ Program.*, 436-441

34) Nakashima Y, Plump A.S, Raines E.W, Breslow J.L, Ross R. (1994). ApoE-deficient mice develop lesions of all phases of atherosclerosis throughout the arterial tree. *Atherioscler Thromb.*, 14(1):133-140

35) Jun J.Y, Ma Z, Segar L. (2011). Spontaneously diabetic Ins2(+/Akita):apoE-deficient mice exhibit exaggerated hypercholesterolemia and atherosclerosis. *Am J Physiol Endocrinol Metab.*, 301(1):E145-154

36) Wang J, Takeuchi T, Tanaka S, Kubo S.K, Kayo T, Lu D, Takata K, Koizumi A, Izumi T. (1999). A mutation in the insulin 2 gene induces diabetes with severe pancreatic beta-cell dysfunction in the Mody mouse. *J Clin Invest.*, 103(1):27-37

37) Cybulsky M.I, Iiyama K, Li H, Zhu S, Chen M, Iiyama M, Davis V, Gutierrez-Ramos J.C, Connelly P.W, Milstone D.S. (2001). A major role for VCAM-1, but not ICAM-1, in early atherosclerosis. *J Clin Invest.*, 107(10):1255-62

3.8 SUPPLEMENTARY MATERIAL FOR CHAPTER 3

Supplementary Table 3.1: Hematology profile

Genotype	**White blood cells ($x10^3$/µl)**	**Neutrophils ($x10^3$/µl)**	**Lymphocytes ($x10^3$/µl)**	**Monocytes ($x10^3$/µl)**	**Eosinophils ($x10^3$/µl)**	**Basophils ($x10^3$/µl)**
ApoE$^{-/-}$	2.16 ±0.26	0.68 ±0.10	1.69 ±0.16	0.17 ±0.02	0.03 ±0.01	0.01 ±0.00
ApoE$^{-/-}$ Ins2$^{+/akita}$	2.65 ±0.24	0.64 ±0.13	1.70 ±0.15	0.15 ±0.01	0.03 ±0.00	0.04 ±0.02

n=3-5

Supplementary Table 3.2: Plasma lipid levels

Genotype	**Plasma Triglycerides (mM)**	**Plasma Cholesterol (mM)**
C57BL/6	0.4 ±0.1	2.3 ±0.2
ApoE$^{+/-}$	0.36 ±0.04	2.48 ±0.17
ApoE$^{+/-}$ Ins2$^{+/akita}$	0.58 ±0.08	2.83 ±0.16
ApoE$^{-/-}$	1.10 ±0.13 *	6.44 ±0.60 $^{****/\dagger\dagger\dagger\dagger/\ddagger\ddagger\ddagger\ddagger}$
ApoE$^{-/-}$Ins2$^{+/akita}$	1.46 ±0.12 *	8.15 ±0.34 $^{****/\dagger\dagger\dagger\dagger/\ddagger\ddagger\ddagger\ddagger}$

*P<0.05 and ****P<0.00005 compared to C56BL/6,

††††P<0.00005 compared to ApoE$^{+/-}$,

‡‡‡‡P<0.00005 compared to ApoE$^{+/-}$ Ins2$^{+/akita}$,

n=5

Supplementary Figure 3.1: Negative controls for immunofluorscence and immunohistochemistry staining. A) Pre-immune goat IgG was used in place of the primary antibody. B) Pre-immune mouse IgG was used in place of primary antibody as a negative control for P-selectin staining, pre-immune rat IgG was used as a negative control for Mac-3 staining, and pre-immune rabbit IgG was used as a negative control for both E-selectin and VCAM-1. Scale bar equals 100μm.

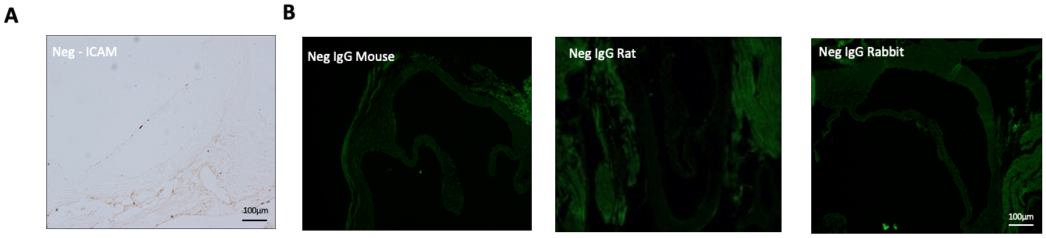
A
Neg - ICAM
100µm
B
Neg IgG Mouse
Neg IgG Rat
Neg IgG Rabbit
100µm

Supplementary Figure 3.2: Analysis of the effects of hyperglycemia on HAEC gene expression of eNOS, iNOS, vWF and PECAM. HAEC cultured in 5mM glucose were exposed to an additional 25mM glucose or 25mM mannitol for 24 hours. The expression of eNOS, iNOS, vWF and PECAM was quantified by reverse transcription-polymerase chain reaction (RT-PCR) and normalized to β-actin expression. n= 4-6, *P<0.05.

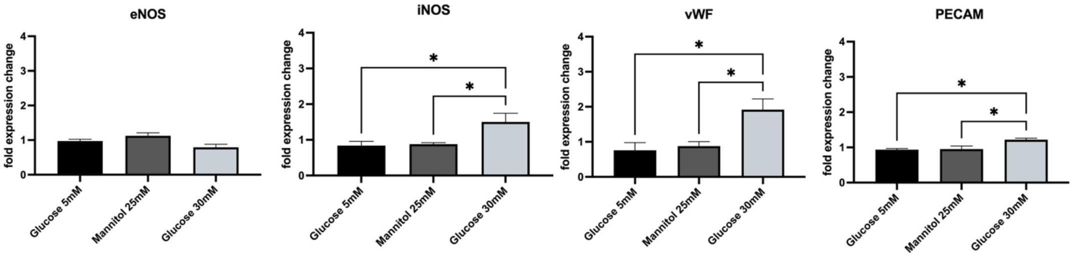
eNOS
iNOS
vWF
PECAM
fold expression change
0
1
2
3
4
*
*
Glucose 5mM
Mannitol 25mM
Glucose 30mM

Supplementary Figure 3.3: Atherosclerotic progression in ApoE$^{+/-}$ and ApoE$^{+/-}$Ins2$^{+/akita}$ mice. Representative images of cross sections of aortic sinus stained with Masson's trichrome from 5 and 25 week-old ApoE$^{+/-}$ and ApoE$^{+/-}$Ins2$^{+/akita}$ mice. No plaques are visible. Scale bar equals 500µm. n=5.

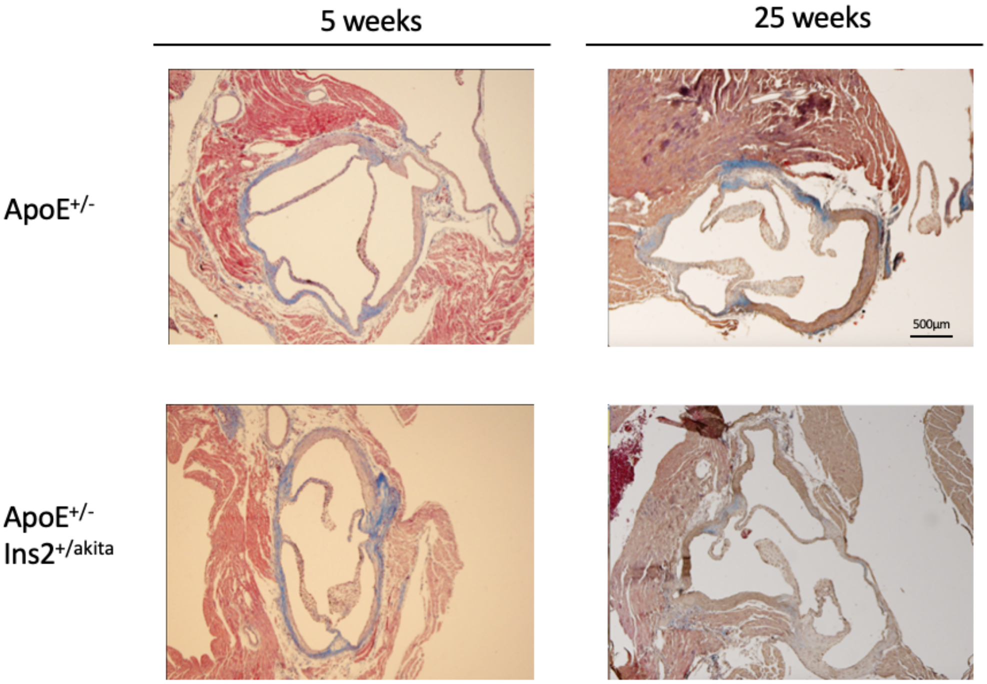
5 weeks
25 weeks
ApoE+/-
ApoE+/-
Ins2+/akita
500µm

CHAPTER 4: Investigating the effects of elevated glucose concentration on human aortic endothelial cell activation

Lauren Mastrogiacomo[1,2], Christian Jacobsen-Perez[1] and Geoff Werstuck[1,2]

[1]Thrombosis and Atherosclerosis Research Institute, Hamilton, ON, Canada.

[2]Department of Medicine, McMaster University, Hamilton, ON, Canada.

4.1 FOREWORD

This study investigates the effects of elevated glucose concentration on endothelial cell (EC) activation. Results suggest that elevated glucose concentrations cause EC activation and expression of adhesion proteins. When endoplasmic reticulum (ER) stress or glycogen synthase kinase (GSK)3α/β is inhibited, there is a reduction in adhesion protein expression. Monocyte attachment was increased in elevated glucose concentrations and decreased with the inhibition of ER stress and GSK3α/β. Data suggests a role of ER stress-GSK3α/β in glucose induced EC activation.

The experiments in this study were conducted by Lauren Mastrogiacomo with assistance from Christian Jacobsen-Perez. The manuscript was written by Lauren Mastrogiacomo in collaboration with Dr. Geoff Werstuck. This manuscript is in preparation for submission.

4.2 ABSTRACT

Diabetes is a risk factor for the development of cardiovascular disease (CVD). The major underlying cause of CVD is atherosclerosis. An understanding of the mechanism that links risk factors to accelerated development of atherosclerosis will help identify potential therapeutic targets. EC activation is an early predictor of atherogenesis and atherosclerosis initiation. Adhesion proteins are present on activated ECs and allow the recruitment of circulating monocytes to bind and migrate to the subendothelial layer, initiating plaque production. Hyperglycemia has been seen to accelerate plaque production in atherosclerotic mouse models, therefore we hypothesize that elevated glucose levels cause early EC activation and therefore early initiation of atherosclerosis. Results from this study show that human aortic endothelial cells (HAECs) cultured in elevated glucose concentrations have increased expression of adhesion proteins (P-selectin, E-selectin, and VCAM-1), and increased THP-1 cell binding. HAEC cultured in elevated glucose and 4-phenylbutyric acid (4-PBA), an ER stress attenuator, or tideglusib, an GSK3α/β inhibitor, reduce adhesion protein expression and THP-1 cell binding. Overall results from this study support that elevated glucose concentrations cause EC activation through the ER stress-GSK3α/β pathway.

4.3 INTRODUCTION

Despite significant advances in our understanding of the pathogenesis of CVDs, as well as the development of effective drug treatments, CVDs remain a leading cause of death worldwide[1,2]. Risk factors for the development of CVD include hypertension, dyslipidemia, obesity, and diabetes[3], however the molecular mechanisms that link these risk factors to the accelerated development of CVD are not well understood. Delineation of these pathways will lead to the identification of specific molecular targets that may provide better therapeutic options in the future.

A major underlying cause of CVD is atherosclerosis[4]. Atherosclerosis involves the accumulation of lipids and inflammatory cells within the walls of medium to large arteries leading to the restriction of blood flow[5]. Atherosclerotic plaques can rupture and trigger the formation of a thrombus, which can lead to further complications such as myocardial infarction or stroke[4,5,6].

Endothelial activation is an early stage in the pathogenesis of atherosclerosis[7,8,9,10]. ECs line the vasculature and form a single layer of semi-permeable cells[11,12]. They contribute to vascular homeostasis via regulation of vascular tone, permeability and vessel wall inflammation[12,13]. EC activation results in the presentation of cell surface adhesion proteins, including P-selectin, E-selectin, intercellular adhesion molecule (ICAM)-1 and VCAM-1[14], the release of chemokines and cytokines, and altered vascular permeability[14,15]. The presence of the adhesion proteins facilitates the attachment and infiltration of circulating monocytes to the subendothelial layer, where they differentiate into macrophages[14]. Macrophages efferocytose modified lipoprotein particles and cellular debris, becoming lipid engorged foams cells that form a fatty streak in the artery wall[16]. The continued accumulation and growth of foam cell/macrophages results in enlarged, advanced atherosclerotic plaques.

Previous studies from our lab and others have shown that CVD risk factors, including diabetes, can induce endoplasmic reticulum (ER) stress in the cells of the vascular wall[17]. The ER is involved in cellular homeostasis and survival, and specifically functions to facilitate protein folding and lipid biosynthesis[17,18]. The accumulation of misfolded proteins, and/or an increase in protein synthesis, can disrupt ER homeostasis and trigger ER stress[17,18]. ER stress activates the unfolded protein response (UPR), which helps return the cell to homeostasis[17,18]. Chronic activation of ER stress can lead to the activation of apoptotic pathways[17,18].

Hyperglycemia-induced ER stress signalling through GSK3α/β in lesional macrophages is an important pathway driving atherogenesis, and inhibition of GSK3α/β has been associated with attenuated atherogenesis and atherosclerotic regression[19,20]. It has been suggested that elevated glucose levels can induce ER stress pathways, resulting in endothelial activation and therefore the initiation of plaque development[21,22,23]. To date, very little is known about the potential role of ER stress-GSK3α/β signalling in ECs, as it pertains to the development and progression of atherosclerosis.

We hypothesize that hyperglycemia causes early EC activation through induction of the ER stress-GSK3α/β pathway. To test this hypothesis, cell culture systems and small molecule strategies to impair ER stress-GSK3α/β signalling are utilized in this study. Understanding the molecular mechanism of how hyperglycemia causes EC activation will help uncover potential therapeutic targets to limit the cardiovascular risk of diabetes.

4.4 MATERIAL AND METHODS

Cell lines and drug treatment

Human aortic endothelial cells

HAEC (ATCC, Manassas, VA) were cultured in Endothelial Cell Growth Medium-2 Bulletkit (Lonza, Basel, Switzerland) supplemented with 1% penicillin-streptomycin in culture flasks at 37°C in 5% CO_2. Cells were grown to confluency and then split into a 12 well plate at a seeding density of $5x10^5$ cells/well. Experiments were performed on cells at passage 4-10. Cells were cultured in regular media (containing 5mM glucose), high mannitol (media containing 5mM glucose + 25mM mannitol), high glucose (media containing 5mM glucose + additional 25mM glucose - totalling 30mM glucose) for 24 hours. Subsets of cells were treated with 3mM 4-phenylbutyric acid (4-PBA) (Sigma-Aldrich, St-Louis, MO), 25μM tideglusib (MedChemExpress, Monmouth Junction, NJ), or 10 ng/mL tumour necrosis factor alpha (TNFα)(Sigma-Aldrich, St-Louis, MO) for 24 hours.

THP-1 Cells

THP-1 cells are a human monocytic cell line derived from an acute monocytic leukemia patient[24]. THP-1 cells were cultured in RPMI-1640 Medium (ATCC modification) (Thermo Fisher Scientific, Waltham, MA). Cells were grown in an untreated cell culture flask to a density of $1x10^6$ cells/mL. Experiments were performed on cells at passage 5-10.

Analysis of gene expression

HAECs were harvested in TRIzol (Thermo Fisher Scientific, Waltham, MA) and total RNA was isolated using the TRIzol RNA isolation method. RNA was quantified using a Nanodrop spectrophotometer (Thermo Fisher Scientific, Waltham, MA). cDNA was synthesized using the High-Capacity cDNA Reverse Transcription Kit (Thermo Fisher Scientific, Waltham, MA). Gene expression was analysed using SYBR Green with ROX (Thermo Fisher Scientific, Waltham, MA) and the StepOnePlus Real-Time PCR System (RT-PCR) (Thermo Fisher Scientific, Waltham, MA) (see Table 4.1 for primers). Samples were analysed in technical triplicates and the comparative cycle threshold (Ct) method was used to determine gene expression. Expression levels were normalised to a β-actin internal control.

Table 4.1: Primer sequences

	Primer Sequence
Human P-selectin	F: 5’- TGAGCACTGCTTGAAGAAAAAGC -3’ R: 5’- CACGTATTCACATTCTGGCCC -3’
Human E-selectin	F: 5’- AGAGGTTCCTTCCTGCCAAG -3’ R: 5’- CAGAGCCATTGAGGGTCCAT-3’
Human VCAM-1	F: 5’- CCCTTGACCGGCTGGAGATT –3’ R: 5’- CTGGGGGCAACATTGACATAAAGTG -3’
Human ICAM-1	F: 5’- GCAGACAGTGACCATCTACAGCTT -3’ R: 5’- CTTCTGAGACCTCTGGCTTCGT – 3’
Human eNOS	F: 5′- TGG ACC TGG ATA CCC GGA C-3′ R: 5′- TGG TGA CTT TGG CTA GCT GGT 3′
Human iNOS	F: 5′- GTT TCT GGC AGC AGC GGC TC-3′ R: 5′- GCT CCT CGC TCA AGT TCA GC-3′
Human vWF	F: 5’- TAA GAG GGC AAC ACA AAC G – 3’ R: 5’- ATC TTC ACC TGC CCA CTC C – 3’
Human PECAM	F: 5’- CCA GTG TCC CCA GAA GCA AA – 3’ R: 5’- TGA TAA CCA CTG CAA TAA GTC CTT TC– 3’
Human β-actin	F: 5’ - ACC GAG CGC GGC TAC AG – 3’ R: 5’ - CTT AAT GTG ACG CAC GAT TTC – 3’

F – forward primer, R- reverse primer

Monocyte cell attachment assay

HAEC were cultured in a 24 well plate at a seeding density of 8x10^4 cells/well. Once attached HAEC were subjected to various glucose concentrations and treatments, as described above. To assess THP-1 cell attachment, THP-1 cells were stained with calcein AM (1:1000 dilution, Thermo Fisher Scientific, Waltham, MA) for 1 hour at 37°C in 5% CO_2. Calcein-labelled THP-1 cells (1x10^4 cells/well) were added to the cultured HAEC in a 24 well plate and incubated for 30 minutes at 37°C on a rocker platform. After the 30-minute incubation, unattached THP-1 cells were removed and HAEC were rinsed with PBS. Nine images were taken per well and THP-1 attachment was quantified using Image J software (Version1.15j8, https://imagej.nih.gov/ij/index.html). Calcein-labelled THP-1 attachment in the absence of HAEC was used as a negative control. After the experiment, trypsin was used to remove the cells and they were counted using a cell counter (Invitrogen, Waltham, MA).

GSK3α/β expression

HAECs were collected in lysis buffer (4xSDS PAGE sample buffer). Total protein extracts were separated by SDS-PAGE. Proteins were transferred to a polyvinylidene difluoride membrane (Bio-Rad, Hercules, CA) and blocked with 5% non-fat milk in TBST (10mM Tris, pH 8.0, 150mM NaCl, 0.5% Tween 20) for 45 minutes. The membrane was probed with primary antibodies against GSK3α/β (1:1000 dilution (Cell signalling, Danvers, MA)) or β-actin (1:3000 dilution (Sigma Aldrich, St. Louis, MO)) overnight at 4°C. The membrane was washed and incubated for 1 hour with horseradish peroxidase-conjugated anti-rabbit (1:200, Agilent (DAKO), Santa Clara, CA) or anti-mouse (1:200, Agilent (DAKO), Santa Clara, CA) antibody. Blots were washed with TBST and developed with the enhanced chemiluminescence system (ECL) (Millipore, Burlington, MA). Images were captured using a Molecular imager ChemiDoc XRS+ (Bio-Rad, Hercules, CA).

Statistical analysis

Statistical analysis was performed using Graph Pad Prism 9 and expressed as +/- SEM. Mean values were compared using one or two-way ANOVA test followed by Tukey's multiple comparisons test. Each experiment included 3-8 replicates for each condition. For all experiments, a P value of <0.05 was considered to be statically significant. *$P<0.05$, **$P<0.005$, ***$P<0.0005$, ****$P<0.00005$.

4.5 RESULTS

Adhesion protein expression is induced in HAEC exposed to elevated glucose concentrations

To assess the effects of elevated glucose concentration on ECs, HAEC were cultured for 24 hours in control media containing 5mM glucose, high mannitol (control media + 25mM mannitol) or high glucose (control media +

25mM glucose - totalling 30mM glucose). Mannitol treatments were included to control for the potential effects of osmotic stress. The expression levels of adhesion proteins were determined using RT-PCR analysis. Expression levels were normalised to a β-actin control. The expression of P-selectin, E-selectin and VCAM-1 were significantly increased in HAECs exposed to high glucose (30mM glucose), compared to control media (5mM glucose) or mannitol (5mM glucose + 25mM mannitol) controls (Figure 4.1). ICAM-1 expression remained unchanged between experimental groups. The addition of mannitol did not significantly alter expression of any of the factors examined. These results suggest that hyperglycemia may play a direct role in endothelial activation and early initiation of monocyte recruitment.

Figure 4.1: Effects of elevated glucose concentration on HAEC. HAEC were treated with control media (5mM glucose), mannitol (control +25mM mannitol) and high glucose (control media +25mM glucose) and gene expression of adhesion proteins was assessed using RT-PCR analysis. Expression levels were normalised to a β-actin control. n=4-6 **P<0.005 and ***P<0.0005. ns=not significant.

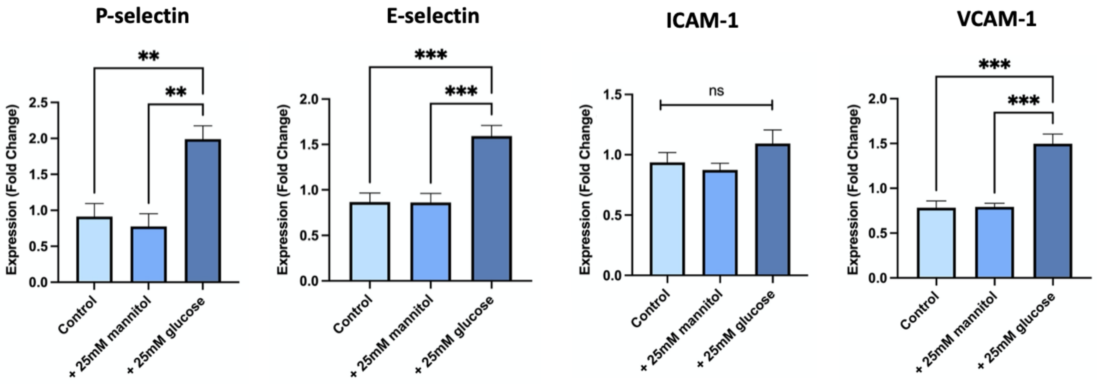
P-selectin
**
**
Expression (Fold Change)
0.0
0.5
1.0
1.5
2.0
2.5
Control
+ 25mM mannitol
+ 25mM glucose
E-selectin
***
***
Expression (Fold Change)
0.0
0.5
1.0
1.5
2.0
Control
+ 25mM mannitol
+ 25mM glucose
ICAM-1
ns
Expression (Fold Change)
0.0
0.5
1.0
1.5
Control
+ 25mM mannitol
+ 25mM glucose
VCAM-1
***
***
Expression (Fold Change)
0.0
0.5
1.0
1.5
2.0
Control
+ 25mM mannitol
+ 25mM glucose

4-PBA reduces adhesion protein expression

Previous research has suggested that CVD risk factors, including hyperglycemia, may promote atherogenesis by a mechanism involving ER stress[17,21,22,22]. In order to determine if ER stress is involved in glucose-induced endothelial activation, 4-PBA, a known attenuator of ER stress[25], was added to HAEC exposed to normal and high glucose concentrations. Gene expression was then analysed by RT-PCR and normalised to a β-actin control. To ensure that the 4-PBA treatment was sufficient to reduce ER stress in HAEC, the expression of two ER stress response genes, calreticulin and glucose regulated protein (GRP78), was assessed (Supplementary Figure 4.1). Elevated glucose concentration (30mM glucose) induced ER stress, as indicated by significantly enhanced expression of both calreticulin and GRP78, compared to HAEC exposed to control media (5mM glucose) or mannitol (5mM glucose + 25mM mannitol). Treatment of the cells with 4-PBA resulted in reduced calreticulin and GRP78 expression, suggesting that 3mM 4-PBA was sufficient to attenuate ER stress in HAEC.

As previously observed, elevated glucose levels significantly increase P-selectin, E-selectin and VCAM-1, but not ICAM-1, gene expression in HAEC (Figure 4.2). The addition of 4-PBA to HAEC cultured in control media (5mM glucose) had no significant effect on adhesion marker expression. Addition of 4-PBA to HAECs exposed to high glucose concentrations (30mM glucose) resulted in a significant reduction in the expression of E-selectin, ICAM-1 and VCAM-1 (Figure 4.2). Interestingly, the addition of 4-PBA further enhanced P-selectin expression in cells cultured in both control and high glucose media. This suggests that ER stress pathways may be involved in endothelial activation and that attenuating endothelial ER stress can reduce some endothelial activation markers (E-selectin, ICAM-1 and VCAM-1).

Figure 4.2: Effects of 4-PBA on glucose induced HAEC activation. HAEC were cultured in control media (5mM glucose), mannitol (control media +25mM mannitol), high glucose (control media +25mM glucose) in the presence or absence of 3mM 4-PBA. Gene expression of adhesion proteins was assessed by RT-PCR analysis. Gene expression was normalised to a β-actin control. n=3-6 $^*P<0.05$, $^{**}P<0.005$, $^{***}P<0.0005$.

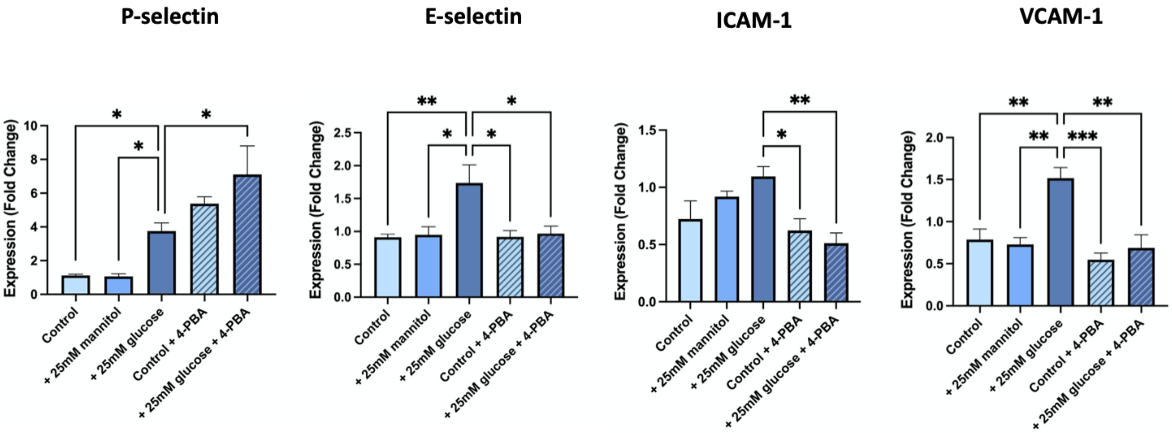
P-selectin
E-selectin
ICAM-1
VCAM-1
Expression (Fold Change)
0
2
4
6
8
10
0.0
0.5
1.0
1.5
2.0
2.5
*
**
***
Control
+ 25mM mannitol
+ 25mM glucose
Control + 4-PBA
+ 25mM glucose + 4-PBA

Tideglusib reduces the expression of adhesion proteins

Previous research from our lab and others have suggested that ER stress signals through GSK3α/β to promote atherogensis[26,27,28]. Very little is known about the function of GSK3α/β in ECs, however, both kinases are expressed in HAECs (Supplementary Figure 4.2). In order to assess the potential role of endothelial GSK3α/β signalling in adhesion protein expression, tideglusib, a GSK3α/β inhibitor[29], was added to cultured HAEC. The effect on adhesion protein expression was analysed using RT-PCR and normalised to a β-actin control.

Tideglusib (25μM) had no significant effect on the expression of ER stress markers, calreticulin and GRP78, in cells cultured in control or high glucose media, suggesting that GSK3α/β lies downstream of the adaptive ER stress response (Supplementary Figure 4.1). The addition of tideglusib to HAEC cultured in control media (5mM glucose) did not affect P-selectin, E-selectin, or VCAM-1 expression levels, but interestingly resulted in a decrease in ICAM-1 expression (Figure 3). The addition of tideglusib to HAEC cultured in high glucose (30mM glucose) resulted in a significant decrease in adhesion protein expression for all adhesion markers (P-selectin, E-selectin, ICAM-1 and VCAM-1) compared to HAEC exposed to high glucose levels (30mM glucose) (Figure 4.3). Together, these data suggest that ER stress signalling through GSK3α/β does play a role in glucose-induced endothelial activation and that this pathway could contribute to accelerated atherogenesis observed in hyperglycemic conditions.

Figure 4.3: Effects of tideglusib on glucose induced HAEC activation. HAEC were treated with control media (+5mM media), mannitol (control media +25mM mannitol), high glucose (control media +25mM glucose) in the presence or absence of tideglusib (25µM). RT-PCR analysis determined gene expression levels. Expression levels were normalised to a β-actin control. n=3-6 $^{*}P<0.05$, $^{**}P<0.005$, $^{***}P<0.0005$, $^{****}P<0.00005$.

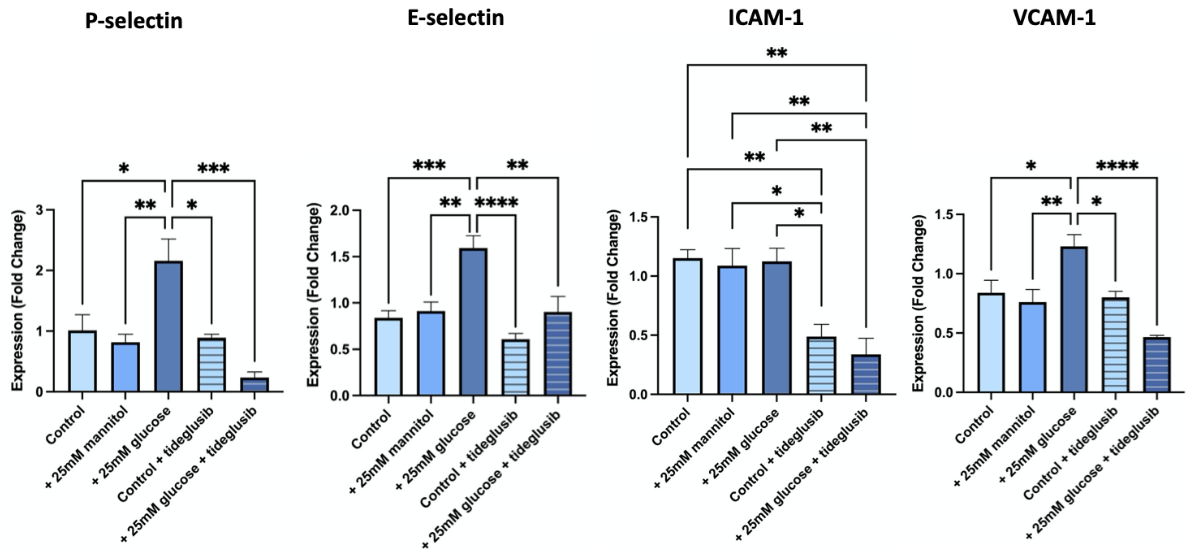
P-selectin
E-selectin
ICAM-1
VCAM-1
Expression (Fold Change)
0
1
2
3
0.0
0.5
1.0
1.5
2.0
Control
+ 25mM mannitol
+ 25mM glucose
Control + tideglusib
+ 25mM glucose + tideglusib
*
**
***
****

The effect of elevated glucose concentration and the role of ER stress-GSK3α/β signalling on other markers of endothelial activation

Endothelial activation has been associated with the induced expression of other factors, including eNOS, iNOS, vWF and PECAM-1[30,31,32,33]. In order to determine the effects of elevated glucose concentration and the role of ER stress-GSK3α/β signalling on these factors, gene expression of these markers was assessed in HAEC cultured in control or high glucose conditions (Figure 4.4). iNOS, vWF and PECAM-1 expression was significantly elevated in HAEC exposed to high glucose (30mM glucose) compared to HAEC cultured in control media (5mM glucose) or high mannitol (5mM glucose + 25mM mannitol). The addition of 4-PBA (3mM) to HAEC significantly reduced gene expression of each of these factors and the addition of tideglusib (25μM) reduced expression of iNOS and PECAM-1 (Figure 4.4). eNOS gene expression was not significantly altered between experimental groups involving any of the treatments (Figure 4.4).

Figure 4.4: eNOS, iNOS, vWF and PECAM-1 expression in HAEC. HAEC were treated with control media (5mM glucose), high mannitol (control media +25mM mannitol), high glucose (control media +25mM glucose), in the presence of absence of 25μM tideglusib or 3mM 4-PBA and gene expression of markers were evaluated using RT-PCR analysis. All results were normalised to a β-actin control. n=3-7. *P<0.05, **P<0.005, ***P<0.0005, ****P<0.00005. ns=not significant.

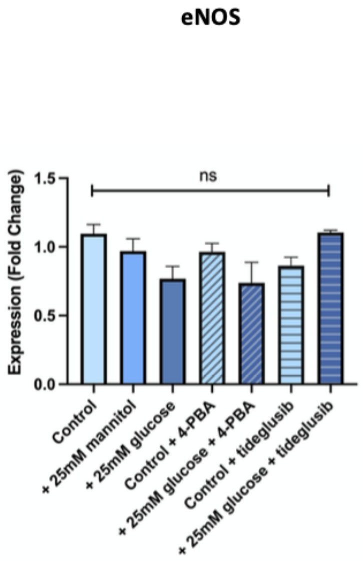
eNOS
ns
Expression (Fold Change)
1.5
1.0
0.5
0.0
Control
+ 25mM mannitol
+ 25mM glucose
Control + 4-PBA
+ 25mM glucose + 4-PBA
Control + tideglusib
+ 25mM glucose + tideglusib

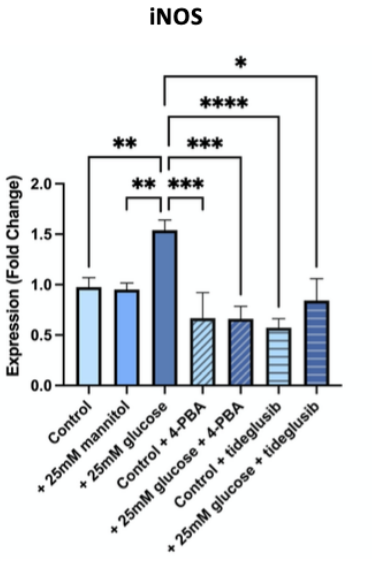
iNOS
*
****
**
***
**
***
Expression (Fold Change)
2.0
1.5
1.0
0.5
0.0
Control
+ 25mM mannitol
+ 25mM glucose
Control + 4-PBA
+ 25mM glucose + 4-PBA
Control + tideglusib
+ 25mM glucose + tideglusib

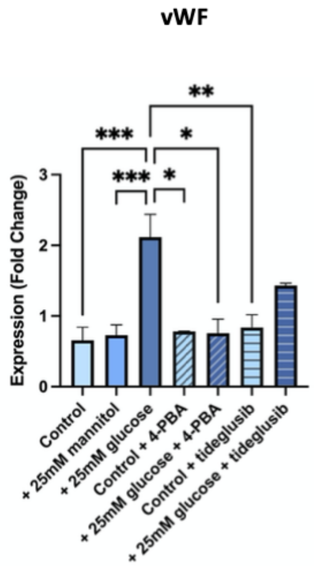
vWF
**
***
*
***
*
Expression (Fold Change)
3
2
1
0
Control
+ 25mM mannitol
+ 25mM glucose
Control + 4-PBA
+ 25mM glucose + 4-PBA
Control + tideglusib
+ 25mM glucose + tideglusib

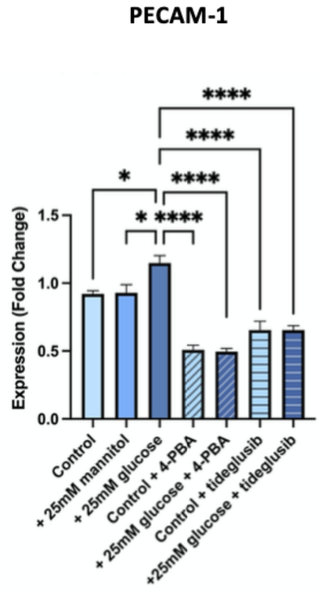
PECAM-1
****
****
*
****
*
****
Expression (Fold Change)
1.5
1.0
0.5
0.0
Control
+ 25mM mannitol
+ 25mM glucose
Control + 4-PBA
+ 25mM glucose + 4-PBA
Control + tideglusib
+25mM glucose + tideglusib

ECs exposed to elevated glucose concentrations have increased monocyte adhesion

To assess the functionality of the upregulated adhesion proteins, and their ability to bind to monocytes, a THP-1 cell attachment assay was performed. HAEC, cultured in control or elevated glucose concentrations, were treated with 4-PBA or tideglusib for 24 hours, as described above. Cells were washed and placed in control media (5mM glucose). TNFα has been shown to promote endothelial activation and the presentation of adhesion proteins, thus facilitating monocyte recruitment[34,35,36]. Therefore TNFα was used as a positive control in this experiment. Calcein-labelled THP-1 monocytes were added to all wells and the cells were placed on a rocker platform for 30 minutes. There was a significant increase in monocyte attachment to HAEC exposed to high glucose (30mM glucose) or TNFα (5mM glucose + 10ng/ml TNFα), compared to HAEC cultured in control media (5mM glucose) or high mannitol (5mM glucose + 25mM mannitol) (Figure 4.5). This finding suggests that the enhanced adhesion protein expression, observed under hyperglycemic conditions, results in the presentation of functional adhesion proteins on the surface of HAECs. The addition of tideglusib (25μM) or 4-PBA (3mM) to HAEC cultured in high glucose (total 30mM glucose), significantly reduced monocyte attachment (Figure 4.5). These findings are consistent with our observation that impaired ER stress-GSK3α/β signalling results in reduced adhesion protein expression in HAEC (Figure 4.2 and Figure 4.3).

Figure 4.5: THP-1 cell attachment assay. HAEC were treated for 24 hours in control media (5mM glucose), high mannitol (control media +25mM mannitol), high glucose (control media +25mM glucose), TNFα (control media +10ng/ml TNFα), in the presence or absence of 25μM tideglusib or 3mM 4-PBA. Calcein-labelled THP-1 cells were added to HAEC treated under different conditions for 30 minutes at 37˚C. Fluorescently labelled THP-1 cells were quantified. **A** Representative images of THP-1 cell attachment under varying conditions. **B** Number of THP-1 cells attached to HAEC. n=4-8. ***P<0.0005, ****P<0.00005.

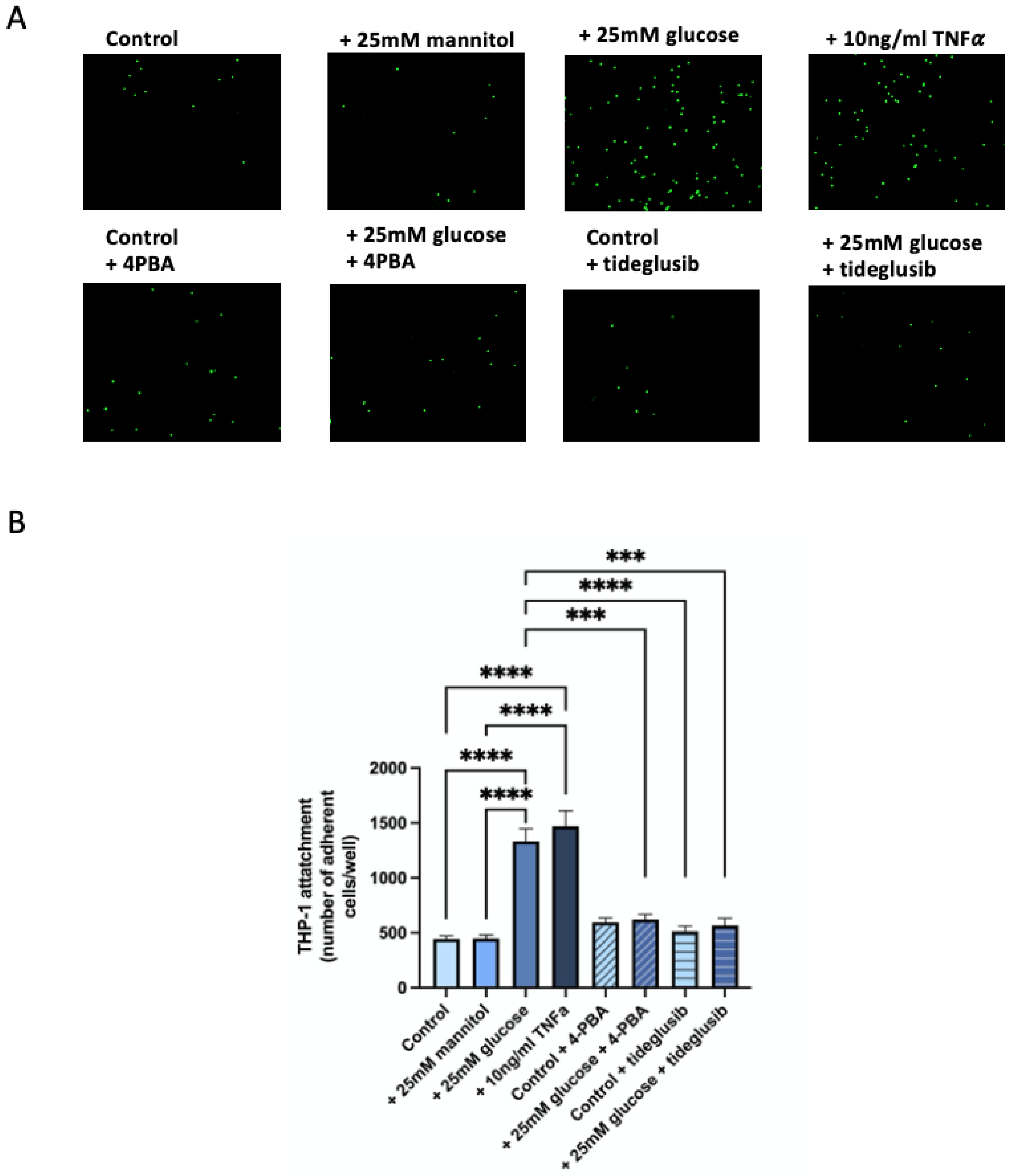
A
Control
+ 25mM mannitol
+ 25mM glucose
+ 10ng/ml TNFα
Control
+ 4PBA
+ 25mM glucose
+ 4PBA
Control
+ tideglusib
+ 25mM glucose
+ tideglusib
B
THP-1 attatchment
(number of adherent
cells/well)
0
500
1000
1500
2000
****
****
****
****
***
****
***
Control
+ 25mM mannitol
+ 25mM glucose
+ 10ng/ml TNFa
Control + 4-PBA
+ 25mM glucose + 4-PBA
Control + tideglusib
+ 25mM glucose + tideglusib

4.6 DISCUSSION

Hyperglycemia and diabetes are well-established risk factors for CVD and the accelerated development of atherosclerosis[37,38,39]. Diabetes is often associated with vascular impairment characterized by altered nitric oxide production, ER stress and endothelial activation[18,40,41,42]. EC activation is widely accepted as an important step in the initiation of atherosclerosis[43,44]. However, our understanding of the molecular mechanisms that link hyperglycemia to the development of CVD is lacking. Previous studies have shown that hyperglycemia can cause ER stress leading to the activation of the UPR[45,46,47,48,49]. The UPR involves the induced expression of ER resident chaperone proteins, the enhanced degradation of unfolded proteins, and if ER stress is not resolved, apoptosis. ER stress has been linked to EC activation[50], however a definitive mechanism has not yet been reported.

In this study we show that HAEC exposed to high glucose concentrations for 24 hours have significantly increased expression of P-selectin, E-selectin and VCAM-1, compared to HAEC cultured in control media or high mannitol. These findings suggest that high glucose levels initiate EC activation, and therefore could contribute to the attachment and migration of monocytes to the subendothelial layer, and early initiation of atherosclerosis. ICAM-1 expression levels were unaffected by high glucose levels, suggesting that ICAM-1 is regulated differently from P-selectin, E-selectin and VCAM-1. In fact, results from a previous study have suggested that ICAM-1 is not essential for atherogenesis[51].

4-PBA is a short branch chain fatty acid that has been shown to alleviate ER stress both in vitro[25] and in vivo[52]. The exposure of HAECs to 4-PBA significantly reduced the expression of ER stress response genes, calreticulin and GRP78, suggesting that these treatment conditions were effective at reducing ER stress levels in HAECs. 4-PBA treatment also attenuated the enhanced gene expression of E-selectin, ICAM-1 and VCAM-1 in HAECs cultured in high glucose concentrations. This finding is consistent with the results of an in vivo study that showed 4-PBA reduced ER stress and decreased expression of E-selectin, ICAM-1 and VCAM-1 in lung ECs[53]. These findings suggest that ER stress plays a direct role in the activation of HAEC and that alleviating ER stress is sufficient to reduce the expression of some adhesion protein markers. Interestingly, in our study, the addition of 4-PBA to high glucose further elevated the expression of P-selectin. This finding suggests that P-selectin may be regulated through alternative pathways/mechanisms relative to the other adhesion proteins.

Previous evidence from our lab and others have suggested that conditions of ER stress can lead to the activation of GSK3α/β[28,54,55]. GSK3α/β are serine/threonine kinases that are involved in the regulation of many metabolic signalling pathways[29,56,57]. In this study we used tideglusib, a small molecule GSK3α/β inhibitor[29], to determine if ER stress was signalling through GSK3α/β in the activation of ECs. Tideglusib did not alter gene expression of ER stress markers, which is a result consistent with our understanding that GSK3α/β is downstream of the adaptive ER stress response[28]. The addition of tideglusib to high glucose treated HAEC significantly reduced adhesion protein expression, suggesting that ER stress signals through GSK3α/β in the upregulation of adhesion protein expression and the activation of ECs.

To assess the functionality of these adhesion proteins, calcein-labelled THP-1 cells (a human monocytic cell line) were added to cultured HAEC. We found that HAEC exposed to high glucose had significantly increased THP-1 cell attachment. The addition of 4-PBA or tideglusib to HAEC exposed to high glucose significantly reduced monocytic attachment, likely due to the reduction in adhesion protein expression. These findings are consistent with glucose-induced ER stress-GSK3α/β playing a central role in endothelial activation. These data are also consistent with recent reports of increased THP-1 cell attachment when human umbilical vein endothelial cells (HUVEC) were treated with elevated glucose levels[58].

Individuals with diabetes are at increased risk of developing CVD[37,38,39], however a complete understanding of the molecular mechanisms that link hyperglycemia/diabetes to atherosclerosis is not yet known. Our results indicate that high glucose levels are sufficient to increase functional adhesion protein expression. Additionally, we have found a potential molecular mechanism by which high glucose levels cause EC activation by signalling through the ER stress-GSK3α/β pathway. Together these findings identify a novel target for new anti-atherogenic therapeutic strategies to reduce endothelial activation. Reducing the effects that hyperglycemia has on the vasculature could prevent or slow the initiation of atherosclerosis in diabetic patients at risk of developing CVD.

4.7 REFERENCES FOR CHAPTER 4

1) Mahmood S.S, Levy D, Vasan R.S, Wang T.J. (2014). The Framingham Heart Study and the epidemiology of cardiovascular disease: a historical perspective. *Lancet.*, 383 (9921):999-1008.

2) Mendoza A, Karch J. (2022). Keeping the beat against time: Mitochondrial fitness in the aging heart. *Front Aging.*, 3:951417.

3) Leon B.M, Maddox T.M. (2015). Diabetes and cardiovascular disease: Epidemiology, biological mechanisms, treatment recommendations and future research. *World J Diabetes.*, 6(13):1246-58.

4) Björkegren J.L.M, Lusis A.J. (2022). Atherosclerosis: Recent developments. *Cell.*, 185(10):1630-1645.

5) Bentzon J.F, Otsuka F, Virmani R, Falk E. (2014). Mechanisms of plaque formation and rupture. *Circ Res.*, 114(12):1852-66.

6) Rafieian-Kopaei M, Setorki M, Doudi M, Baradaran A, Masri H. (2014). Athersclerosis: Process, Indicators, Risk Factors and New Hopes. *Int J Prev Med.*, 5(8):917-946.

7) Celermajer D.S, Sorensen K.E, Gooch V.M, Spiegelhalter D.J, Miller O.I, Sullivan I.D, Lloyd J.K, Deanfield J.E. (1992). Non-invasive detection of endothelial dysfunction in children and adults at risk of atherosclerosis. *Lancet.,* 340(8828):1111-5.

8) Suwaidi J.A, Hamasaki S, Higano S.T, Nishimura R.A, Holmes Jr.D.R, Lerman A. (2000). Long-term follow-up of patients with mild coronary artery disease and endothelial dysfunction. *Circulation,* 101(9):948-54.

9) Davignon J, Ganz P. (2004). Role of endothelial dysfunction in atherosclerosis. *Circulation,* 109(23 Suppl 1):III27-32.

10) Endemann D.H, Schiffrin E.L. (2004). Endothelial dysfunction. *J Am Soc Nephrol.*m 15(8):1983-92

11) Galle J, Quaschning T, Seibold S, Wanner C. (2003). Endothelial dusfunction and inflammation: What is the link?. *Kidney Int.*, 63(suppl 84):S45-S49.

12) Deanfield J.E, Halcox J.P, Rabelink T.J. (2007). Endothelial function and dysfunction: testing and clinical relevance. *Circulation,* 115(10):1285-95.

13) Chia Y.P, Teo A, Yeo T.W. (2022). Overview of the Assessment of Endothelial Function in Humans. *Front Med (Lausanne),* 7:542567.

14) Szmitko P.E, Wang C-H, Weisel R.D, de Almeida J.R, Anderson T.J, Verma S. (2003) New markers of inflammation and endothelial cell activation: Part I. *Circulation,* 108(16):1917-23.

15) Sun H-J, Wu Z-Y, Nie X-W, Bian J-S. (2020). Role of Endothelial Dysfunction in Cardiovascular Diseases: The Link Between Inflammation and Hydrogen Sulfide. *Front Pharmacol.*, 10:1568.

16) Martin C.J, Peters K.N, Behar S.M. (2014). s clean up: efferocytosis and microbial control. *Curr Opin Microbiol.*, 17:17-23.

17) Ozcan L, Tabas I. (2012). Role of Endoplasmic Reticulum Stress in Metabolic Disease and Other Disorders. *Annu Rev Med.*, 63:317-328.

18) Dong Y, Fernandes C, Liu Y, Wu Y, Wu H, Brophy, Deng L, Song K, Wen A, Wong S, Yan D, Towner R, Chen H. (2017). Role of endoplasmic reticulum stress signalling in diabetic endothelial dysfunction and atherosclerosis. *Diab Vasc Dis Res.*, 14(1):14-23.

19) McAlpine C.S, Huang A, Emdin A, Banko N.S, Beriault D.R, Shi Y, Werstuck G.H. (2015). Deletion of Myeloid GSK3α Attenuates Atherosclerosis and Promotes an M2 Macrophage Phenotype. *Arterioscler Thromb Vasc Bio.*, 35(5):1113-22.

20) Patel S, Mastrogiacomo L, Fulmer M, Shi Y, Werstuck G. (2022). Deletion of Macrophage-Specific Glycogen Synthase Kinase (GSK)-3α Promotes Atherosclerotic Regression in LDLR$^{-/-}$ Mice. *Int. J. Mol. Sci.*, 23(16) 9293.

21) Bakker Wineke, Eringa E.C, Sipkema P, van Hinsbergh V.W.M. (2009). Endothelial dysfunction and diabetes: roles of hyperglycemia, impaired insulin signalling and obesity. *Cell Tissue Res.,* 335(1):165-89.

22) Maamoun H, Abdelsalam S.S, Zeidan A, Korashy H.M, Agouni A. (2019). Endoplasmic Reticulum Stress: A Critical Molecular Driver of Endothelial Dysfunction and Cardiovascular Disturbances Associated with Diabetes. *Int J Mol Sci.*, 10(7):1658.

23) Ding H, Aljofan M, Triggle C.R. (2007). Oxidative stress and increased eNOS and NADPH oxidase expression in mouse microvessel endothelial cells. *J Cell Physiol.,* 212(3):682-9

24) *THP-1 - Tib-202 | ATCC*. (n.d.). Retrieved October 26, 2022, from https://www.atcc.org/products/tib-202

25) Hanada S, Harada M, Kumemura H, Omary M.B, Koga H, Kawaguchi T, Taniguchi E, Yoshida T, Hisamoto T, Yanagimoto C, Maeyama, Ueno T, Sata M. (2007). Oxidative stress induces the endoplasmic reticulum stress and facilitates inclusion formation in cultured cells. *J Hepatol.*, 47(1):93-102.

26) Bowes A.J, Khan M.I, Shi Y, Robertson L, Werstuck G.H. (2009). Valporate Attenuates Accelerated Atherosclerosis in Hyperglycemic ApoE-Deficient Mice. *Am J Pathol.*, 174(1):330-342.

27) Choi S-E, Jang H-J, Kang Y, Jung J.G, Han S.J, Kim H.J, Kim D.J, Lee K-W. (2010). Atherosclerosis induced by a high-fat diet is alleviated by lithium chloride via reduction of VCAM expression in ApoE-deficient mice. *Vascul Pharmacol.,* 53(5-6):264-72.

28) McAlpine C.S, Werstuck G.H. (2014). Protein kinase R-like endoplasmic reticulum kinase and glycogen synthase kinase-3α/β regulate foam cell formation. *J Lipid Res.*, 55(11):2320-33.

29) Hostiuc S, Perlea P, Marinescu M, Dogaroiu C, Drima E. (2019). GSK-3 Inhibitors and Tooth Repair: An Ethical Analysis. *Front Pharmacol.*, 9:1495.

30) Förstermann U, Münzel T. (2006). Endothelial nitric oxide synthase in vascular disease: from marvel to menace. *Circulation.*, 113(13):1708-14.

31) Hemmrich K, Suschek C.V, Lerzynski G, Kolb-Bachofen V. (2003). iNOS activity is essential for endothelial stress gene expression protecting against oxidative damage. *J Appl Physiol (1985)*, 95(5):1937.

32) Lip G.Y.H, Blann. (1997). von Willebrand factor: a marker of endothelial dysfunction in vascular disorders?. *Cardiovasc. Res.*,34(2):255-265.

33) Privratsky J.R, Newman P.J. (2014). PECAM-1: regulator of endothelial junctional integrity. *Cell Tissue Res.*, 355(3):607-19.

34) Mackay F, Loetscher, Stueber D, Gehr G, Lesslauer W. (1993). Tumour Necrosis Factor alpha (TNF-alpha)-induced cell adhesion to human endothelial cells is under dominant control of one TNF receptor type, TNF-R55. *J Exp Med.*, 177(5):1277-1286.

35) Pober J.S. (2002) Endothelial activation: intracellular signalling pathways. *Arthritis Res.,* 4 suppl 3(Suppl 3): S109-16.

36) Zhou P, Lu S, Luo Y, Wang S, Yang K, Zhai Y, Sun G, Sun X. (2017). Attenuation of TNF-α-Induced Inflammatory Injury in Endothelial Cells by Ginsenoside Rb1 via Inhibiting NF- κB, JNK and p38 Signalling Pathways. *Front. Pharmacol.*, 8:464.

37) Canto E.D, Ceriello A, Rydén L, Ferrini M, Hansen T.B, Schnell O, Standl E, Beulens J.W. (2019). Diabetes as a cardiovascular risk factor: An overview of global trends of macro and micro vascular complications. *Eur J Prev Cardiol.,* 26 (2-suppl):25-32.

38) Vilahur G, Badimon J.J, Bugiardini R, Badimon L. (2014). Perspectives: The burden of cardiovascular risk factors and coronary heart disease in Europe and worldwide. *Eur Heart J Suppl.*, 16:A7-A11.

39) Yusuf S, Hawken S, Ounpuu S, Dans T, Avezum A, Lanas F, McQueen M, Budaj A, Pais P, Varigos J, Lisheng L. (2004). Effect of potentially modifiable risk factors associated with myocardial infraction in 52

countries (the INTERHEART study): case-control study. *Lancet.*, 364(9438):937-52.

40) Kawano H, Motoyama T, Hirashima O, Hirai N, Miyao Y, Sakamoto T, Kugiyama K, Ogawa H, Yasue H. (1999). Hyperglycemia rapidly suppresses flow-mediated endothelium-dependent vasodilation of brachial artery. *J Am Coll Cardiol.*, 34(1):146-54.

41) Loader J, Montero D, Lorenzen C, Watts R, Méziat C, Reboul C, Stewart S, Walther G. (2015). Acute Hyperglycemia Impairs Vascular Function in Healthy and Cardiometabolic Diseased Subjects: Systemic Review and Meta-Analysis. *Arterioscler Thromb Vasc Biol.*, 35(9):2060-72.

42) Ounpuu S, Negassa A, Yusuf S. (2001). INTER-HEART: A global study of risk factors for acute myocardial infraction. *Am Heart J.*, 141(5):711-21.

43) Mussbacher M, Schossleitner K, Kral-Pointner J.B, Salzmann M, Schrammel A, Schmid J.A. (2022). More than just a Monolayer: the Multifaceted Role of Endothelial Cells in the Pathophysiology of Atherosclerosis. *Curr Atheroscler Rep.*, 24(6):483-492.

44) Boulanger C.M. (2018). Highlight on Endothelial Activation and Beyond. *Arterioscler Thromb Vasc Biol.*, 38(12):e198-e201.

45) Chen C, Zhang B, Xue J, Li Z, Dou S, Chen H, Wang Q, Qu M, Wang H, Zhang Y, Wan L, Zhou Q, Xie L. (2022). Pathogenic Role of Endoplasmic Reticulum Stress in Diabetic Corneal Endothelial Dysfunction. *Invest Ophthalmol Vis Sci.*, 63(3):4.

46) Fiorentino V.T, Procopio T, Mancuso E, Arcidiancono G.P, Andreozzi F, Arturi F, Sciacqua A, Perticone F, Hribal M.L, Sesti G. (2015). SRT1720 counteracts glucosamine-induced endoplasmic reticulum stress and endothelial dysfunction. *Cardiovasc. Res.,* 107(2):295-306.

47) Sheikh-Ali M, Sultan S, Alamir A-R, Hass M.J, Mooradian A.D. (2010). Hyperglycemia-induced endoplasmic reticulum stress in endothelial cells. *Nutrition*, 26(11-12):1146-50.

48) Werstuck G.H, Khan M.I, Femia G, Kim A.J, Tedesco V, Trigatti B, Shi Y. (2006). Glucosamine-induced endoplasmic reticulum dysfunction is associated with accelerated atherosclerosis in a hyperglycemic mouse model. *Diabetes.,* 55(1):93-101.

49) Khan M.I, Pichna B.A, Shi Y, Bowes A.J, Werstuck G.H. (2009). Evidence supporting a role for endoplasmic stress in the development of atherosclerosis in a hyperglycemic mouse model. *Antioxid Redox Signal.*, 11(9): 2289-98.

50) Lenna S, Han R, Trojanowsk. (2014). Endoplasmic reticulum stress and endothelial dysfunction*. IUBMB Life,* 66(8):530-7.

51) Cybulsky M.I, Iiyama K, Li H, Zhu S, Chen M, Iiyama M, Davis V, Gutierrez-Ramos. J-C, Connelly P.W, Milstone D.S. (2001). A major role for VCAM-1, but not ICAM-1, in early atherosclerosis. *J Clin Invest.*, 107(10):1255-1262.

52) Cao S.S, Kaufman R.J. (2012) Unfolded protein response. *Curr Biol.*, 22(16):R622-6.

53) Shah D, Romero F, Guo Z, Sun J, Li J, Kallen C.B, Naik U, Summer R. (2017). Obesity-Induced Endoplasmic Reticulum Stress Causes Lung Endothelial Dysfunction and Promotes Acute Lung Injury. *Am. J. Respir. Cell Mol.,* 57(2).

54) Song L, De Sarno P, Jope R.S. (2002). Central role of glycogen synthase kinase-3beta in endoplasmic reticulum stress-induced caspase-3 activation. *J Biol Chem.*, 277(47):44701-8.

55) Chen Y.Y, Chen G, Fan Z, Luo J, Ke Z-J. (2008). GSK3beta and endoplasmic reticulum stress mediate rotenone-induced death of SK-N-MC neuroblastoma cells. *Biochem Pharmacol.*, 76(1):128-38.

56) Jope R.S, Yuskaitis J, Beurel E. (2007). Glycogen synthase kinase-3 (GSK3): inflammation, diseases, and therapeutics. *Neurochem Res,* 32(4-5): 577-95.

57) Wu X, Stenson M, Abeykoon J, Nowakowski K, Zhang L, Lawson J, Wellik L, Li Y, Krull J, Wenzl K, Novak A.J, Ansell S.M, Bishop G.A, Billadeau D.D, Peng H.W, Giles F, Schmitt D.M, Witzig T.E. (2019). Targeting glycogen synthase kinase 3 for therapeutic benefit in lymphoma. *Blood.,* 134(4):363-373.

58) Pal P.B, Sonowal H, Shukla K, Srivastava S.K, Ramana K.V. (2019). Aldose reductase regulated hyperglycemia-induced HUVEC death via SIRT1/AMPK-α1/mTOR pathway. *J Mol Endocrinol.,* 63(1):11-25.

4.8 SUPPLEMENTARY MATERIAL FOR CHAPTER 4

Supplementary Figure 4.1: ER stress activation in HAEC cultured in elevated glucose concentration. HAEC were cultured for 24 hours in control media (5mM glucose), mannitol (control media +25mM mannitol), high glucose (control media +25mM glucose), in the presence of absence of 25μM tideglusib or 3mM 4-PBA. After 24 hours, ER stress markers were evaluated using RT-PCR analysis. Gene expression was normalised to a β-actin control. **A** Calreticulin gene expression under different conditions. **B** GRP78 gene expression in HAEC under different conditions. n=3-6. *P<0.05, **P<0.005, ***P<0.0005, ****P<0.00005.

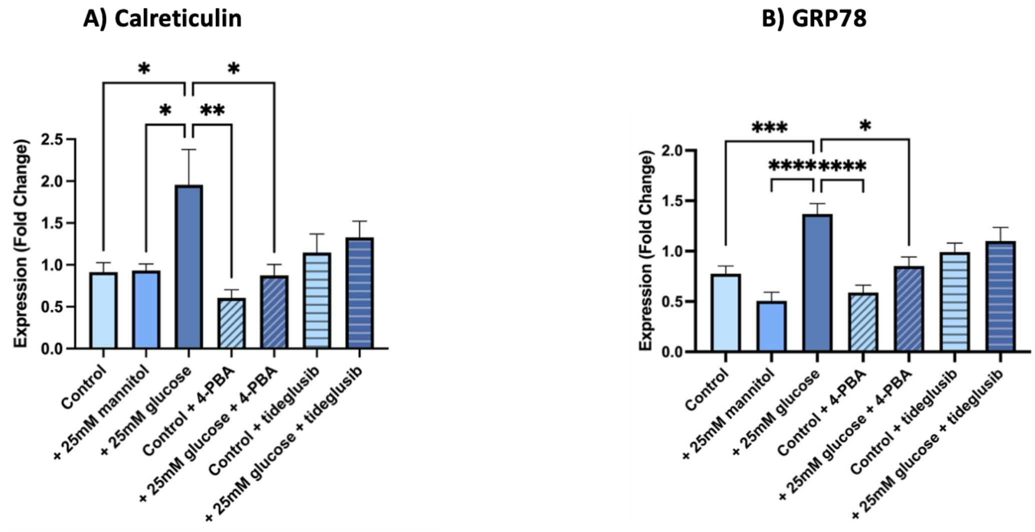
A) Calreticulin

B) GRP78

Supplementary Figure 4.2: Western blot analysis of GSK3α/β expression in HAEC. The blot shows GSK3α(51kDa) and GSK3β (47 kDa) protein expression in 2 HAEC cultures (1+2) grown in control media.

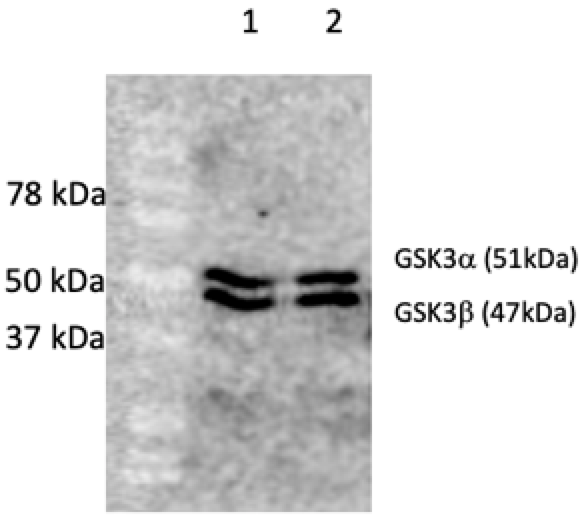
1
2
78 kDa
50 kDa
37 kDa
GSK3α (51kDa)
GSK3β (47kDa)

CHAPTER 5: Investigating the role of endothelial GSK3α/β in atherogenesis

Lauren Mastrogiacomo[1,2] and Geoff Werstuck[1,2]

[1]Thrombosis and Atherosclerosis Research Institute, Hamilton, ON, Canada.

[2]Department of Medicine, McMaster University, Hamilton, ON, Canada.

5.1 FOREWORD

This study investigates the role of endothelial glycogen synthase kinase (GSK)3α and GSK3β in endothelial activation and the initiation of atherosclerosis. Deletion of GSK3α, but not GSK3β, reduces endothelial cell (EC) activation and the development of atherosclerotic lesions. These data suggest that endothelial GSK3α and GSK3β play distinct roles. GSK3α is involved in the activation of the endothelium and is pro-atherogenic in LDLR$^{-/-}$ mice.

The experiments in this study were conducted by Lauren Mastrogiacomo. The manuscript was written by Lauren Mastrogiacomo in collaboration with Dr. Geoff Werstuck. This paper has been submitted to the International Journal of Molecular Sciences (2022).

5.2 ABSTRACT

Atherosclerotic cardiovascular disease (CVD) is the leading cause of death worldwide. Risk factors for developing CVD (hyperglycemia, dyslipidemia, obesity, hypertension and smoking) are associated with endoplasmic reticulum (ER) stress, inflammation, and endothelial activation. When ECs become activated they express adhesion proteins (P-selectin, E-selectin, ICAM-1 and VCAM-1) that recruit monocytes to the subendothelial layer initiating plaque development in the vessel wall. Understanding the mechanism(s) by which ECs increase adhesion protein expression will facilitate the development of therapies aimed at preventing CVD progression and mortality. GSK3α/β are constitutively active kinases which have been associated with many cellular pathways regulating cell viability and metabolism. While roles for myeloid GSK3α/β in the development of atherosclerosis have been established, there is limited knowledge on the potential roles of endothelial GSK3α/β. With the use of Cre recombinase technology, GSK3α/β was knocked out of both ECs and macrophages (Tie2Cre GSK3α/$\beta^{fl/fl}$ LDLR$^{-/-}$). A bone marrow transplant was used to replenish GSK3α/β in the myeloid lineage allowing the assessment of an endothelial-specific GSK3α/β knockout (BMT Tie2Cre GSK3α/$\beta^{fl/fl}$ LDLR$^{-/-}$). In both models, adhesion protein expression, macrophage recruitment and plaque volume were reduced in GSK3α knockout mice. GSK3β knockout had no significant effect. Results from this study are the first to suggest a

pro-atherogenic role of endothelial GSK3α and support existing evidence for targeting GSK3α in the treatment of atherosclerotic CVD.

5.3 INTRODUCTION

Atherosclerosis is a multifactorial inflammatory disease that involves accumulation of lipids and inflammatory cells in the subendothelial layer, causing a narrowing of the artery, altering vascular blood flow, and increasing risk of thrombus formation and/or cardiac complications[1,2,3,4]. Atherosclerotic CVD is the leading cause of mortality worldwide[5,6]. Although effective, current medications target specific risk factors, such as hypertension or dyslipidemia, rather than the disease process itself[7,8]. Understanding the mechanism(s) underlying the initiation and development of atherosclerosis will facilitate the development of more targeted therapies to prevent or reduce the risk for CVD.

The earliest detectable stage in atherogenesis is endothelial activation[9]. The endothelium forms a single layer of semi-permeable cells that line the vasculature that performs critical functions in the maintenance of vascular homeostasis[10]. Risk factors for CVD, including hyperglycemia, hypertension, dyslipidemia and smoking, are each associated with arterial inflammation and activation of the EC layer[11]. EC activation is characterized by expression of leukocyte adhesion proteins, including P-selectin, E-selectin, ICAM-1 and VCAM-1[12]. These adhesion proteins facilitate the recruitment of circulating monocytes to the injured endothelium. Monocytes migrate into the subendothelial layer where they differentiate into macrophages. These macrophages endocytose lipids and cellular debris, becoming lipid engorged foam cells[13,14]. Understanding the mechanism underlying adhesion protein expression could potentially reveal novel therapeutic targets to halt atherogenesis and plaque progression.

GSK3 is an enzyme involved in many cellular signalling pathways[15]. There are two isoforms of GSK3, GSK3α and GSK3β that are 98% homologous in the kinase domain[16]. These isoforms are now known to possess both redundant and isoform-specific functions[17]. A whole body GSK3α knockout mouse model is viable, however a whole body GSK3β knockout mouse dies during mid-gestation[18,19]. Previous research has indicated that a whole body GSK3α knockout attenuates atherosclerosis in mice[20]. Further research has shown that a myeloid-specific knockout of GSK3α can also attenuate atherosclerosis, however not to the extent observed in the whole body GSK3α knockout mouse[21]. These findings suggest that GSK3α plays a pro-atherosclerotic role in other cells of the body.

ECs play a critical role in the initiation of atherosclerosis and little is known about the potential role of GSK3α/β in the endothelium. In this study, Cre-Lox technology was used to create an endothelial GSK3 knockout in LDLR$^{-/-}$ mice in order to investigate the potential role of endothelial GSKα/β in atherogenesis.

5.4 MATERIAL AND METHODS

GSK3α/β knockout mouse strains

Cre-Lox technology was used to generate mice in which GSK3α or GSK3β is specifically ablated in ECs. LDLR$^{-/-}$ mice (B6.129S7-*Ldlr*^{tm1Her}/J, Jackson Laboratory, Bar Harbor, ME) were crossed with mice carrying a loxP-flanked GSK3α (GSK3α$^{fl/fl}$) gene or GSK3β floxed (GSK3β$^{fl/fl}$) gene[22,23] to create GSK3α$^{fl/fl}$ LDLR$^{-/-}$ or GSK3β$^{fl/fl}$ LDLR$^{-/-}$ mice. These mice were then crossed with a mouse that expressed Cre recombinase under the control of the endothelial specific Tie2 promoter (B6.Cg-Tg (Tek-Cre)1Ywa/J, Jackson Laboratories, Bar Harbor, ME) to create Tie2Cre GSK3α$^{fl/fl}$ LDLR$^{-/-}$ or Tie2Cre GSK3β$^{fl/fl}$ LDLR$^{-/-}$ mice. All mouse strains existed in a C57Bl/6 genetic background. Validation and characterization of these mice showed that the ablation of GSK3α and GSK3β occurred in ECs, as well as myeloid lineage cells (Supplementary Figure 5.1). Therefore, these mice were an endothelial /macrophage GSK3α or GSK3β knockout mouse model. To replenish GSK3α or GSK3β in the myeloid lineage, bone marrow from LDLR$^{-/-}$ mice was transplanted into GSK3α$^{fl/fl}$ LDLR$^{-/-}$, GSK3β$^{fl/fl}$ LDLR$^{-/-}$, Tie2Cre GSK3α$^{fl/fl}$ LDLR$^{-/-}$, Tie2Cre GSK3β$^{fl/fl}$ LDLR$^{-/-}$, or LDLR$^{-/-}$ (control) mice (see below). These mice were used as endothelial-selective GSK3α or GSK3β knockout mouse models.

Bone marrow transplant

Eight week old LDLR$^{-/-}$, Tie2Cre LDLR$^{-/-}$, GSK3α$^{fl/fl}$ LDLR$^{-/-}$, GSK3β$^{fl/fl}$ LDLR$^{-/-}$, Tie2Cre GSK3α$^{fl/fl}$ LDLR$^{-/-}$ and Tie2Cre GSK3β$^{fl/fl}$ LDLR$^{-/-}$ mice were irradiated with 667RAD and then 333RAD, 3 hours later, for a total dose of 1000RAD. Irradiated recipient mice were injected with bone marrow harvested from the tibias and femurs of 8 week old donor LDLR$^{-/-}$ mice ($1x10^6$ cells/recipient). The recipient mice were allowed to recover for 4 weeks, during which they received mush food combined with Nutri-cal (Vetoquinol, France) and hydrogel. The bone marrow transplant was validated by isolating DNA from circulating leukocytes using a DNeasy Blood and Tissue Kit (Qiagen, Hilden, Germany) and RT-PCR analysis of peritoneal macrophages (Primers Table 5.1) (Supplementary Figure 5.2A+B).

Table 5.1: Primer sequences

	Primer sequence
GSK3α	F: 5'- GAG CGT TCC CAA GAA GTG G -3' R: 5'- GTG CCT GGT ATA CTA CTC CGA -3'
GSK3β	F: 5'- ATA AAG ATG GCA GCA AGG TAA CCA -3' R: 5'- CTG ACT TCC TGT GGC CTG TCA -3'
vWF	F: 5'-GCA GTG GAG AAC AGT GGT G -3' R: 5'- GTG GCA GCG GGC AAA C -3'
β-actin	F: 5'- GGG GTG TTG AAG GTC TCA AAC -3' R: 5'-GGC ACC ACA CCT TCT ACA ATG -3'

Experimental design

At 12-weeks of age female mice (LDLR$^{-/-}$, Tie2Cre LDLR$^{-/-}$, GSK3α$^{fl/fl}$ LDLR$^{-/-}$, GSK3β$^{fl/fl}$ LDLR$^{-/-}$, Tie2Cre GSK3α$^{fl/fl}$ LDLR$^{-/-}$ and Tie2Cre GSK3β$^{fl/fl}$ LDLR$^{-/-}$), both endothelial/macrophage GSK3α or GSK3β knockout mice and BMT endothelial GSK3α or GSK3β knockout mice, were placed on a high-fat diet ((HFD) containing 21% fat, 0.2% cholesterol with 42% of the calories from fat, Harland Tekland,TD97363) for 3-weeks to establish atherosclerotic plaques. Mice were maintained on a 12-hour light/dark cycle with unlimited access to food and water. All mice were harvested at 15-weeks of age (Supplementary Figure 5.3). All experiments were performed in female mice because 3 weeks of high fat diet feeding produced only minimal lesions in male mice (data not shown). Littermates lacking Cre recombinase were used as controls. Additional controls include LDLR$^{-/-}$ mice and Tie2Cre LDLR$^{-/-}$ mice. Experiments were performed according to the guidelines and regulations of the Canadian Council on Animal care and all animal studies were pre-approved by McMaster University Animal Research Ethics Board.

Tissue harvesting

Mice were anesthetized and a midline laparotomy incision was made. PBS was flushed through the apex of the heart to rinse the vasculature. The whole aorta was carefully removed and cleaned from surrounding muscle and adventitial fat. Other tissues included heart, lung, liver, and skeletal muscle were also removed from some mice for further analysis.

EC isolation

ECs were isolated using a protocol adapted from *Chen S. et al*[24]. Whole aortas were longitudinally dissected, and the tunica intima side of the vessel was washed in 50µl of 0.25% Trypsin (Gibco, Waltham, MA) for 2 minutes at 37°C in 5% CO_2[24]. ECs were collected and placed in 10ml media (EGM™-2 Endothelial Cell Growth Medium-2 BulletKit (Lonza, Basel, Switzerland) supplemented with 1% penicillin-streptomycin). This process was repeated 4 times. The collected cells were centrifuged at 500 rpm for 10 minutes, the supernatant was discarded, and cells were resuspended in TRIzol Reagent (Thermo Fisher Scientific, Waltham, MA). The identity of the isolated cells was confirmed by assessing vWF gene expression by RT-PCR (Supplementary Figure 5.1C).

Macrophage collection

To collect peritoneal macrophages, 1mL of thioglycolate (10%, Sigma-Aldrich, St. Louis, MO) was injected into the peritoneal cavity. After 5 days, the mouse was euthanized, and 10mL of 0.05mM EDTA-PBS was injected into the peritoneal cavity. The peritoneum was massaged to achieve maximum yield, and the macrophages were collected using a 10mL syringe. Macrophages were centrifuged and resuspended in DMEM media (supplemented with 20%

FBS, 1% pen strep and 1% L-glutamine) and plated in a 6 well plate. After 2 hours the plates were washed 3 times with PBS, to remove red blood cells and other debris. Macrophage RNA was isolated using the TRIzol Reagent method (Thermo Fisher Scientific, Waltham, MA).

Assessing tissue specific GSK3α and GSK3β gene expression

Total RNA was isolated from peritoneal macrophages, lung, liver, skeletal muscle and aortic ECs using the TRIzol reagent method (Thermo Fisher Scientific, Waltham, MA) and cDNA was synthesized using the High-Capacity cDNA Reverse Transcription Kit (Thermo Fischer Scientific, Waltham, MA). The expression of GSK3α and GSK3β was quantified using the SYBR Green (with ROX) method (Thermo Fischer Scientific, Waltham, MA) and the StepOnePlus Real-Time PCR System (Thermo Fischer Scientific, Waltham, MA) (Primers Table 5.1). Samples were run in technical triplicates. The comparative Ct method was used to determine relative gene expression and expression levels were normalized to a β-actin control.

Analysis of blood and plasma

Mice were fasted for 4 hours. Fasting blood glucose levels were measured using a OneTouch Verio Flex Meter (Lifescan, Inc., Milpitas, CA), fasting plasma total cholesterol and triglyceride levels were determined using the colormetric

Infinity Cholesterol or Infinity Triglyceride Kit (Thermo Fisher Scientific, Waltham, MA). Assays were performed according to the manufacturer's instructions.

Atherosclerotic plaque analysis

Hearts were embedded in paraffin and 5µm thick serial sections of the aortic sinus were collected on glass slides[25]. Sections were deparaffinised and then stained with Weigert's Hematoxylin (Sigma-Aldrich, St. Louis, MI). The slides were further stained with Biebrich scarlet-acid fuchsin solution and alanine blue (Sigma-Aldrich, St. Louis, MI). Coverslips were attached using DPX mounting media and images were captured using the Olympus DP71 digital camera (Olympus imaging, Centre Valley, PA) mounted on a Leitz Laborlux S bright-field microscope (Leica Microsystems, Concord, ON). Atherosclerotic plaque areas were determined from 12 serial sections per mouse. The atherosclerotic volumes were determined using ImageJ software (Version1.15j8, https://imagej.nih.gov/ij/index.html), as previously described[25].

Analysis of EC activation

Endothelial activation was assessed through immunofluorescent and immunohistochemical analyses. Sections of aortic sinus were immunostained with antibodies against P-selectin (Novus Biologicals, Littleton, CO, NB100-65392 1:50 dilution), E-selectin (Novus Biologicals, Littleton, CO, NBP1-45545 1:100 dilution), VCAM-1 (Abcam, Cambridge, UK, ab134047 1:50

dilution), vWF (Agilent Dako, Santa Clara, CA, A008202 1:50 dilution or Proteintech, Rosemount, IL, 66682-1-Ig, 1:100) and CD107b+/Mac3 (BD Biosciences, Franklin Lakes, NJ, 550292 1:50 dilution). Primary antibodies were detected with appropriate conjugated secondary antibodies (Alexa Fluor 488 anti-mouse, Alexa Fluor 488 anti-rabbit or Alexa Fluor 488 anti-rat – all from Thermo Fisher Scientific, Waltham, MA) and the percentage of the endothelium stained in each case was determined by immunofluorescence. Immunohistochemistry was used to assess ICAM-1 expression, using a primary antibody (R&D Systems, Minneapolis, MN, BAF796 1:50 dilution) and the appropriate biotinylated anti-goat secondary antibody (Thermo Fisher Scientific, Waltham, MA). Horseradish peroxidase and 3,3’ diaminobenzidine (DAB) (Agilent, Santa Clara, CA) was used to detect immunohistochemical staining. Negative controls for staining were performed using pre-immune IgG in place of the primary antibody (Supplementary Figure 5.4).

Statistical analysis

Analysis of data was performed on Graph Pad Prism 9 and analyzed using a t-test, one or two-way ANOVA test followed by a multiple comparison test. All error bars on graphs represent the standard error of the mean (+/- SEM). For all experiments, a P value of <0.05 was considered to be statically significant. *P<0.05, **P<0.005, ***P<0.0005, ****P<0.00005.

5.5 RESULTS

The Tie2Cre recombinase is not endothelial specific

In this study, Tie2Cre GSK3α$^{fl/fl}$ LDLR$^{-/-}$ and Tie2Cre GSK3β$^{fl/fl}$ LDLR$^{-/-}$ mice were created in order to investigate the endothelial-specific role(s) of GSK3α and GSK3β. It has previously been reported that the Tie2Cre mouse strain (B6.Cg-Tg (Tek-cre)1Ywa/J) may express Cre recombinase activity in some myeloid lineages[26]. Previous work from our lab has found that deletion of GSK3α in macrophages attenuated atherosclerosis in LDLR$^{-/-}$ mice[21]. Therefore, it was important to determine the specificity of GSK3α/β knockout in our Tie2Cre strains. Peritoneal macrophages and ECs were isolated from GSK3α$^{fl/fl}$ LDLR$^{-/-}$, GSK3β$^{fl/fl}$ LDLR$^{-/-}$, Tie2Cre GSK3α$^{fl/fl}$ LDLR$^{-/-}$ and Tie2Cre GSK3β$^{fl/fl}$ LDLR$^{-/-}$ mice and the gene expression of GSK3α or GSK3β was analysed. RT-PCR analysis showed that macrophages and ECs from Tie2Cre GSK3α$^{fl/fl}$ LDLR$^{-/-}$ showed a significant decrease in GSK3α, but not GSK3β, expression, compared to GSK3α$^{fl/fl}$ LDLR$^{-/-}$ mice (Supplementary Figure 5.1A). No significant differences were observed in GSK3α or GSK3β expression in the lungs, liver, or skeletal muscle. RT-PCR analysis from Tie2Cre GSK3β$^{fl/fl}$ LDLR$^{-/-}$ mice showed a significant decrease in macrophage and endothelial GSK3β, but not GSK3α, compared to GSK3β$^{fl/fl}$ LDLR$^{-/-}$ mice (Supplementary Figure 5.1B). No significant differences were observed in gene expression in lung, liver or skeletal muscle. These results indicate that, in these Tie2Cre strains, GSK3 is affected in macrophages, as well as ECs. Therefore, this is not an endothelial specific model. This mouse model will be referred to hereon as an endothelial /macrophage knockout of GSK3α or GSK3β.

Endothelial/macrophage knockout of GSK3α attenuates atherosclerosis

To determine the effect of an endothelial/macrophage GSK3α or GSK3β knockout on atherogenesis, mice were placed on a HFD to initiate plaque formation. After 3 weeks of HFD feeding, no significant differences were observed in plasma lipids or body weight of Tie2Cre GSK3$\alpha^{fl/fl}$ LDLR$^{-/-}$ mice, compared to age matched LDLR$^{-/-}$ or Tie2Cre LDLR$^{-/-}$ controls (Table 5.2). Mice carrying the GSK3$\beta^{fl/fl}$ allele tended to present with elevated plasma triglycerides, body weight and adipose weight, relative to Tie2Cre LDLR$^{-/-}$ control. This appears to be a result of non-GSK3 related differences in this strain as the effect was independent of Cre recombinase activity.

Table 5.2: Metabolic parameters for endothelial/macrophage knockout mice

Genotype		**Blood glucose (mM)**	**Plasma Triglycerides (mM)**	**Plasma Cholesterol (mM)**	**Body Weight (g)**	**Liver Weight (g)**	**Adipose Weight (g)**	**Pancreas weight (g)**
	LDLR$^{-/-}$	10.85 ± 0.81	2.30 ± 0.22	11.23 ± 0.42	22.71 ± 0.97	1.30 ± 0.16	0.31 ± 0.06	0.13 ± 0.01
	Tie2Cre LDLR$^{-/-}$	9.39 ± 0.37	2.12 ± 0.18	11.11 ± 0.16	20.40 ± 0.78	1.00 ± 0.05	0.18 ± 0.03	0.11 ± 0.00
GSK3α$^{fl/fl}$	GSK3α$^{fl/fl}$ LDLR$^{-/-}$	9.56 ± 0.61	2.06 ± 0.12	10.18 ± 0.25	22.61 ± 0.77	1.11 ± 0.07	0.22 ±0.03	0.12 ± 0.00
	Tie2Cre GSK3α$^{fl/fl}$ LDLR$^{-/-}$	9.86 ± 0.85	2.43 ± 0.19	10.38 ± 0.41	21.56 ± 0.55	1.04 ± 0.08	0.22 ± 0.02	0.13 ± 0.01
GSK3β$^{fl/fl}$	GSK3β$^{fl/fl}$ LDLR$^{-/-}$	10.92 ± 1.35	2.71 ± 0.52	11.39 ± 0.29	27.35 ± 0.58 **/††††	1.27 ± 0.05	0.48 ± 0.05 ††	0.14 ± 0.01
	Tie2Cre GSK3β$^{fl/fl}$ LDLR$^{-/-}$	10.75 ± 1.26	4.33 ± 0.56 */†	11.44 ± 0.43	25.55 ± 1.47 **/††††	1.16 ± 0.17	0.24 ± 0.06 †	0.16 ± 0.00

*P<0.05 and **P<0.005 compared to LDLR$^{-/-}$

†P <0.05, ††P<0.005, ††††P<0.00005 compared to Tie2Cre LDLR$^{-/-}$

n= 7-9

Plaque volumes were visualized and quantified using Masson's trichrome staining. LDLR$^{-/-}$, Tie2Cre LDLR$^{-/-}$, GSK3α$^{fl/fl}$ LDLR$^{-/-}$ and GSK3β$^{fl/fl}$ LDLR$^{-/-}$ mice showed no difference in plaque volume, suggesting that neither the Tie2Cre recombinase nor GSK3α$^{fl/fl}$/GSK3β$^{fl/fl}$ had an effect on atherosclerotic plaque formation (Supplementary Figure 5.5). GSK3α$^{fl/fl}$ LDLR$^{-/-}$ and GSK3β$^{fl/fl}$ LDLR$^{-/-}$ mice, lacking the Tie2Cre recombinase, were chosen as controls for the remainder of this study, as they are littermates with the experimental mice.

It was observed that Tie2Cre GSK3α$^{fl/fl}$ LDLR$^{-/-}$ mice have significantly smaller plaque volume, compared to age matched GSK3α$^{fl/fl}$ LDLR$^{-/-}$ mice (Figure 5.1C). No significant difference was detected between Tie2Cre GSK3β$^{fl/fl}$ LDLR$^{-/-}$ and GSK3β$^{fl/fl}$ LDLR$^{-/-}$ controls. This suggests that endothelial/macrophage GSK3α is an important contributor to plaque accumulation, and supports previous findings, that GSK3α and GSK3β display different functional roles in the context of atherosclerosis [19,21,27,28].

Figure 5.1: Atherosclerosis in endothelial/macrophage GSK3α/β knockout mice. A Representative images of Masson's trichrome staining of cross sections of aortic sinus from 15 week old control or endothelial/macrophage GSK3α/β knockout mice. Scale bar represents 100μm. **B** Quantification of plaque area at the aortic sinus of the 15 week old mice. **C** Plaque volume quantification in the aortic sinus of control and endothelial/macrophage GSK3α/β knockout mice. n=7-8 (**B-C**), *<P0.05, **P<0.005, ***P<0.0005, †P<0.05, ††††P<0.00005, ns=not significant.

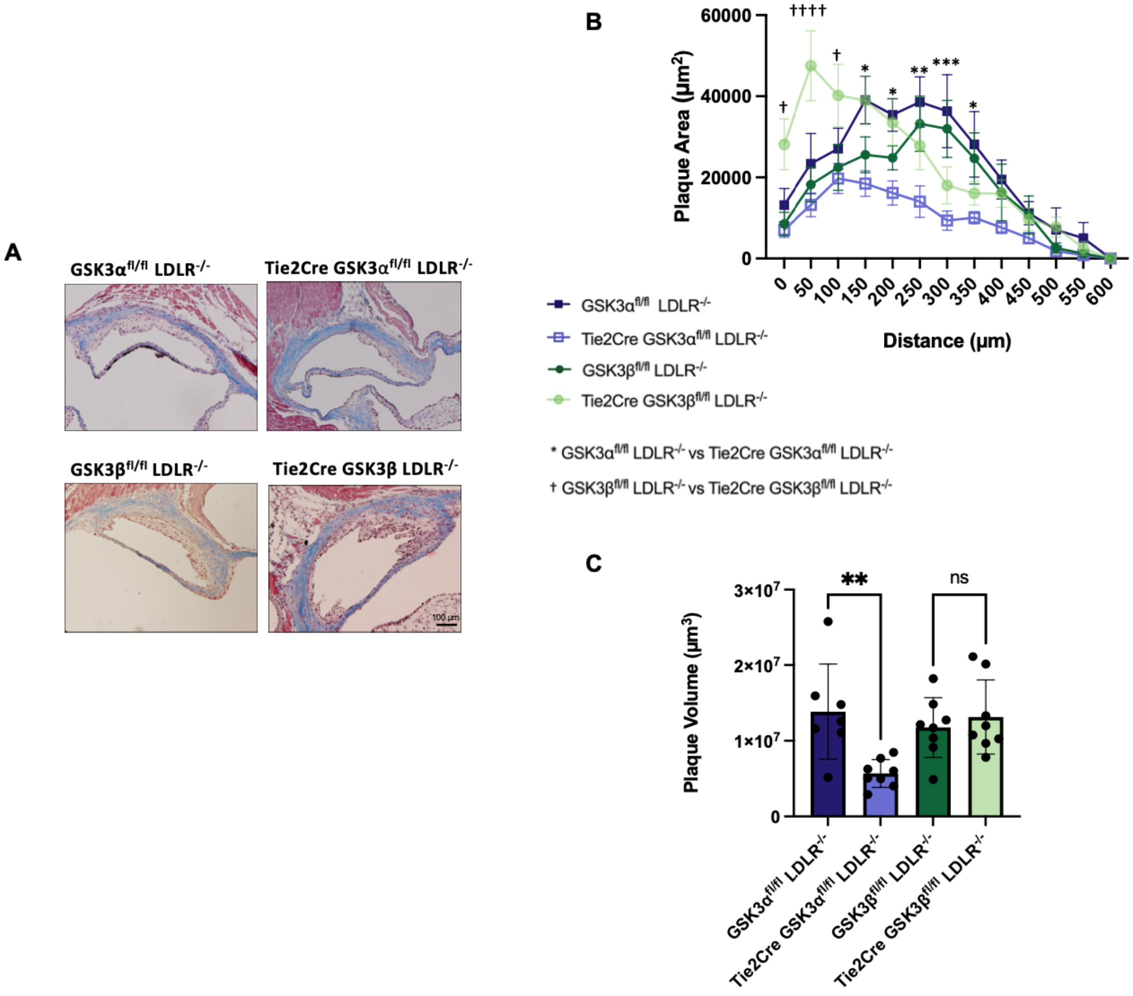
A
GSK3α fl/fl LDLR-/-
Tie2Cre GSK3α fl/fl LDLR-/-
GSK3β fl/fl LDLR-/-
Tie2Cre GSK3β LDLR-/-
100 µm
B
Plaque Area (µm²)
60000
40000
20000
0
Distance (µm)
0 50 100 150 200 250 300 350 400 450 500 550 600
††††
†
*
**
***
GSK3α fl/fl LDLR-/-
Tie2Cre GSK3α fl/fl LDLR-/-
GSK3β fl/fl LDLR-/-
Tie2Cre GSK3β fl/fl LDLR-/-
* GSK3α fl/fl LDLR-/- vs Tie2Cre GSK3α fl/fl LDLR-/-
† GSK3β fl/fl LDLR-/- vs Tie2Cre GSK3β fl/fl LDLR-/-
C
Plaque Volume (µm³)
3×10⁷
2×10⁷
1×10⁷
0
**
ns
GSK3α fl/fl LDLR-/-
Tie2Cre GSK3α fl/fl LDLR-/-
GSK3β fl/fl LDLR-/-
Tie2Cre GSK3β fl/fl LDLR-/-

Endothelial activation is reduced in endothelial/macrophage knockout of GSK3α

EC activation is widely accepted as an important event in monocyte recruitment and the initiation of atherosclerosis[29,30]. To assess endothelial activation, sections of aortic sinus from 15 week old mice were immunostained with antibodies against P-selectin, E-selectin, VCAM-1 and ICAM-1. Endothelial staining was verified by co-staining with the endothelial marker, vWF (Supplementary Figure 5.6). Results indicate that Tie2Cre GSK3α$^{fl/fl}$ LDLR$^{-/-}$ mice have significantly reduced expression of P-selectin, E-selectin and VCAM-1 compared to age matched GSK3α$^{fl/fl}$ LDLR$^{-/-}$ controls (Figure 5.2B-D). No significant difference was detected in adhesion protein expression between Tie2Cre GSK3β$^{fl/fl}$ LDLR$^{-/-}$ and GSK3β$^{fl/fl}$ LDLR$^{-/-}$ mice. These data are the first indication that GSK3α plays a role in endothelial activation. There was no difference in ICAM-1 expression in any experimental groups (Figure 5.2E). The specificity of the staining is supported by sections of the aortic sinus stained with appropriate pre-immune IgG in place of the primary antibody (Supplementary Figure 5.4).

Figure 5.2: Adhesion protein expression in endothelial/macrophage GSK3α/β knockout mice. A Representative images of stained aortic sinus cross sections from 15 week old endothelial/macrophage GSK3α/β knockout and control mice. Scale bar represents 100μm. Quantification of percentage of endothelium showing immunofluorescent staining of P-selectin (**B**) E-selectin (**C**) and VCAM-1 (**D**). **E** Quantification of immunohistochemistry staining of ICAM-1 expression on the endothelium. n=6-8 (**B-E**), *P<0.05, ***P<0.0005. ns=not significant.

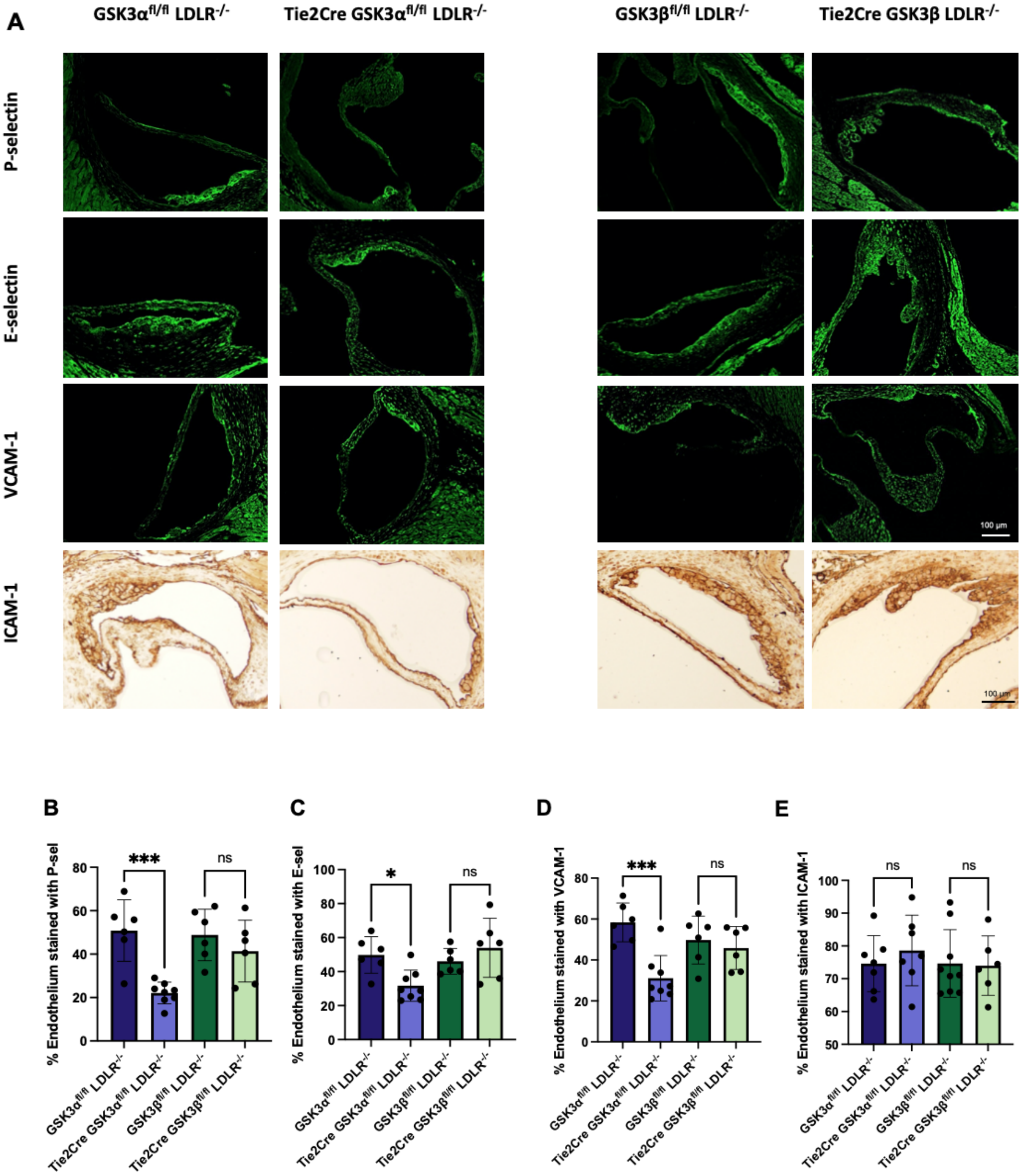
A
GSK3α fl/fl LDLR-/-
Tie2Cre GSK3α fl/fl LDLR-/-
GSK3β fl/fl LDLR-/-
Tie2Cre GSK3β LDLR-/-
P-selectin
E-selectin
VCAM-1
ICAM-1
100 µm
100 µm
B
% Endothelium stained with P-sel
***
ns
C
% Endothelium stained with E-sel
*
ns
D
% Endothelium stained with VCAM-1
***
ns
E
% Endothelium stained with ICAM-1
ns
ns
GSK3α fl/fl LDLR-/-
Tie2Cre GSK3α fl/fl LDLR-/-
GSK3β fl/fl LDLR-/-
Tie2Cre GSK3β fl/fl LDLR-/-

Sections were stained with an antibody against CD107b^{+}/Mac-3^{+} (Mac-3) to assess monocyte/macrophage recruitment. Tie2Cre GSK3α$^{fl/fl}$ LDLR$^{-/-}$ mice had significantly reduced Mac-3 staining, compared to age matched control mice (Figure 5.3). There was no significant difference in monocyte/macrophage content between Tie2Cre GSK3β$^{fl/fl}$ LDLR$^{-/-}$ and GSK3β$^{fl/fl}$ LDLR$^{-/-}$ control mice, these findings support a role for endothelial and macrophage GSK3α in monocyte/macrophage recruitment.

Figure 5.3: Monocyte/macrophage recruitment in endothelial/macrophage GSK3α/β knockout mice. A Representative images of cross sections of aortic sinus from 15 week old endothelial/macrophage GSK3α/β knockout and control mice stained with an antibody against Mac-3. Scale bar represents 100μm. **B** Quantification of percentage of the intima stained with anti-Mac-3 antibody. n=7-8 (**B**), **P<0.005. ns=not significant.

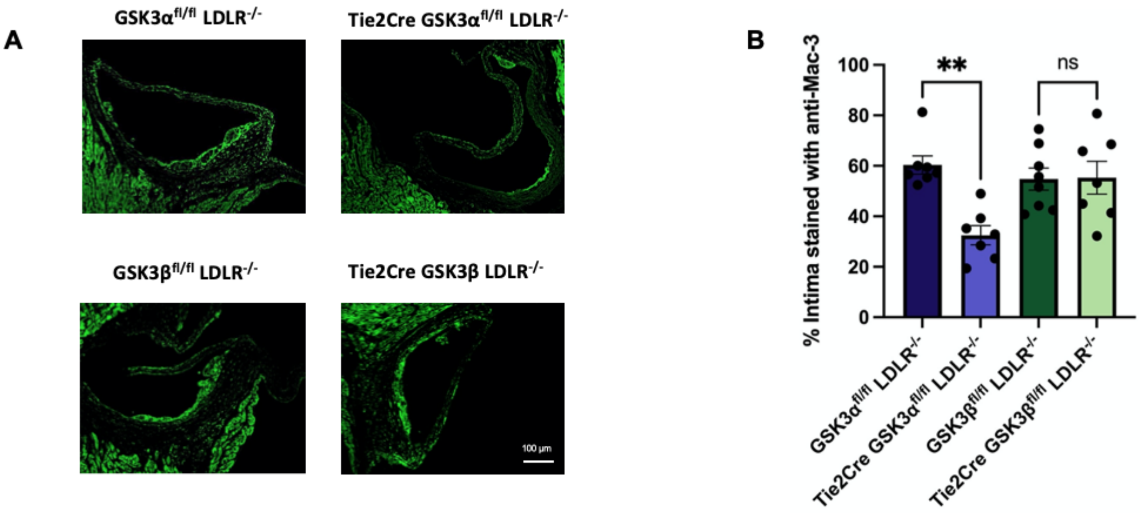
A
GSK3α$^{fl/fl}$ LDLR$^{-/-}$
Tie2Cre GSK3α$^{fl/fl}$ LDLR$^{-/-}$
GSK3β$^{fl/fl}$ LDLR$^{-/-}$
Tie2Cre GSK3β LDLR$^{-/-}$
100 μm
B
% Intima stained with anti-Mac-3
100
80
60
40
20
0
**
ns
GSK3α$^{fl/fl}$ LDLR$^{-/-}$
Tie2Cre GSK3α$^{fl/fl}$ LDLR$^{-/-}$
GSK3β$^{fl/fl}$ LDLR$^{-/-}$
Tie2Cre GSK3β$^{fl/fl}$ LDLR$^{-/-}$

Bone marrow transplant (BMT) replenished GSK3α and GSK3β expression in myeloid cells

It is possible that the effects on endothelial activation and monocyte /macrophage recruitment, observed above, were an indirect result of macrophage-specific deficiency in GSK3α. A bone marrow transplant was performed to replace myeloid expression of GSK3α and GSK3β, thereby facilitating the assessment of the effects of endothelial GSK3α or GSK3β deficiencies directly.

BMTs were performed on both control and experimental mice. In order to determine if the BMT was successful, DNA was isolated from circulating leukocytes, and the presence of intact genes encoding GSK3α and GSK3β was verified (Supplementary Figure 5.2A). The expression of GSK3α or GSK3β was confirmed in isolated peritoneal macrophages by RT-PCR analysis (Supplementary Figure 5.2B). No significant difference in GSK3α or GSK3β expression was detected, suggesting that the BMT was successful. This mouse model will be referred to as the endothelial knockout of GSK3α or GSK3β.

Interestingly, plaques in mice receiving a BMT were significantly smaller than in the mice that did not receive a BMT indicating that the procedure itself did have an effect on atherosclerotic progression (Supplementary Figure 5.7). Therefore, direct comparisons of atherosclerotic progression in macrophage

/endothelial GSK3 knockout mice and BMT endothelial GSK3 knockout mice are not presented.

Endothelial knockout of GSK3α attenuates atherosclerosis

To determine the role of GSK3α or GSK3β in ECs during atherogenesis, bone marrow from 8 week old LDLR$^{-/-}$ mice was transplanted into lethally irradiated 8 week old LDLR$^{-/-}$, Tie2Cre LDLR$^{-/-}$, GSK3α$^{fl/fl}$ LDLR$^{-/-}$, GSK3β$^{fl/fl}$ LDLR$^{-/-}$, Tie2Cre GSK3α$^{fl/fl}$ LDLR$^{-/-}$ and Tie2Cre GSK3β$^{fl/fl}$ LDLR$^{-/-}$ recipient mice. After 4 weeks of recovery, the success of the BMT was verified, and mice were placed on a HFD for 3 weeks. No significant difference was detected in blood glucose, plasma triglycerides, plasma cholesterol, liver weight, adipose weight or pancreas weight between mouse models (Table 5.3). As previously observed, the body weight of BMT GSK3β$^{fl/fl}$ LDLR$^{-/-}$ mice was significantly higher than controls. Plaque volume of the controls (BMT LDLR$^{-/-}$, BMT Tie2Cre LDLR$^{-/-}$, BMT GSK3α$^{fl/fl}$ LDLR$^{-/-}$ and BMT GSK3β$^{fl/fl}$ LDLR$^{-/-}$) was assessed, and no significant difference was identified between control groups (Supplementary Figure 5.8), suggesting that Tie2Cre, GSK3α$^{fl/fl}$ or GSK3β$^{fl/fl}$ do not affect plaque development. BMT GSK3α$^{fl/fl}$ LDLR$^{-/-}$ or BMT GSK3β$^{fl/fl}$ LDLR$^{-/-}$ mice were used as controls for the remaining experiments, as they are littermates of the experimental mice.

Table 5.3: Metabolic parameters for BMT endothelial knockout mice

Genotype		**Blood glucose (mM)**	**Plasma Triglycerides (mM)**	**Plasma Cholesterol (mM)**	**Body Weight (g)**	**Liver Weight (g)**	**Adipose Weight (g)**	**Pancreas weight (g)**
	BMT LDLR$^{-/-}$	9.6 ± 0.16	1.99 ± 0.22	9.65 ± 0.21	19.54 ± 0.72	0.89 ± 0.04	0.16 ± 0.06	0.12 ±0.05
	BMT Tie2Cre LDLR$^{-/-}$	10.15 ± 1.14	2.67 ± 0.27	8.89 ± 0.51	21.93 ± 0.34	1.33 ± 0.20	0.23 ± 0.01	0.31 ± 0.23
BMT GSK3α$^{fl/fl}$	BMT GSK3α$^{fl/fl}$ LDLR$^{-/-}$	11.54 ± 0.88	1.97 ± 0.15	8.25 ± 0.28	25.36 ± 1.43	1.29 ± 0.09	0.28 ± 0.06	0.10 ± 0.01
	BMT Tie2Cre GSK3α$^{fl/fl}$ LDLR$^{-/-}$	12.08 ± 0.60	1.63 ± 0.12	7.71 ± 0.26	21.56 ± 0.82	1.13 ± 0.10	0.18 ± 0.03	0.09 ± 0.01
BMT GSK3β$^{fl/f}$	BMT GSK3β$^{fl/fl}$ LDLR$^{-/-}$	11.6 ± 0.56	1.58 ± 0.22	7.01 ± 0.34	28.12 ± 1.51 **/†/‡‡	1.41 ± 0.15	0.42 ± 0.19	0.12 ± 0.01
	BMT Tie2Cre GSK3β$^{fl/fl}$ LDLR$^{-/-}$	10.2 ± 0.49	2.02 ± 0.24	7.31 ± 0.33	22.40 ± 0.70	1.00 ±0.07	0.18 ± 0.02	0.09 ± 0.00

**P<0.005 compared to BMT LDLR$^{-/-}$

†P<0.05 compared to BMT Tie2Cre LDLR$^{-/-}$

‡‡P<0.005 compared to BMT Tie2Cre GSK3β$^{fl/fl}$ LDLR$^{-/-}$

n= 7-10

To investigate the endothelial specific role of GSK3, plaque volumes of the BMT endothelial GSK3α or GSK3β knockout mice were quantified. Results show that BMT Tie2Cre GSK3α$^{fl/fl}$ LDLR$^{-/-}$ mice have significantly smaller plaques than control mice (Figure 5.4B-C). No significant difference was seen between BMT Tie2Cre GSK3β$^{fl/fl}$ LDLR$^{-/-}$ and the BMT GSK3β$^{fl/fl}$ LDLR$^{-/-}$ control. This suggests that endothelial GSK3α specifically contributes to atherogenesis and supports previous data that GSK3α and GSK3β play different functions in the context of atherogenesis [19,21,27,28].

Figure 5.4: Atherosclerosis in BMT endothelial GSK3α/β knockout mice. A Representative images of Masson's trichrome staining of cross sections of aortic sinus from 15 week old BMT control or BMT endothelial GSK3α/β knockout mice. Scale bar represents 100μm. **B** Quantification of plaque area at the aortic sinus of the 15 week old mice. **C** Plaque volume quantification in the aortic sinus of BMT control and BMT endothelial GSK3α/β knockout mice. n=7-10 (**B-C**), *<P0.05, **<P0.05. ns=not significant.

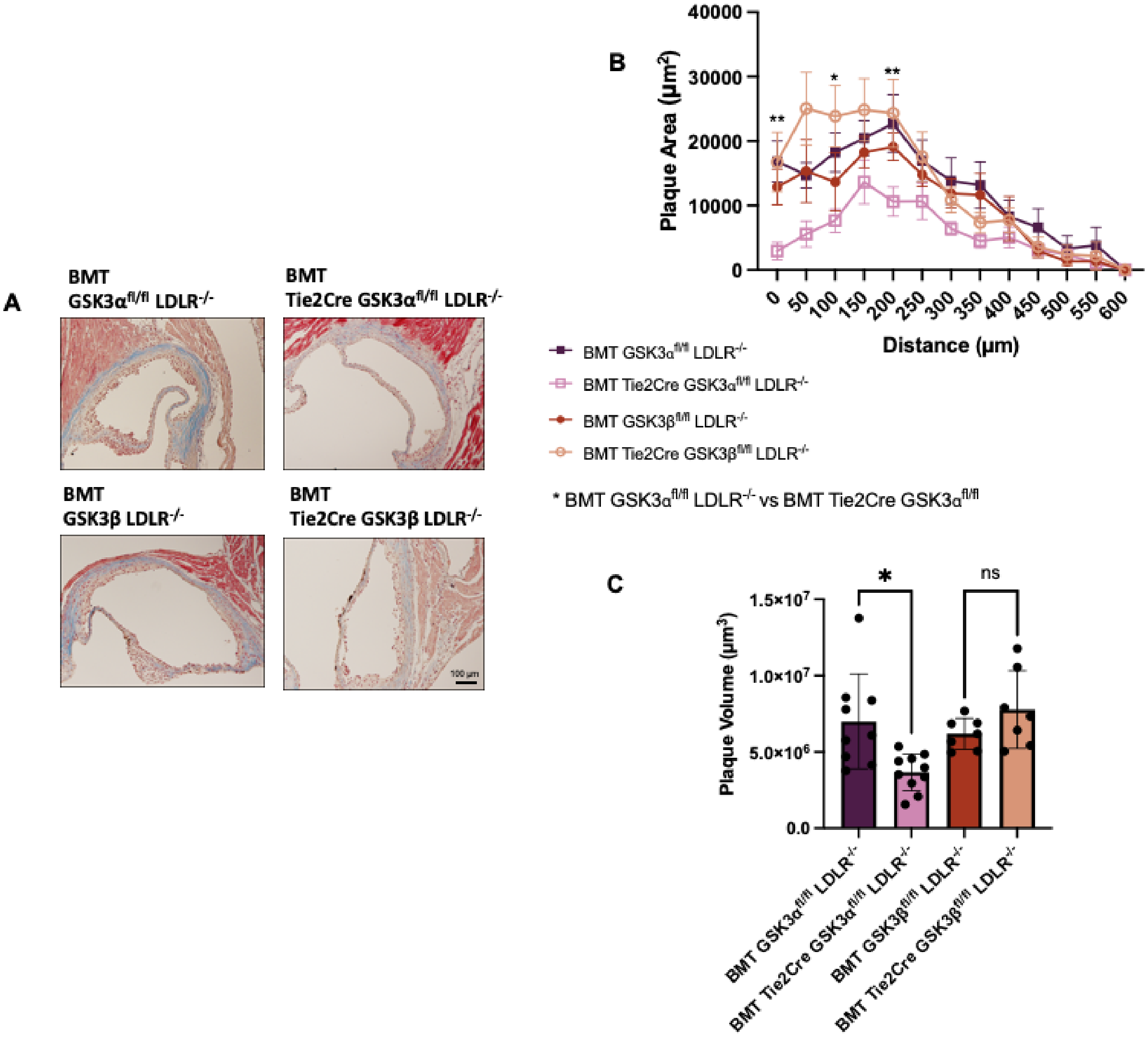
A
BMT GSK3α$^{fl/fl}$ LDLR$^{-/-}$
BMT Tie2Cre GSK3α$^{fl/fl}$ LDLR$^{-/-}$
BMT GSK3β LDLR$^{-/-}$
BMT Tie2Cre GSK3β LDLR$^{-/-}$
100 µm
B
Plaque Area (µm^2)
40000
30000
20000
10000
0
**
*
**
0 50 100 150 200 250 300 350 400 450 500 550 600
Distance (µm)
BMT GSK3α$^{fl/fl}$ LDLR$^{-/-}$
BMT Tie2Cre GSK3α$^{fl/fl}$ LDLR$^{-/-}$
BMT GSK3β$^{fl/fl}$ LDLR$^{-/-}$
BMT Tie2Cre GSK3β$^{fl/fl}$ LDLR$^{-/-}$
* BMT GSK3α$^{fl/fl}$ LDLR$^{-/-}$ vs BMT Tie2Cre GSK3α$^{fl/fl}$
C
Plaque Volume (µm^3)
1.5×10^7
1.0×10^7
5.0×10^6
0.0
*
ns
BMT GSK3α$^{fl/fl}$ LDLR$^{-/-}$
BMT Tie2Cre GSK3α$^{fl/fl}$ LDLR$^{-/-}$
BMT GSK3β$^{fl/fl}$ LDLR$^{-/-}$
BMT Tie2Cre GSK3β$^{fl/fl}$ LDLR$^{-/-}$

Endothelial activation is reduced in endothelial GSK3α knockout mice

To determine the effects that endothelial GSK3α or GSK3β knockout have on endothelial activation, sections of aortic sinus from BMT endothelial knockout mice were immunostained for adhesion markers. BMT Tie2Cre GSK3α$^{fl/fl}$ LDLR$^{-/-}$ mice had significantly less staining of P-selectin, E-selectin and VCAM-1 compared to age matched BMT GSK3α$^{fl/fl}$ LDLR$^{-/-}$ controls (Figure 5.5B-D). No significant difference was detected between BMT Tie2Cre GSK3β$^{fl/fl}$ LDLR$^{-/-}$ and BMT GSK3β$^{fl/fl}$ LDLR$^{-/-}$. There was no difference in ICAM-1 expression in any experimental groups (Figure 5.5E). These results, combined with the results above, suggest that endothelial GSK3α plays a role in adhesion protein expression thereby affecting/increasing plaque accumulation.

Figure 5.5: Adhesion protein expression in BMT endothelial GSK3α/β knockout mice*.* A Representative images of stained cross sections of aortic sinus from 15 week old BMT endothelial GSK3α/β knockout and BMT control mice. Scale bar represents 100μm. Quantification of percentage of endothelium showing immunofluorescent staining of P-selectin (**B**) E-selectin (**C**) and VCAM-1 (**D**). **E** Quantification of immunohistochemistry staining of ICAM-1 expression on the endothelium. n=5-8 (**B-E**), **P<0.005, ***P<0.0005. ns=not significant.

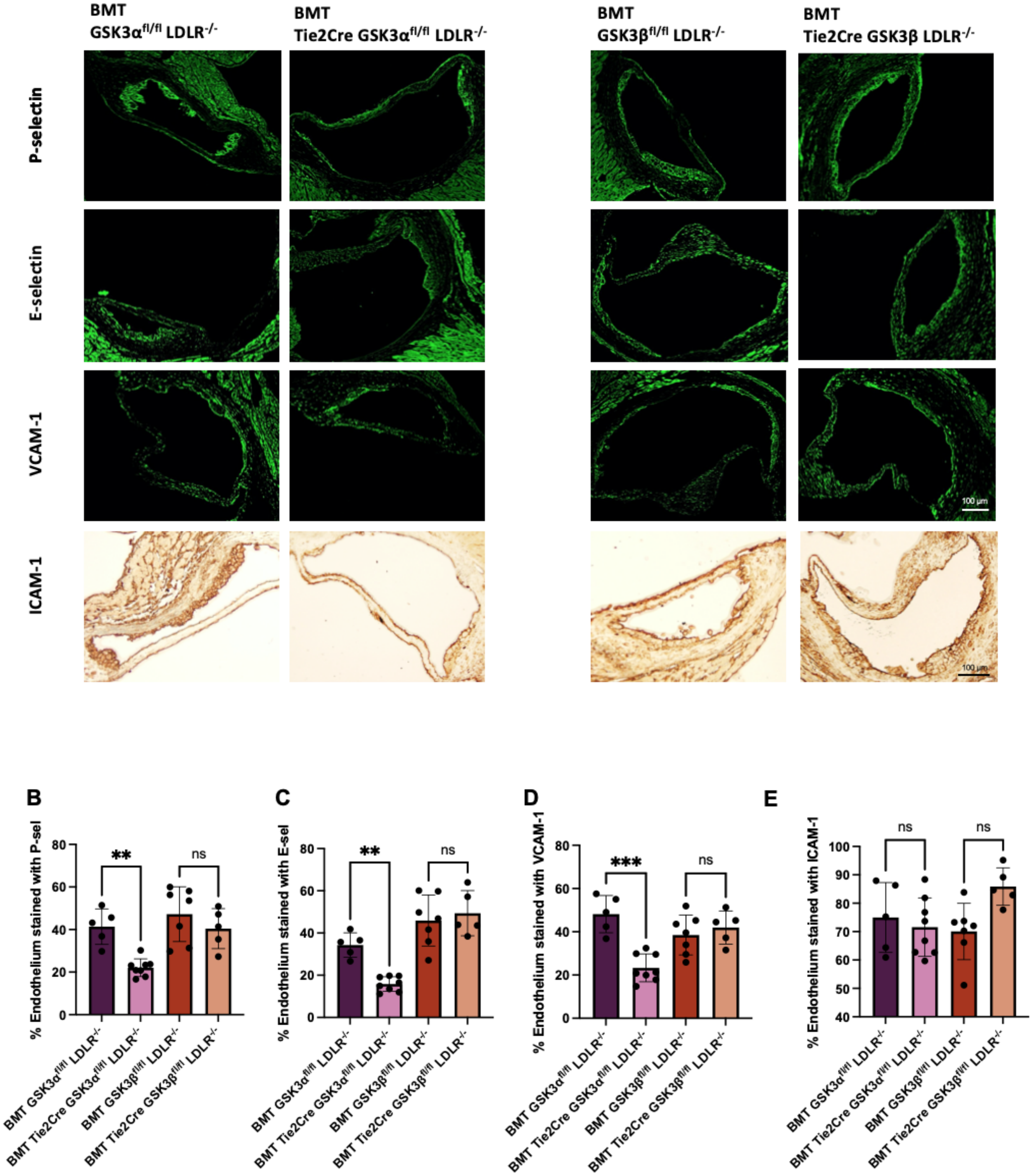
BMT GSK3α$^{fl/fl}$ LDLR$^{-/-}$
BMT Tie2Cre GSK3α$^{fl/fl}$ LDLR$^{-/-}$
BMT GSK3β$^{fl/fl}$ LDLR$^{-/-}$
BMT Tie2Cre GSK3β LDLR$^{-/-}$
P-selectin
E-selectin
VCAM-1
ICAM-1
100 µm
100 µm
B
% Endothelium stained with P-sel
C
% Endothelium stained with E-sel
D
% Endothelium stained with VCAM-1
E
% Endothelium stained with ICAM-1
**
***
ns
0
20
40
60
80
50
70
90
100
BMT GSK3α$^{fl/fl}$ LDLR$^{-/-}$
BMT Tie2Cre GSK3α$^{fl/fl}$ LDLR$^{-/-}$
BMT GSK3β$^{fl/fl}$ LDLR$^{-/-}$
BMT Tie2Cre GSK3β$^{fl/fl}$ LDLR$^{-/-}$

To assess monocyte/macrophage recruitment, aortic sinus sections were stained with an antibody against Mac-3. BMT Tie2Cre GSK3α$^{fl/fl}$ LDLR$^{-/-}$ had significantly reduced Mac-3 staining, compared to age matched control mice (Figure 5.6). There was no significant difference in monocyte/macrophage recruitment between BMT Tie2Cre GSK3β$^{fl/fl}$ LDLR$^{-/-}$ and BMT GSK3β$^{fl/fl}$ LDLR$^{-/-}$ control mice. These findings suggest that the effect of endothelial GSK3α knockout on endothelial activation results in a significant reduction in monocyte /macrophage recruitment.

Figure 5.6: Monocyte/macrophage recruitment in endothelial GSK3α/β knockout mice. A Representative images of sections of aortic sinus from 15 week old BMT endothelial GSK3α/β knockout and BMT control mice stained with anti-Mac-3. Scale bar represents 100μm. **B** Quantification of percentage of intima stained with anti-Mac-3 immunofluorescent staining. n=7-8 (**B**). **P<0.005. ns=not significant.

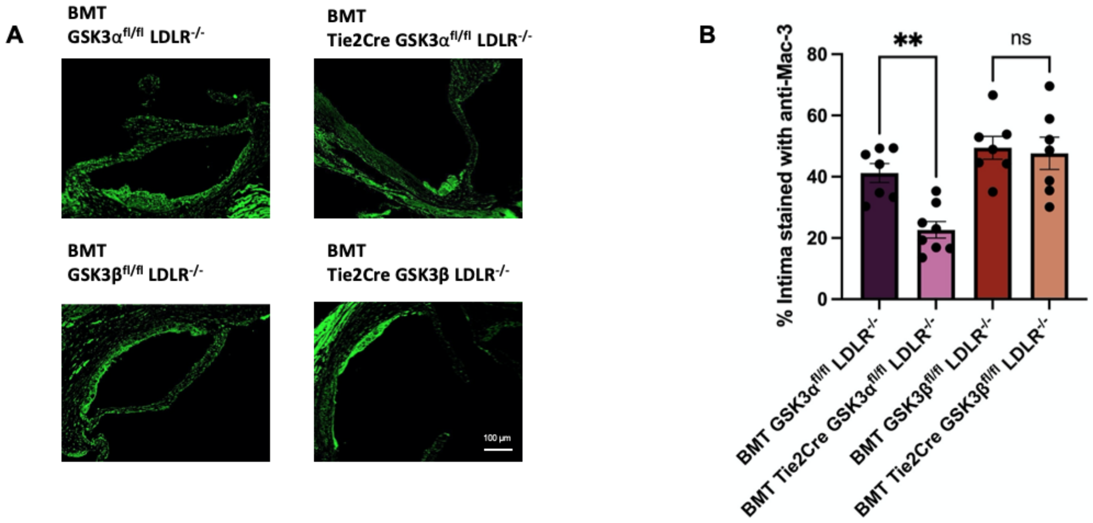
A
BMT
GSK3α$^{fl/fl}$ LDLR$^{-/-}$
BMT
Tie2Cre GSK3α$^{fl/fl}$ LDLR$^{-/-}$
BMT
GSK3β$^{fl/fl}$ LDLR$^{-/-}$
BMT
Tie2Cre GSK3β LDLR$^{-/-}$
100 µm
B
% Intima stained with anti-Mac-3
80
60
40
20
0
**
ns
BMT GSK3α$^{fl/fl}$ LDLR$^{-/-}$
BMT Tie2Cre GSK3α$^{fl/fl}$ LDLR$^{-/-}$
BMT GSK3β$^{fl/fl}$ LDLR$^{-/-}$
BMT Tie2Cre GSK3β$^{fl/fl}$ LDLR$^{-/-}$

5.6 DISCUSSION

EC activation is believed to be the initiating step in the pathogenesis of atherosclerosis[31]. Activated ECs express adhesion proteins that facilitate the recruitment of circulating monocytes to the artery wall. These monocytes differentiate into macrophages which drive further plaque growth and development. Understanding the mechanism by which cardiovascular risk factors promote atherosclerosis will facilitate the development of therapies to inhibit this process.

In this study we examine the effect of dyslipidemia on the endothelium and specifically focus on the role of GSK3α/β in this process using Tie2Cre recombinase to selectively ablate GSK3 in ECs. As previously noted the Tie2Cre mouse model may not be endothelial specific[26]. Characterization of these novel mouse strains (Tie2Cre GSK3α/β$^{fl/fl}$ LDLR$^{-/-}$) revealed that GSK3α and GSK3β were eliminated in macrophages, as well as ECs. Therefore, this model was used to examine the combined effects of endothelial/macrophage GSK3α or GSK3β knockout. Endothelial/macrophage knockout of GSK3α (Tie2Cre GSK3α$^{fl/fl}$ LDLR$^{-/-}$) significantly reduced the expression of endothelial activation markers (P-selectin, E-selectin, VCAM-1) and monocyte/macrophage recruitment, compared to the age matched control (GSK3α$^{fl/fl}$ LDLR$^{-/-}$). ICAM-1 staining showed no difference which has been reported in another atherosclerotic mouse model[32]. Likely as a result of these effects, atherosclerotic plaque size was also significantly reduced in endothelial/macrophage GSK3α knockout mice. These findings indicate that endothelial and/or macrophage GSK3α plays an important role in atherogenesis. Deletion of endothelial/macrophage GSK3β had no significant effect on adhesion protein expression, monocyte/macrophage recruitment, or plaque size. The limitation of these experiments was the inability to clearly distinguish the effects of endothelial from macrophage GSK3α knockout on endothelium activation and atherogenesis.

Previous work from our lab has shown that macrophage knockout of GSK3α does have the effect of reducing atherosclerotic plaque area and volume[21]. Therefore, knocking out GSK3α in the myeloid lineage is likely having an effect on plaque size in this model. To replenish GSK3α in the myeloid lineage, a BMT was performed in order to create an endothelial selective GSK3α or GSK3β knockout mouse model. Results suggest that an endothelial selective GSK3α knockout significantly reduced adhesion protein expression, monocyte /macrophage recruitment, and atherosclerotic plaque area/volume, compared to age matched BMT GSK3α$^{fl/fl}$ LDLR$^{-/-}$ controls. Deletion of endothelial GSK3β had no effect on adhesion protein expression, monocyte/macrophage recruitment, or plaque size, suggesting that endothelial GSK3β may not be an important contributor to atherogenesis. More research is required to assess the possibility of targeting endothelial and/or macrophage GSK3α as a therapy to slow or attenuate atherogenesis. Future studies using small molecule isoform-specific inhibitors for GSK3α[33] will help to test the potential for specific GSK3α inhibition as a therapy to treat CVD.

This is the first report to indicate a specific role for endothelial GSK3α and further supports the potential of targeting GSK3α as a therapy in the treatment or prevention of atherosclerotic CVD.

Acknowledgments: We thank Dr Bradley Doble (University of Manitoba) and Dr Jim Woodgett (University of Toronto) for the generous gift of the floxed-GSK3α and floxed-GSK3β mice.

5.7 REFERENCES FOR CHAPTER 5

1) Lusis A.J. (2000) Atherosclerosis. *Nature,* 407(6801):233-41

2) Fave C, Montagnana M. (2018). Atherosclerosis Is an Inflammatory Disease which Lacks a Common Anti-inflammatory Therapy: How Human Genetics Can Help to This Issue. A Narrative Review. *Front. Pharmacol.*, 9:55

3) Kobiyama K, Ley K. (2018). Atherosclerosis. *Circ Res.*, 123(10):1118-1120.

4) Warboys C.M, Amini N, de Luca A, Evans P.C. (2011). The role of blood flow in determining the sites of atherosclerotic plaques. *F1000 Med Rep.*, 3:5.

5) Barquera S, Pedroza-Tobías A, Medina C, Hernández-Barrera L, Bibbins-Domingo K, Lozano R, Moran A.E. (2015). Global Overview of the Epidemiology of Atherosclerotic Cardiovascular Disease. *Arch Med Res.*, 46(5):328-38.

6) Herrington W, Lacey B, Sherliker P, Armitage J, Lewington S. (2016). Epidemiology of Atherosclerosis and the Potential to Reduce the Global Burden of Atherothrombotic Disease. *Circ Res.,* 118(4):535-46.

7) Wirtz V.J, Kaplan W.A, Kwan G.F, Laing R.O. (2016). Access to Medications for Cardiovascular Diseases in Low-and Middle-Income Countries. *Circulation,* 133(21):2076-85.

8) Wald N.J, Law M.R. (2003). A strategy to reduce cardiovascular disease by more than 80%. *BMJ.*, 326(7404):1419.

9) Theodorou K, Boon R.A. (2018). Endothelial Cell Metabolism in Atherosclerosis. *Front Cell Dev Biol.*, 6:82.

10) Chia P.Y, Teo A, Yeo T.W. (2020). Overview of the Assessment of Endothelial Function in Humans. *Front Med (Lausanne)*., 7:542567.

11) Hadi H.A.R, Carr C.S, Suwaidi J.A. (2005). Endothelial dysfunction: Cardiovascular risk factors, therapy, and outcome. *Vasc Health Risk Manag.*, 1(3):183-98.

12) Hunt B.J, Jurd K.M. (1998). Endothelial cell activation. A central pathophysiological process. *BMJ.*, 316(7141):1328-9.

13) Michiels C. (2003). Endothelial cell functions. *J Cell Physiol.*, 196(3):430-43.

14) Markin A.M, Sobenin I.A, Grechko A.V, Zhang D, Orekhov A.N. (2020). Cellular Mechanisms of Human Atherogenesis: Focus on Chronification of Inflammation and Mitochondrial Mutations. *Front Pharmacol.*, 11:642.

15) Beurel E, Grieco S.F, Jope R.S. (2015). Glycogen synthase kinase-3 (GSK3): regulation, actions, and diseases. *Pharmacol Ther.*, 148:114-31.

16) Kaidanovich-Beilin O, Woodgett J.R. (2011). GSK-3: Functional Insights from Cell Biology and Animal Models. *Front Mol Neurosci.*, 4:40.

17) Woodgett J.R, Cohen P. (1984). Multisite phosphorylation of glycogen synthase: Molecular basis for the substrate specificity of glycogen synthase kinase-3 and casein kinase-II (glycogen synthase kinase-5). *BBA.*, 778(3):339-347

18) Hoeflich K.P, Luo J, Rubie E.A, Tsao M.S, Jin O, Woodgett. (2000) Requirement for glycogen synthase kinase-3beta in cell survival and NF-kappaB activation. *Nature,* 406(6791):86-90.

19) MacAulay K, Doble B.W, Patel S, Hansotia T, Sinclair E.M, Drucker D.J, Nagy A, Woodgett J.R. (2007). Glycogen synthase kinase 3alpha-specific regulation of murine hepatic glycogen metabolism. *Cell Metab.*, 6(4):329-37.

20) Banko N.S, McAlpine C.S, Venegas-Pino D.E, Raja P, Shi Y, Khan M.I, Werstuck G.H. (2014). Glycogen synthase kinase 3α deficiency attenuates atherosclerosis and hepatic steatosis in high fat diet-fed low density lipoprotein receptor-deficient mice. *Am J Pathol.*, 184(12):3394-404.

21) McAlpine C.S, Huang A, Emdin A, Banko N.S, Beriault D.R, Shi Y, Werstuck G.H. (2015). Deletion of Myeloid GSK3α Attenuates Atherosclerosis and Promotes an M2 Macrophage Phenotype. *Aterioscler Thromb Vasc Biol.*, 35(5):1113-22.

22) Patel S, Macaulay K, Woodgett J.R. (2011). Tissue-specific analysis of glycogen synthase kinase-3α (GSK-3α) in glucose metabolism: effect of strain variation. *PloS One*., 6(1):e15845.

23) Patel S, Doble B.W, MacAulay K, Sinclair E.M, Drucker D.J, Woodgett J.R. (2008). Tissue-specific role of glycogen synthase kinase 3beta in glucose homeostasis and insulin action. *Mol Cell Biol*., 28(20): 6314-28.

24) Chen S, Sega M, Agarwal A. (2004). “Lumen digestion” technique for isolation of aortic endothelial cells from heme oxygenase-1 knockout mice. *Biotechniques.*, 37(1):84-6.

25) Venegas-Pino D.E, Banko N, Khan M.I, Shi Y, Werstuck G.H. (2013). Quantative analysis and characterization of atherosclerotic lesions in the murine aortic sinus. *J Vis Exp.*, (82):50933.

26) Kisanuki Y.Y, Hammer R.E, Miyazaki J, Williams S.C, Richardson J.A, Yanagisawa. (2001). Tie2Cre transgenic mice: a new model for endothelial cell-lineage analysis in vivo. *Dev Biol*., 230(2):230-42.

27) Wand Q.M, Park I.K, Fiol C.J, Roach P.J, DePaoli-Roach A.A. (1994). Isoform differences in substrate recognition by glycogen synthase kinase 3 alpha and 3 beta in phosphorylation of phosphatase inhibitor 2. *Biochemistry.,* 33(1):143-7.

28) Soutar M.P.M, Kim W-Y, Williamson R, Peggie M, Hastie C.J, Mclauchlan H, Snider W.D, Gordon-Weeks P.R, Sutherland C. (2010). Evidence that glycogen synthase kinase-3 isoforms have distinct substrate preference in the brain. *J Neurochem.*, 115(4):974-83.

29) Sun C, He B, Sun M, Lv X, Wang F, Chen J, Zhang J, Ye Z, Wen J, Liu P. (2021). Yes-Associated Protein in Atherosclerosis and Related

Complications: A Potential Therapeutic Target That Requires Further Exploration. *Front Cardiovasc Med.*, 8:704208.

30) Mestas J, Ley K. (2008). Monocyte-endothelial cell interactions in the development of atherosclerosis. *Trends Cardiovasc Med.*, 18(6):228-32.

31) Jebari-Benslaiman S, Galicia-García U, Larrea-Sebal A, Olaetxea J.R, Alloza I, Vandenbroeck K, Benito-Vicente A, Martín C. (2022). Pathophysiology of Atherosclerosis. *Int J Mol Sci.*, 23:6):3346

32) Cybulsky M.I, Iiyama K, Li H, Zhu S, Chen M, Iiyama M, Davis V, Gutierrez-Ramos. J-C, Connelly P.W, Milstone D.S. (2001). A major role for VCAM-1, but not ICAM-1, in early atherosclerosis. *J Clin Invest.*, 107(10):1255-1262.

33) Wagner F.F, Benajiba L, Campbell A.J, Weïwer M, Sacher J.R, Gale J.P, Ross L, Puissant A, Alexe G, Conway A, Back M, Pikman Y, Galinsky I, DeAngelo A.J, Stone R.M, Kaya T, Shi X, Robers M.B, Machleidt T, Wilkinson J, Hermine O, Kung A, Stein A.J, Lakshminarasimhan D, Hemann M.T, Solnick E, Zhang Y-L, Pan J.Q, Stegmaier K, Holson E.B. (2018). Exploiting an Asp-Glu “switch” in glycogen synthase kinase 3 to design paralog-selective inhibitors for use in acute myeloid leukemia. *Sci Transl Med.*, 10(431).

5.8 SUPPLEMENTARY MATERIAL FOR CHAPTER 5

Supplementary Figure 5.1: Characterizing the endothelial/macrophage GSK3α/β knockout mouse model. A Gene expression of GSK3α and GSK3β was assessed in macrophages, lung, liver, skeletal muscle and ECs from GSK3α$^{fl/fl}$ LDLR$^{-/-}$ and Tie2Cre GSK3α$^{fl/fl}$ LDLR$^{-/-}$ mice. **B** Gene expression of GSK3α/β was assessed in macrophages, lung, liver, skeletal muscle and ECs from GSK3β$^{fl/fl}$ LDLR$^{-/-}$ and Tie2Cre GSK3α$^{fl/fl}$ LDLR$^{-/-}$ mice. Gene expression was normalised to a β-actin control. **C** To verify that the cells isolated from murine aortas were, in fact, ECs, the expression of endothelial marker, vWF was assessed. n=3-7 (**A-C**). *P<0.05, **P<0.005, ***P<0.0005, ****P<0.00005. ns=not significant.

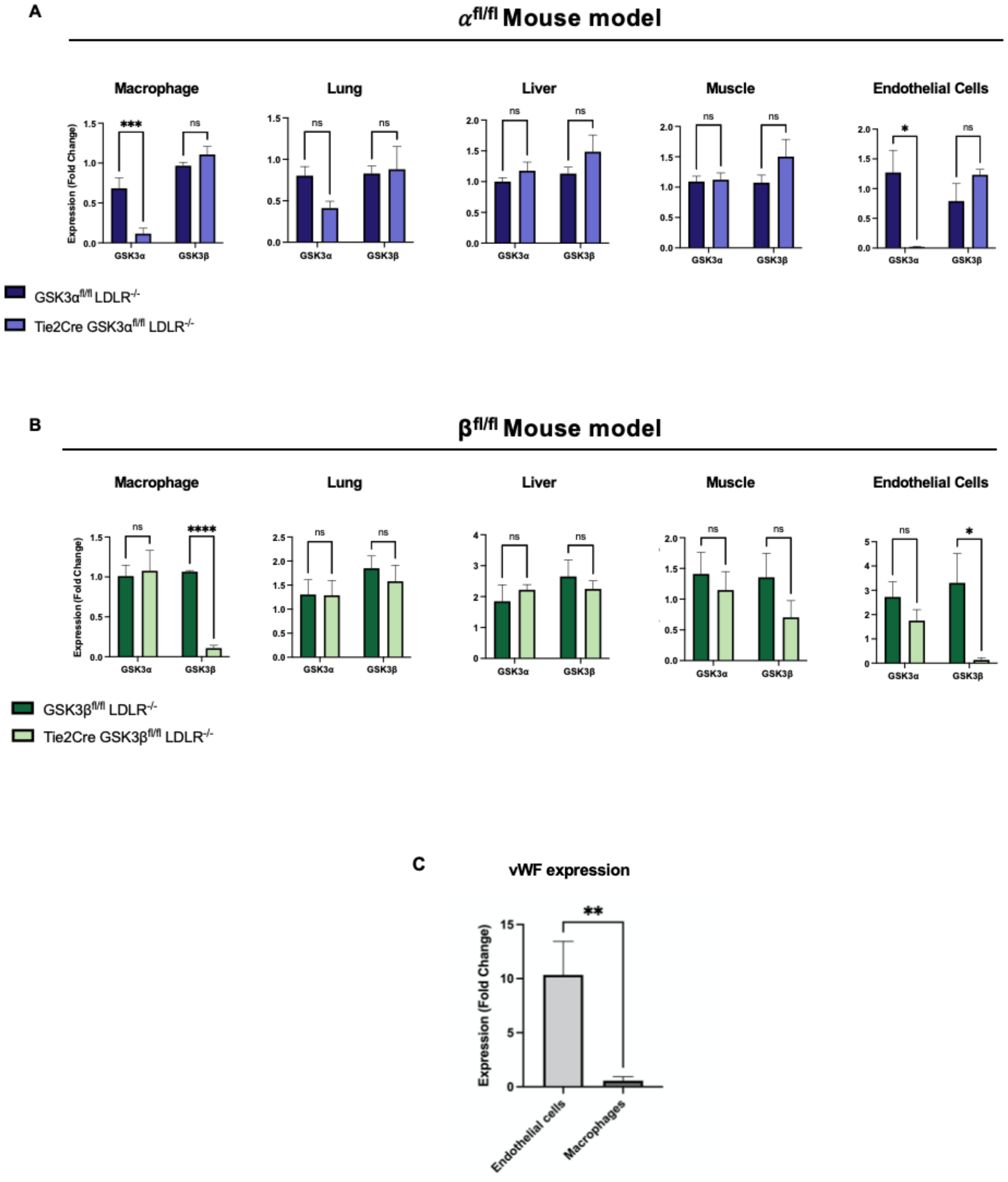
A
$\alpha^{fl/fl}$ Mouse model
Macrophage
Lung
Liver
Muscle
Endothelial Cells
Expression (Fold Change)
***
*
ns
GSK3α
GSK3β
GSK3α$^{fl/fl}$ LDLR$^{-/-}$
Tie2Cre GSK3α$^{fl/fl}$ LDLR$^{-/-}$
B
$\beta^{fl/fl}$ Mouse model
Macrophage
Lung
Liver
Muscle
Endothelial Cells
Expression (Fold Change)
****
*
ns
GSK3α
GSK3β
GSK3β$^{fl/fl}$ LDLR$^{-/-}$
Tie2Cre GSK3β$^{fl/fl}$ LDLR$^{-/-}$
C
vWF expression
Expression (Fold Change)
**
Endothelial cells
Macrophages

Supplementary Figure 5.2: Confirmation that BMT restored GSK3α and GSK3β in macrophages. A PCR analysis of genomic DNA from blood cells from BMT GSK3α$^{fl/fl}$ LDLR$^{-/-}$, LDLR$^{-/-}$, GSK3α$^{fl/fl}$ LDLR$^{-/-}$, and Tie2Cre GSK3α$^{fl/fl}$ LDLR$^{-/-}$ mice. Results confirm that BMT mice have the GSK3α wildtype (WT) gene restored. **B** RT-PCR analysis of GSK3α/β expression in macrophages isolated from BMT GSK3α$^{fl/fl}$ LDLR$^{-/-}$,BMT Tie2Cre GSK3α$^{fl/fl}$ LDLR$^{-/-}$, BMT GSK3β$^{fl/fl}$ LDLR$^{-/-}$, and BMT Tie2Cre GSK3β$^{fl/fl}$ LDLR$^{-/-}$ mice after a BMT. n=3 (**B**). ns=not significant.

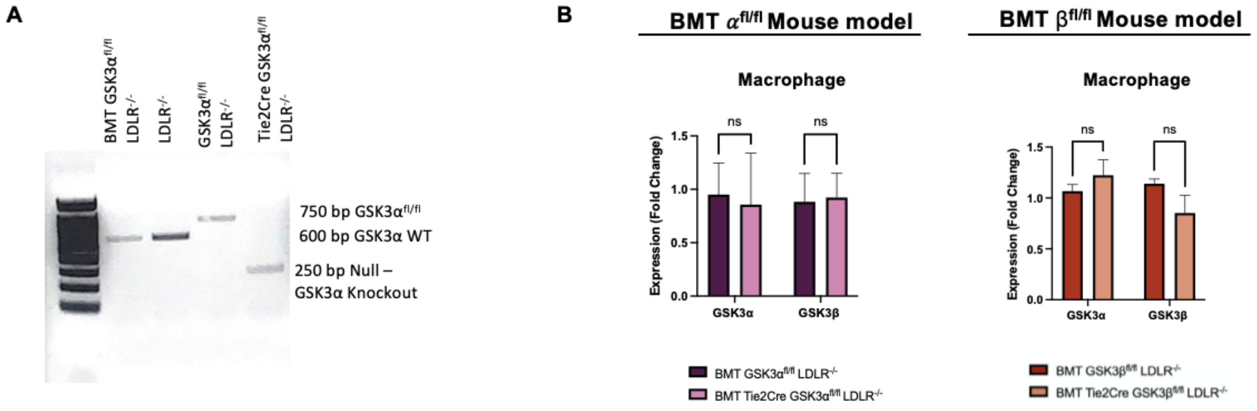
A
BMT GSK3α$^{fl/fl}$ LDLR$^{-/-}$
LDLR$^{-/-}$
GSK3α$^{fl/fl}$ LDLR$^{-/-}$
Tie2Cre GSK3α$^{fl/fl}$ LDLR$^{-/-}$
750 bp GSK3α$^{fl/fl}$
600 bp GSK3α WT
250 bp Null – GSK3α Knockout
B
BMT α$^{fl/fl}$ Mouse model
Macrophage
Expression (Fold Change)
1.5
1.0
0.5
0.0
ns
ns
GSK3α
GSK3β
BMT GSK3α$^{fl/fl}$ LDLR$^{-/-}$
BMT Tie2Cre GSK3α$^{fl/fl}$ LDLR$^{-/-}$
BMT β$^{fl/fl}$ Mouse model
Macrophage
Expression (Fold Change)
1.5
1.0
0.5
0.0
ns
ns
GSK3α
GSK3β
BMT GSK3β$^{fl/fl}$ LDLR$^{-/-}$
BMT Tie2Cre GSK3β$^{fl/fl}$ LDLR$^{-/-}$

Supplementary Figure 5.3: Experimental design. A Experimental plan for analysis of endothelial/macrophage GSK3 knockout mice. Genotyped mice were placed on a HFD for 3 weeks and harvested at 15 weeks of age. **B** Experimental plan for BMT endothelial GSK3α/β knockout mice. Genotyped mice received a BMT at 8 weeks of age. After 4 weeks of recovery the mice were placed on a HFD for 3 weeks and harvested at 15 weeks of age.*Figure created using Biorender.com 2022.*

A Endothelial/macrophage GSK3α or GSK3β knockout mouse model

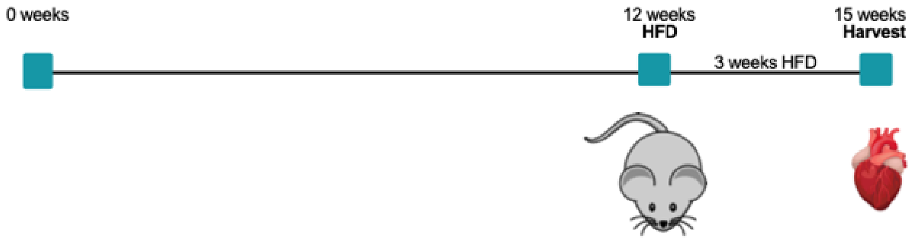
0 weeks
12 weeks
HFD
3 weeks HFD
15 weeks
Harvest

B BMT - Endothelial GSK3α or GSK3β knockout mouse model

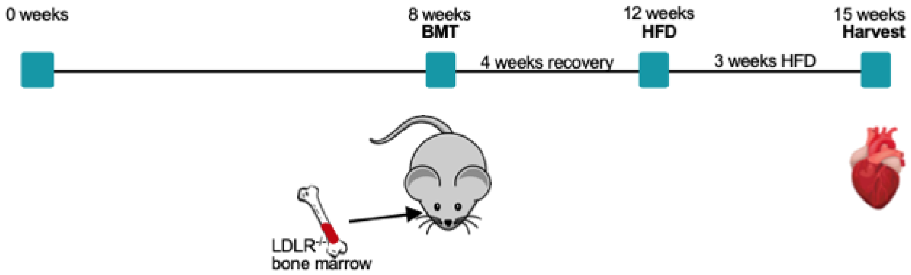
0 weeks
8 weeks
BMT
4 weeks recovery
12 weeks
HFD
3 weeks HFD
15 weeks
Harvest
LDLR-/-
bone marrow

Supplementary Figure 5.4: Negative controls for immunofluorescence and immunohistochemistry staining. A Pre-immune IgG rabbit was used in place of primary antibody as a negative control for both E-selectin and VCAM-1 staining. Pre-immune IgG rat was used in place of primary antibody as a negative control for Mac-3 staining. Pre-immune IgG mouse was used in place of primary antibody as a negative control for P-selectin staining**. B** Pre-immune goat IgG was used in place of the primary antibody for a negative control for ICAM-1 staining. Scale bar represents 100µm.

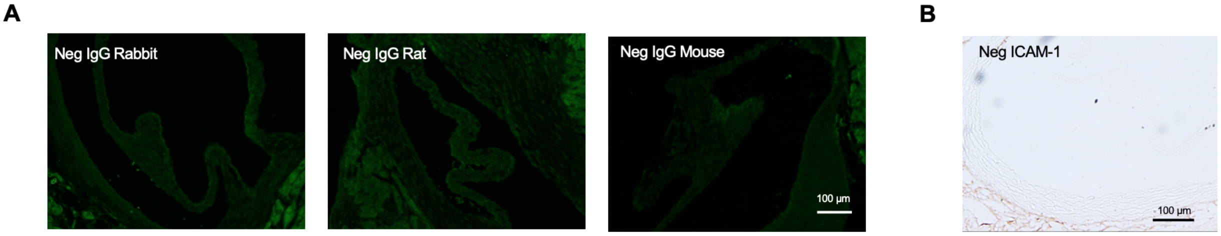
A
Neg IgG Rabbit
Neg IgG Rat
Neg IgG Mouse
100 µm
B
Neg ICAM-1
100 µm

Supplementary Figure 5.5: Atherosclerosis in control mice from the endothelial/macrophage GSK3α/β knockout mouse model. A Representative images of aortic sinus cross sections from 15 week old control LDLR$^{-/-}$, Tie2Cre LDLR$^{-/-}$, GSK3α$^{fl/fl}$ LDLR$^{-/-}$ and GSK3β$^{fl/fl}$ LDLR$^{-/-}$ mice stained with Masson's trichrome. Scale bar represents 100μm. **B** Plaque volume quantification in the aortic sinus of control mice. n=4-8 (**B)**. ns=not significant.

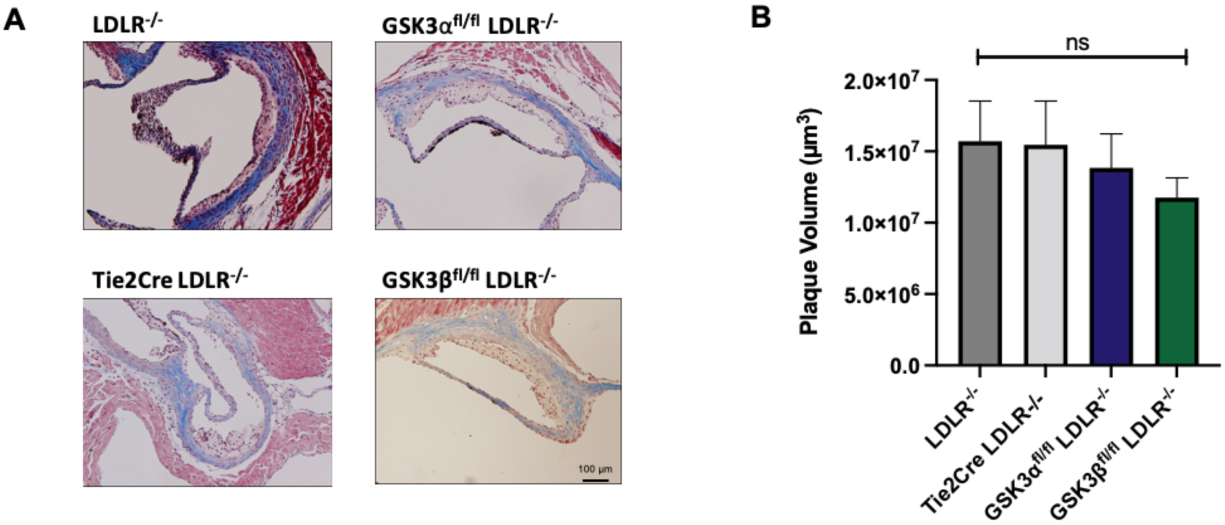
A
LDLR-/-
GSK3αfl/fl LDLR-/-
Tie2Cre LDLR-/-
GSK3βfl/fl LDLR-/-
100 µm
B
ns
2.0×10^7
1.5×10^7
1.0×10^7
5.0×10^6
0.0
Plaque Volume (µm^3)
LDLR-/-
Tie2Cre LDLR-/-
GSK3αfl/fl LDLR-/-
GSK3βfl/fl LDLR-/-

Supplementary Figure 5.6: Co-staining of adhesion protein and vWF. Representative images of aortic cross sections stained with antibodies against vWF and P-selectin, E-selectin or VCAM-1. Green represents the adhesion proteins (P-selectin, E-selectin of VCAM-1), red represents vWF staining and blue represents DAPI. Yellow represents where both proteins are present. Scale bar represents 50μm.

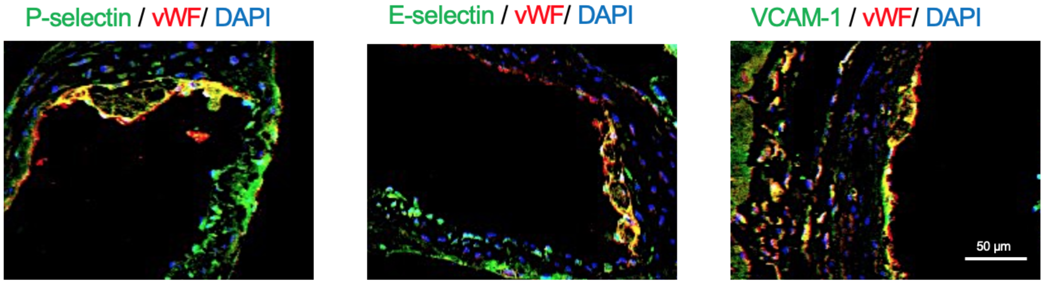

P-selectin / vWF/ DAPI

E-selectin / vWF/ DAPI

VCAM-1 / vWF/ DAPI

Supplementary Figure 5.7: Atherosclerosis assessment comparison between non-BMT mice and BMT mice. Plaque volume quantification in the aortic sinus of non-BMT mice and BMT mice in LDLR$^{-/-}$ mice, α$^{fl/fl}$ mouse model and the β$^{fl/fl}$ mouse model. n=4-10, *<P 0.05, **<P0.05.

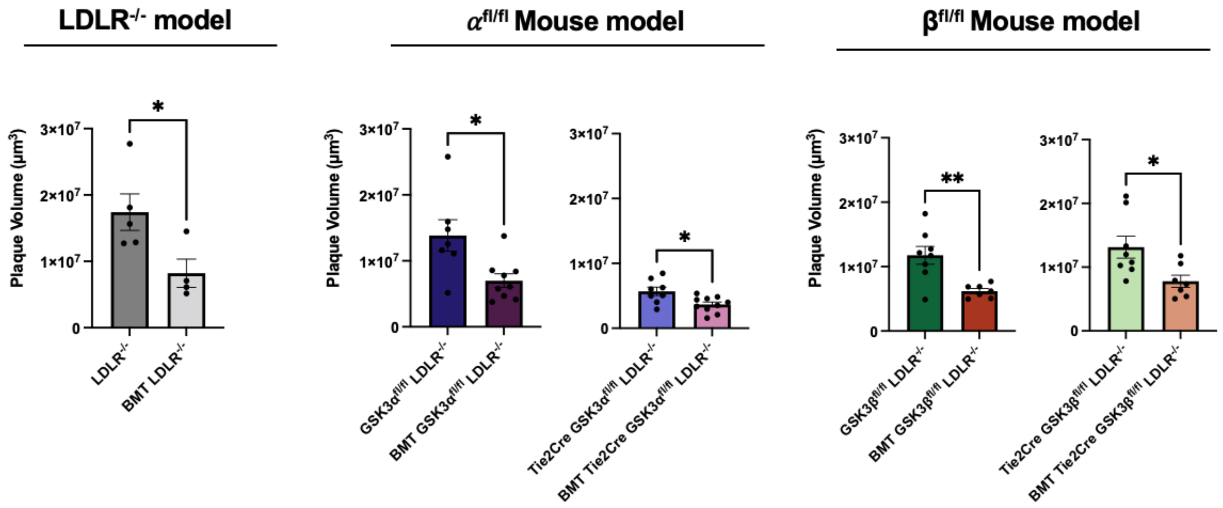
LDLR-/- model
αfl/fl Mouse model
βfl/fl Mouse model
Plaque Volume (μm3)
3×10^7
2×10^7
1×10^7
0
*
**
LDLR-/-
BMT LDLR-/-
GSK3αfl/fl LDLR-/-
BMT GSK3αfl/fl LDLR-/-
Tie2Cre GSK3αfl/fl LDLR-/-
BMT Tie2Cre GSK3αfl/fl LDLR-/-
GSK3βfl/fl LDLR-/-
BMT GSK3βfl/fl LDLR-/-
Tie2Cre GSK3βfl/fl LDLR-/-
BMT Tie2Cre GSK3βfl/fl LDLR-/-

Supplementary Figure 5.8: Atherosclerosis assessment in control mice from the BMT endothelial GSK3α/β knockout mouse model. A Representative images of Masson's trichrome staining of aortic sinus cross sections from 15 week old control BMT LDLR$^{-/-}$, BMT Tie2Cre LDLR$^{-/-}$, BMT GSK3α$^{fl/fl}$ LDLR$^{-/-}$ and BMT GSK3β$^{fl/fl}$ LDLR$^{-/-}$ mice. Scale bar represents 100μm. **B** Plaque volume quantification in the aortic sinus of control mice. n=4-9, ns=not significant.

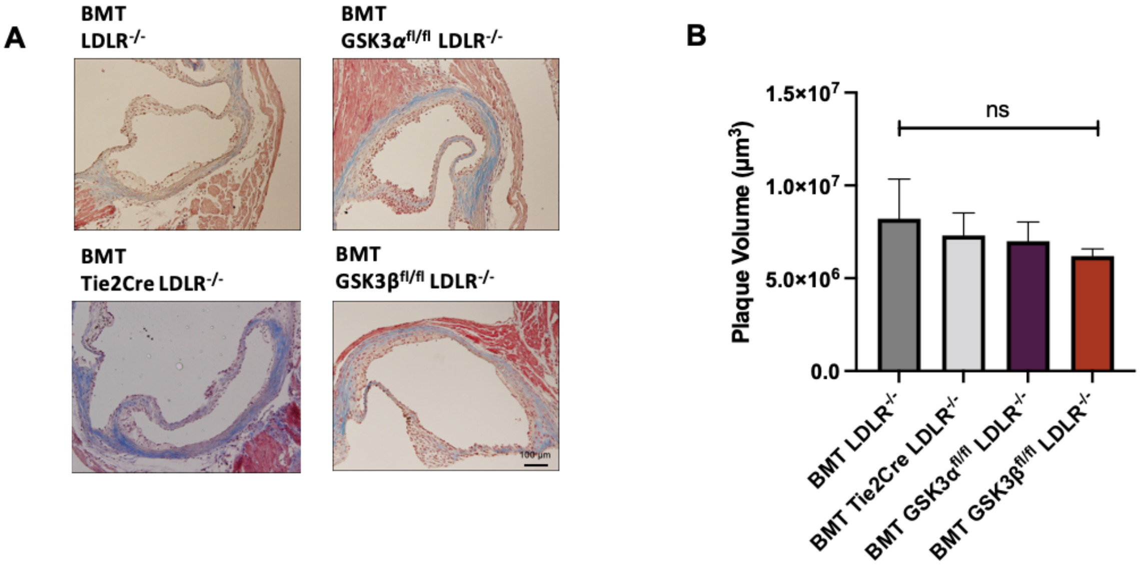
A
BMT LDLR$^{-/-}$
BMT GSK3α$^{fl/fl}$ LDLR$^{-/-}$
BMT Tie2Cre LDLR$^{-/-}$
BMT GSK3β$^{fl/fl}$ LDLR$^{-/-}$
100 μm
B
Plaque Volume (μm^3)
1.5×10^7
1.0×10^7
5.0×10^6
0.0
ns
BMT LDLR$^{-/-}$
BMT Tie2Cre LDLR$^{-/-}$
BMT GSK3α$^{fl/fl}$ LDLR$^{-/-}$
BMT GSK3β$^{fl/fl}$ LDLR$^{-/-}$

CHAPTER 6: General Discussion

Cardiovascular disease (CVD) is presently the leading cause of death worldwide. Atherosclerosis is a major underlying cause of CVD[169,170]. Risk factors that are known to increase the risk of developing atherosclerosis and CVD include; hyperglycemia, dyslipidemia, hypertension, obesity and smoking[171]. Despite advancements in research, as well as the development of medications for the treatment of CVD risk factors, mortality related to atherosclerotic CVD continues to rise[172].

The INTERHEART study identified diabetes as a risk factor for CVD[171]. Diabetic patients have a 2-4 fold increased risk of developing CVD, compared to individuals without diabetes. It is estimated that up to 80% of diabetes related deaths are due to CVD[173]. Diabetes is characterized by elevated glucose levels[174], therefore it has been suggested that elevated glucose levels may directly cause vascular complications associated with the development of CVD. This is supported by research identifying hyperglycemia as an independent risk factor for CVD[175,176,177]. The purpose of the research detailed in this thesis is to begin to identify a potential mechanism by which CVD risk factors, including hyperglycemia and dyslipidemia, activate endothelial cells (ECs) to initiate atherosclerosis. Understanding these pathways will facilitate the identification of new therapeutic targets for CVD prevention.

Briefly, the three manuscripts in this thesis outline:

1) The effects of hyperglycemia on early endothelial activation and the initiation of atherosclerosis (published in *Am J Pathol* 2022).
2) Investigating the effects of elevated glucose concentration on human aortic endothelial cell activation (in preparation for submission).
3) Investigating the role of endothelial GSK3α/β in atherogenesis (submitted to *Int J Mol Sci,* 2022).

Hyperglycemia causes early EC activation

The findings presented in Chapter 3 suggest a direct role for hyperglycemia in early EC activation, and the initiation of atherogenesis. Our results show that 25 week old hyperglycemic and dyslipidemic mice ($ApoE^{-/-}Ins2^{+/akita}$) present with increased plaque size, compared to age matched dyslipidemic controls ($ApoE^{-/-}$ mice). This is consistent with previous reports showing that hyperglycemia can accelerate the development of atherosclerosis[159,178,179,180,181,182]. Adhesion protein expression was assessed and compared in 5 and 25 week old $ApoE^{-/-}Ins2^{+/akita}$ and $ApoE^{-/-}$ mice using immunofluorescence staining techniques. Results suggest that at 5 weeks of age, before detection of plaque development, hyperglycemic mice have increased endothelial expression of P-selectin, E-selectin and VCAM-1 in the aortic sinus. To determine the specific role of hyperglycemia, in the absence of dyslipidemia, atherosclerosis and endothelial activation were assessed in hyperglycemic, normolipidemic ApoE$^{+/-}$Ins2$^{+/akita}$ mice. At 5 weeks and 25 weeks of age, no atherosclerosis was detectable in either ApoE$^{+/-}$Ins2$^{+/akita}$ or ApoE$^{+/-}$ mice, suggesting that hyperglycemia is not sufficient to promote atherogenesis in the absence of dyslipidemia. ApoE$^{+/-}$Ins2$^{+/akita}$ mice had elevated P-selectin, E-selectin and VCAM-1 expression on ECs located in the aortic sinus at 5 and 25 weeks of age, and increased monocyte/macrophage recruitment to the EC layer, relative to normoglycemia, normolipidemic ApoE$^{+/-}$ controls. This suggests that elevated glucose concentrations are sufficient to activate EC, however, in the absence of dyslipidemia, no detectable plaque is formed. Treatment with an SGLT-2 inhibitor significantly reduced blood glucose levels in the ApoE$^{+/-}$Ins2$^{+/akita}$ mice. This reduction in blood glucose was associated with a significant reduction of P-selectin, E-selectin, VCAM-1, as well as monocyte/macrophage recruitment. These findings suggest that regulating/reducing glucose levels will directly improve EC health and may block the initiation of atherosclerosis. A summary of the findings from this Chapter is shown in Figure 6.1.

Figure 6.1: Summary of findings from Chapter 3. In vitro and in vivo studies suggest that hyperglycemia causes EC activation. In vivo, evidence for the functionality of the activated endothelium is supported by increased monocyte infiltration and accelerated atherogenesis. Hyperglycemia is sufficient to induce endothelial activation, however dyslipidemia is required for accelerate plaque development. Blood glucose lowering with an SGLT-2 inhibitor attenuates EC activation and decreased monocyte attachment in mice. *Figure created using Biorender.com 2022.*

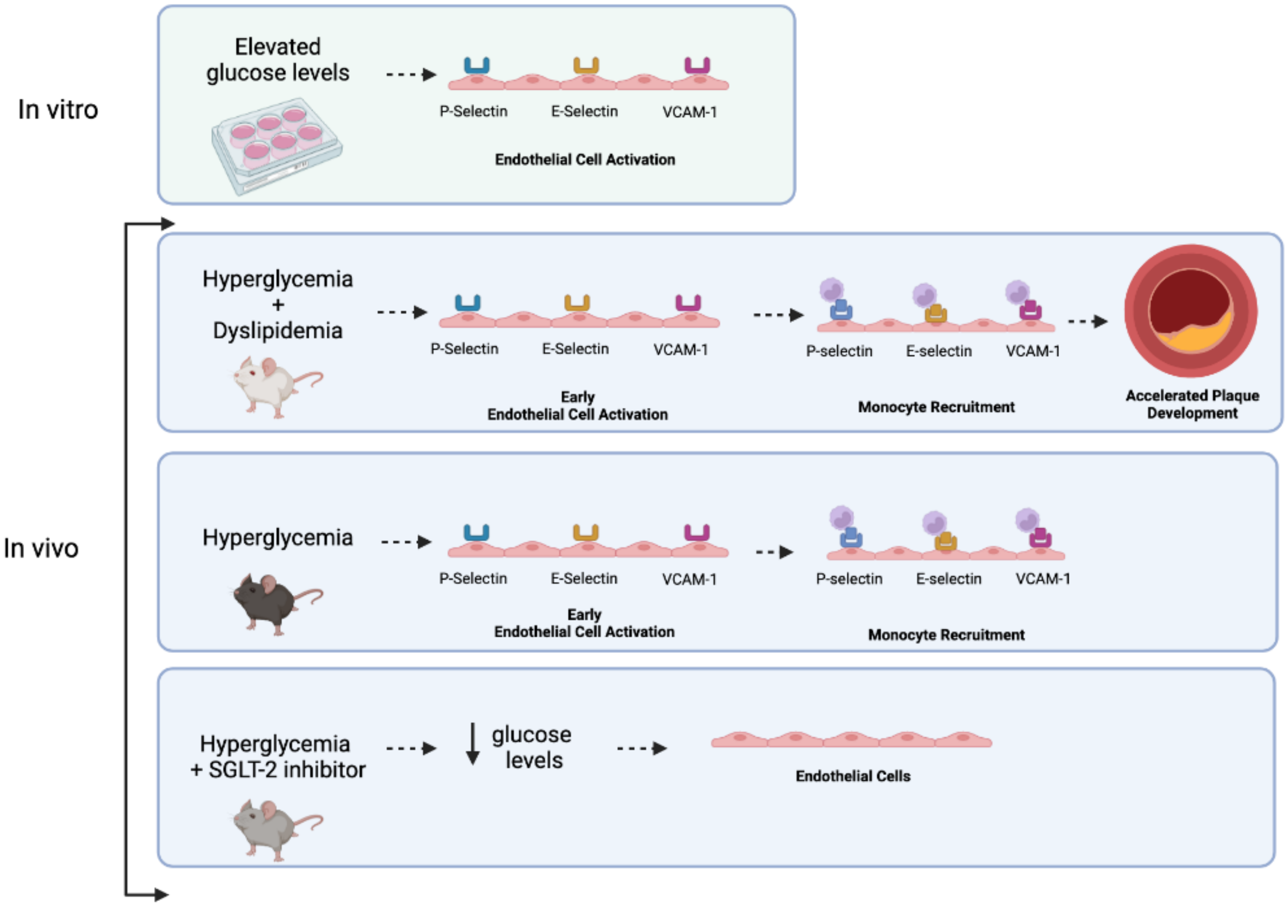
In vitro
Elevated glucose levels
P-Selectin
E-Selectin
VCAM-1
Endothelial Cell Activation
In vivo
Hyperglycemia + Dyslipidemia
P-Selectin
E-Selectin
VCAM-1
Early Endothelial Cell Activation
P-selectin
E-selectin
VCAM-1
Monocyte Recruitment
Accelerated Plaque Development
Hyperglycemia
P-Selectin
E-Selectin
VCAM-1
Early Endothelial Cell Activation
P-selectin
E-selectin
VCAM-1
Monocyte Recruitment
Hyperglycemia + SGLT-2 inhibitor
↓ glucose levels
Endothelial Cells

Previous work has assessed the effects of hyperglycemia on the vasculature. Children with type 1 diabetes showed increased intima-medial thickening and lower flow mediated dilation compared to non-diabetic controls[183]. The outcome of this study suggested that endothelial dysfunction is present in type 1 diabetic children and may predispose them for early development of CVD[183]. A multicenter study assessed the risk of non-lipid related CVD risk factors, including dysglycemia[184]. The outcome showed that individuals with impaired glucose levels had more extensive fatty streaks in the right coronary artery[184]. These studies suggest a role of hyperglycemia in early endothelial activation and monocyte/macrophage infiltration to the subendothelium.

Previous work done on mice had shown that hyperglycemia accelerates plaque development in ApoE$^{-/-}$Ins2$^{+/akita}$ mice[178]. This increase in plaques volume was also seen in other hyperglycemic mouse models using streptozotocin (STZ) injections, to eliminate pancreatic beta cells[179], and induce hyperglycemia in ApoE$^{-/-}$ mice[159,180,181,182]. However, EC activation was not accessed in these models. EC activation is considered to be the earliest stage in atherogenesis, therefore it is important to understand how hyperglycemia interacts and affects ECs.

In this study, EC activation has been defined as the significant up regulation of the expression of adhesion proteins, including P-selectin, E-selectin and VCAM-1. A previous study investigated the specific contribution of individual adhesion proteins by knocking out ICAM-1, P-selectin or E-selectin in ApoE$^{-/-}$ mice. Mice with any one of the individual adhesion proteins knockout showed significantly smaller atherosclerotic lesions[185]. Another study knocked out ICAM-1 and knocked down VCAM-1 in LDLR$^{-/-}$ mice[64],as a knockout of VCAM-1 is embryonically lethal[186,187]. In this model, VCAM-1 mRNA and protein levels were knocked down to 2-8%[64]. This study revealed that mice with VCAM-1 deficiency showed reduced atherosclerotic lesion volume whereas ICAM-1 deficient mice showed no difference in atherosclerotic lesion formation[64]. This suggests a more important role of VCAM-1 in the initiation of atherosclerosis in LDLR$^{-/-}$ mice[64]. Studies performed in mice have looked at the importance of endothelial activation in the context of dyslipidemia and atherosclerosis, however there has been limited focus on how hyperglycemia affects EC activation.

SGLT-2 inhibitors are currently FDA approved for clinical use in the treatment of type 2 diabetes[188,189,190]. SGLT-2 inhibitors are used to lower blood glucose levels by suppressing glucose reabsorption in the proximal convoluted tubule of the kidney[191]. Recent studies showed that SGLT-2 inhibitors improve CVD outcomes, as well as reduce body weight, however the mechanisms underlying the cardiovascular benefit are not fully understood[192,193,194,195]. It has been suggested in some clinical trials, that the use of SGLT-2 inhibitors were successful in improving endothelial function[196,197,198,199].

Taken together, research to date has outlined the importance of hyperglycemia and vascular interactions/complications. Chapter 3 outlines that adhesion proteins are upregulated in responses to elevated glucose levels. This allows recruitment of monocytes and the initiation of atherogenesis earlier than in normoglycemic controls. This may explain, at least in part, why hyperglycemic mice have larger plaques compared to normoglycemic sex and age matched controls. The finding that the activation of ECs is reversible after glucose levels are reduced supports the importance of blood glucose control to prevent CVD.

CVD risk factors may cause EC activation by signalling through the endoplasmic reticulum (ER) stress-glycogen synthase kinase (GSK)3α/β pathway

Chapter 4 investigates a potential pathway by which hyperglycemia, and potentially other CVD risk factors, may upregulate adhesion protein expression and therefore accelerate atherosclerosis. In this study, cultured HAEC cells showed increased P-selectin, E-selectin, and VCAM-1 expression when exposed to elevated glucose concentrations. The expression of ER stress response proteins, GRP78 and calreticulin, were also induced by exposure to elevated glucose concentration. The addition of 4-PBA, an ER stress inhibitor, or tideglusib, a GSK3α/β inhibitor, reduced adhesion protein expression in HAEC treated with elevated glucose. This suggests a role of ER stress and GSK3α/β in EC activation.

As expected, treatment with 4-PBA also reduced the expression of ER stress markers (calreticulin and GRP-78) suggesting that 4-PBA was alleviating ER stress. In contrast, HAEC treated with tideglusib showed no change in calreticulin and GRP-78 expression, compared to untreated HAEC. This suggests that GSK3α/β is downstream of the adaptive ER stress response, a finding that is consistent with previous reports[144,182,200].

A THP-1 monocyte adhesion assay was performed to assess the functionality of the adhesion protein expression on HAEC under elevated glucose concentrations. Results show that HAECs cultured in elevated glucose concentrations had enhanced THP-1 cell attachment compared to normal glucose controls. Additionally the treatment of HAECs with 4-PBA or tideglusib reduced adhesion of THP-1 cells. The results from this study are consistent with the in vivo data presented in Chapter 3 - that elevated glucose levels are sufficient to elevate functional adhesion protein expression and monocyte binding. In addition, this study shows that alleviation of ER stress, or GSK3α/β inhibition reduces endothelial activation and reduces recruitment of monocytes. Together, these data suggest that hyperglycemia causes endothelial activation through the ER stress-GSK3α/β pathway (Figure 6.2).

Figure 6.2: Summary of findings from Chapter 4. In vitro studies showed that elevated glucose levels cause an increase in calreticulin and GRP78 (ER stress markers), elevated gene expression of P-selectin, E-selectin and VCAM-1, and an increase in monocyte recruitment. The addition of 4-PBA reduced ER stress and EC activation. The addition of tideglusib to elevated glucose concentrations still showed elevated GRP78 and calreticulin, however there was a decrease in EC activation. Findings summarized in this paper suggest that elevated glucose levels cause signalling through ER stress-GSK3α/β resulting in the activation of ECs and the recruitment of monocytes. This may be a mechanism by which hyperglycemia causes accelerated atherosclerosis. *Figure created using Biorender.com 2022.*

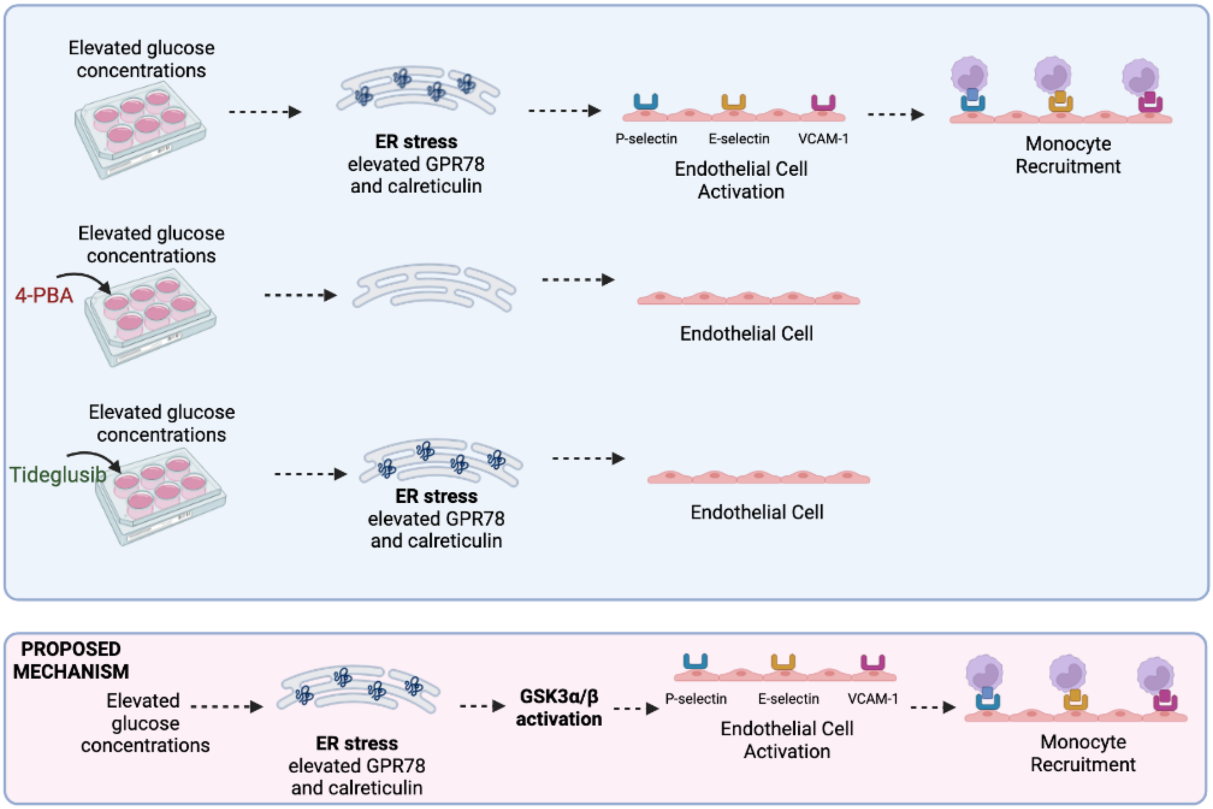
Elevated glucose concentrations
ER stress
elevated GPR78 and calreticulin
P-selectin
E-selectin
VCAM-1
Endothelial Cell Activation
Monocyte Recruitment
Elevated glucose concentrations
4-PBA
Endothelial Cell
Elevated glucose concentrations
Tideglusib
ER stress
elevated GPR78 and calreticulin
Endothelial Cell
PROPOSED MECHANISM
Elevated glucose concentrations
ER stress
elevated GPR78 and calreticulin
GSK3α/β activation
P-selectin
E-selectin
VCAM-1
Endothelial Cell Activation
Monocyte Recruitment

A definitive mechanism associating CVD risk factors, in this case specifically hyperglycemia, and EC activation is presently unknown. Risk factors of CVD have been shown to promote ER stress and ER stress has been identified at every stage of plaque development[201]. Atherosclerotic mice lacking the ER stress effector CHOP were shown to have a reduction in atherosclerotic lesion volume at the aortic sinus[202]. 4-PBA is FDA approved for clinical use and is currently used to treat patients with urea disorders[203]. It is an ER stress alleviator that prevents the aggregation of unfolded proteins[203]. Supplementation with 4-PBA attenuates atherosclerosis in ApoE$^{-/-}$ and LDLR$^{-/-}$ mice[204,205]. In a study using hyperglycemic rats, it was shown that reduction of ER stress improved endothelial function, assessed by the vessel's ability to vasodilate[206]. Atherosclerosis was not a part of this study. These findings suggest ER stress promotes atherosclerosis progression and alters endothelial function.

GSK3α/β is thought to lie downstream of ER stress and contribute to atherosclerosis progression[132, 144,182,207]. Tideglusib is a pan GSK3α/β inhibitor that was originally developed for the treatment of neurological disorders[208,209]. Presently, tideglusib is being used in clinical trials for congenital myotonic dystrophy and amyotrophic lateral sclerosis[210,211,212]. Currently there is limited research on GSK3α/β inhibition and its relation to EC activation. In vitro research has suggested GSK3β expression in ECs is increased under elevated glucose concentrations[213]. In this study there was no assessment of EC activation.

Another study involved the treatment of HUVEC with TNFα (responsible for the upregulation of adhesion proteins), and saw an elevation in VCAM-1 expression[214]. Inhibition of GSK3α/β in TNFα treated cells reduced VCAM-1 expression[214]. Other adhesion proteins were not assessed in this study. Further investigation is needed to delineate the specific role of GSK3α/β in EC activation.

Additional research is needed to determine if other CVD risk factors cause upregulation of adhesion proteins, and if this is regulated through ER stress-GSK3α/β signalling. This thesis supports the role of ER stress-GSK3α/β signalling and the upregulation of functional adhesion proteins expression (P-selectin, E-selectin, VCAM-1) on HAEC. Together these data identify multiple potential therapeutic targets (including ER stress and/or GSK3α/β) for the treatment of vascular diseases.

GSK3α plays a role in EC activation and atherosclerotic progression

Chapter 5 investigates the specific roles of GSK3α and GSK3β in endothelial activation and atherogenesis in a mouse model. A novel mouse model was created to knockout GSK3α or GSK3β in ECs (Tie2Cre GSK3α$^{fl/fl}$ LDLR$^{-/-}$ or Tie2Cre GSK3β$^{fl/fl}$ LDLR$^{-/-}$). It was discovered that Tie2Cre recombinase was not just restricted to ECs and that GSK3α/β expression in macrophages was also affected. Mice with an endothelial/macrophage GSK3α (Tie2Cre GSK3α$^{fl/fl}$LDLR$^{-/-}$) knockout had reduced plaque volume, and showed reduced EC activation (P-selectin, E-selectin, VCAM-1). The reduction in plaque volume was not surprising as previous studies had shown that macrophage deficiency of GSK3α was sufficient to significantly attenuate plaque growth. In order to delineate the specific role of endothelial GSK3α/β, BMT was used to replenish the myeloid lineage with GSK3α and GSK3β, to create an endothelial selective GSK3α or GSK3β knockout mouse model (BMT Tie2Cre GSK3α$^{fl/fl}$ LDLR$^{-/-}$ or BMT Tie2Cre GSK3β$^{fl/fl}$ LDLR$^{-/-}$). Results from Masson's Trichrome staining analysis showed that endothelial GSK3α knockout mice had reduced plaque volume. Endothelial GSK3α knockout mice also had a reduction in P-selectin, E-selectin and VCAM-1 expression at the aortic sinus. Monocyte /macrophage recruitment was also reduced in GSK3α knockout mice (both endothelial/macrophage and endothelial knockout). Interestingly, across all groups, endothelial/macrophage or endothelial-selective GSK3β knockout mice showed no substantial effect on plaque volume, adhesion protein expression or monocyte/macrophage recruitment. Additionally, ICAM-1 expression remained unaffected by the endothelial/macrophage or endothelial GSK3α/GSK3β knockout in these mice. Overall, the results of this study are consistent with the previous findings and further suggest a specific role for GSK3α in endothelial activation and adhesion protein expression resulting in accelerated atherosclerotic progression (Figure 6.3).

Figure 6.3: Summary of findings from Chapter 5. Both endothelial /macrophage and endothelial GSK3α knockout mice have reduced EC activation, reduced monocyte/macrophage recruitment, and reduced plaque volume, compared to age matched GSK3α LDLR$^{-/-}$ or BMT GSK3α LDLR$^{-/-}$ controls. The overall findings of this study suggest that dyslipidemia activates GSK3α causing EC activation, monocyte recruitment and accelerated atherosclerosis. *Figure created using Biorender.com 2022.*

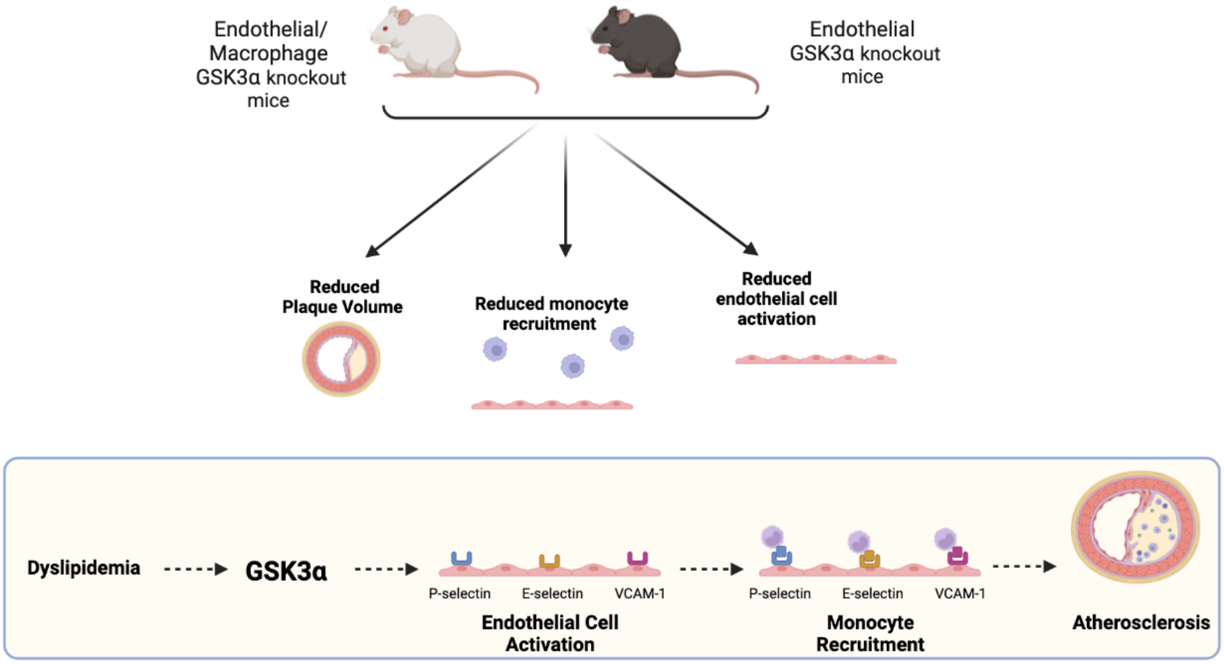
Endothelial/
Macrophage
GSK3α knockout
mice
Endothelial
GSK3α knockout
mice
Reduced
Plaque Volume
Reduced monocyte
recruitment
Reduced
endothelial cell
activation
Dyslipidemia
GSK3α
P-selectin
E-selectin
VCAM-1
Endothelial Cell
Activation
P-selectin
E-selectin
VCAM-1
Monocyte
Recruitment
Atherosclerosis

Presently, the relevant signalling factors lying directly upstream and downstream of GSK3α are unknown. Further research is required to fully understand this pathway and these studies may lead to the identification of even better targets for therapies. Additionally, a greater understanding of the individual role of the isoforms is also required. Previous research has shown that GSK3β is vital for embryonic development and survival in mice[215]. A whole body GSK3α knockout is a viable and fertile mouse model[216]. The role for GSK3α has been suggested in atherosclerosis development. A whole body knockout of GSK3α in an atherosclerotic mouse model attenuated atherosclerosis[144]. Pharmacological inhibition of GSK3α/β (using valproate) reduced plaque volume in dyslipidemic[204], and hyperglycemic/dyslipidemic mice[182]. Another pharmacological inhibition study using lithium to inhibit GSK3α/β in an atherosclerotic mouse model showed a reduction in plaque volume, as well as decrease in VCAM-1 expression and monocyte recruitment[164]. Additionally myeloid specific knockout of GSK3α reduced plaque formation[127] and it was more recently discovered that this knockout can promote atherosclerotic regression[165].

The downstream signalling pathways through which GSK3α activates pro-atherogenic processes are not known. One potential mechanism may involve activation of NF-κB resulting in the upregulation of adhesion protein expression. It has been suggested that GSK3α/β inhibition reduces NF-κB activity in pancreatic cancer cell (PCC) lines[217,218]. Another study using PCC concluded that GSK3α/β maintains NF-κB activity by regulating IKK activity[218]. IKK phosphorylates the inhibitory IκB protein attached to NF-κB[219]. Phosphorylation of IκB results in its disassociation from NF-κB, allowing NF-κB to migrate to the nucleus and initiate gene transcription[219]. Additionally fibroblasts from GSK3β whole body knockout embryos (collected on day 12.5 of gestation) treated with TNFα, showed reduced NF-κB activity compared to wildtype embryos[220]. These studies suggest a role for GSK3α/β and NF-κB activation. One study involved the creation of an atherosclerotic mouse model in which NF-κB was specifically down regulated in EC only. Results suggest that mice with the EC specific NF-κB inhibition had significantly reduced plaques, compared to wildtype controls[221]. Furthermore, NF-κB activation has also been associated with increased adhesion protein expression[222,223,224,225]. Putting this research together, combined with results from this thesis, GSK3α could be increasing adhesion protein expression through NF-κB activation. Further research is required to explore this possibility.

Cre-recombinase technology allowed us to research the individual roles of endothelial GSK3α and GSK3β in the initiation and progression of atherosclerosis, and EC activation in vivo. Research highlighted in this thesis suggests that GSK3α specifically plays a role in EC activation. This was outlined in Chapter 4 and Chapter 5. Inhibition of GSK3α/β in HAEC and a specific knockout of endothelial GSK3α in mice showed reduced expression of adhesion proteins. Chapter 5 concludes that endothelial GSK3α plays a pro-atherogenic role in atherosclerosis progression in mice, whereas GSK3β appears to not play a major role. We believe that CVD risk factors cause EC activation through the ER stress-GSK3α pathway.

Limitations

As with all studies, this research has limitations that should be taken into consideration in future studies. First, there are many CVD risk factors associated with increased risk for CVD. Research outlined in this thesis was limited to the effects of hyperglycemia and dyslipidemia in relation to EC activation and atherosclerosis initiation and progression. Therefore, further research is needed to assess how other CVD risk factors (obesity, hypertension, smoking etc.) also cause EC activation and accelerated atherosclerosis development. The potential role of GSK3α should also be investigated in these models.

Secondly, these studies investigate the potential role of ER stress-GSK3α signalling in the progression of atherosclerosis. Clinically relevant interventions will have to be effective on established atherosclerotic CVD that is usually diagnosed after symptoms are present. Whilst mechanistically interesting and informative, the results of this study do not inform on the potential effects of GSK3α inhibition in existing plaques. Future studies will involve the use of specific small molecule inhibitors for GSK3α and GSK3β[226]. These will permit studies in which specific isoforms are inhibited at particular times during atherosclerosis.

Finally, in these studies, assessment of EC activation is limited to the expression of 4 key proteins, however there are other proteins and EC functions that could be assessed. A more thorough investigation of endothelial activation should be carried out in future research. Other potential endothelial specific markers for future projects could be VE-Cadherin, CD31/PECAM-1 and CD105/endoglin. Other studies could involve the intimal-media thickening[227,228], NO production and the ability of the vessel to vasodilate[228]. These studies will give a more complete picture of the effects of specific interventions and the molecular mechanisms involved.

Future Directions

Future studies should be focused on further exploration of GSK3α to better understand its role in the endothelium as it relates to atherogenesis and, as a potential anti-atherogenic target for CVD therapy.

Specific small molecule inhibitors for GSK3α and GSK3β have been recently created[226]. BRD0705 is the GSK3α specific inhibitor, and BRD3731 is the GSK3β specific inhibitor. These small molecule inhibitors will allow much more flexibility in the investigation of the role(s) of GSK3α/β in atherogenesis.

These studies could be done in LDLR$^{-/-}$ mice, ApoE$^{-/-}$ mice, or any other animal model of atherosclerosis. Additionally, inhibition can be introduced at any point in disease development. This research will allow us to assess the use of pharmacological intervention and inhibition of GSK3α in vivo.

Another future direction would be to identify the relevant downstream factors involved in GSK3α and GSK3β signalling. The direct downstream substrates of GSK3α could be determined using phospho-proteomic analysis. ECs would be collected from Tie2Cre GSK3α$^{fl/fl}$ LDLR$^{-/-}$ (experimental) and GSK3α$^{fl/fl}$ LDLR$^{-/-}$ (control) mice and analysed relative to each other. Phospho-proteomics looks at the differential phosphorylation of proteins. The difference in protein phosphorylation patterns between the two groups would permit the identification of key proteins that are specifically phosphorylated by GSK3α activity. These proteins could then be specifically studied to determine their potential role in EC activation in atherogenesis.

Significance

Atherosclerotic cardiovascular disease is a major health concern in today's society. In order to develop new targeted therapies, cellular and molecular mechanisms that lead to disease initiation and progression need to be understood. The data present in this thesis identifies the association between hyperglycemia and dyslipidemia and ECs activation, as well as a critical role for GSK3α in EC activation and atherosclerotic progression.

Specifically, this thesis outlines;

1. Hyperglycemia (a CVD risk factor) alone is sufficient to cause EC activation. Reduction in glucose levels using an SGLT-2 inhibitor, reduces adhesion protein expression on ECs in an ApoE$^{+/-}$Ins2$^{+/akita}$ mouse model.
2. Hyperglycemia, and potentially other CVD risk factors, cause EC activation by signalling through the ER stress-GSK3α/β pathway.
3. Endothelial GSK3α signalling specifically mediates EC activation and atherosclerosis progression.

EC activation is an important process of atherosclerosis initiation. Observations from this thesis extend our understanding of how CVD risk factors, in particular hyperglycemia and dyslipidemia, may contribute to EC activation and the progression of atherosclerosis (Figure 6.4). Furthermore, this research has uncovered GSK3α as a potential anti-atherogenic target.

Figure 6.4: Summary of the findings from this thesis. CVD risk factors, hyperglycemia and dyslipidemia, cause ER stress. ER stress leads to GSK3α activation (signalling through the PERK pathway was suggested in previous papers[144,182,200,207]). GSK3α activation results in the upregulation of adhesion protein expression, promoting the initiation and progression of atherosclerosis.

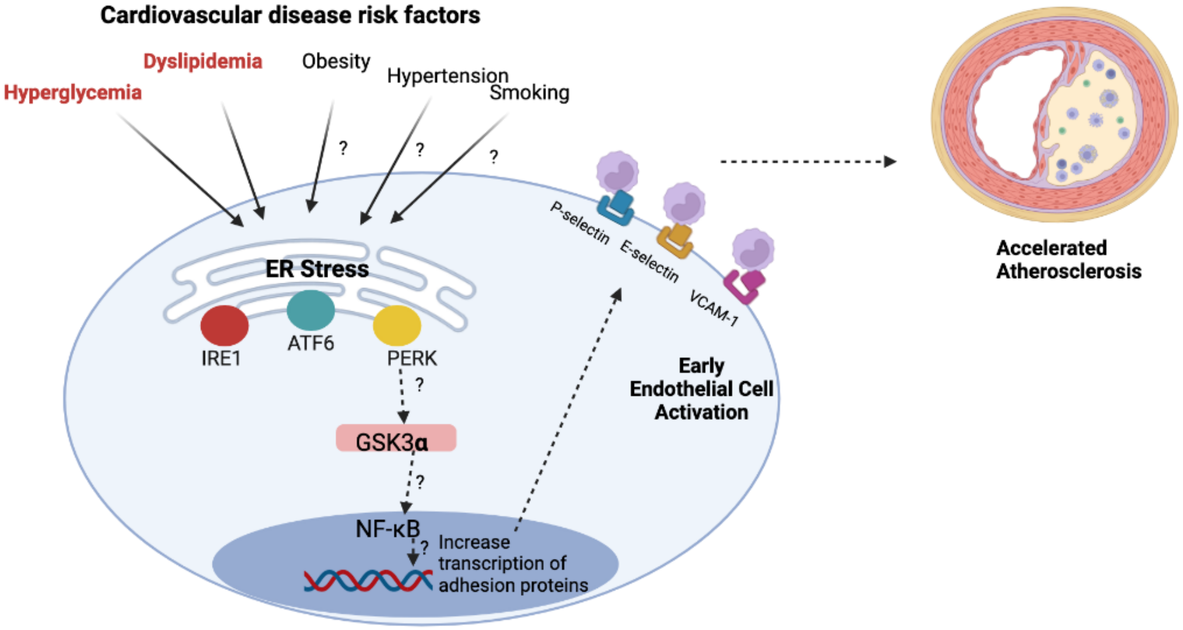
Cardiovascular disease risk factors
Hyperglycemia
Dyslipidemia
Obesity
Hypertension
Smoking
?
?
?
ER Stress
IRE1
ATF6
PERK
?
GSK3α
?
NF-κB
?
Increase transcription of adhesion proteins
P-selectin
E-selectin
VCAM-1
Early Endothelial Cell Activation
Accelerated Atherosclerosis

6.1 REFERENCES FOR INTRODUCTION AND GENERAL DISCUSSION

1) World Health Organization. (2013) Global action plan for prevention and control of noncommunicable diseases 2013-2020.

2) Joseph P, Leong D, McKee M, Anand S.S, Schwal, J-D, Teo K, Mente A, Yusuf S. (2017) Reducing the Global Burden of Cardiovascular Disease, Part 1: The Epidemiology and Risk Factors. *Circ Res.*, 121(6):677-694.

3) Roth G.A, Mensah G.A, Johnson C.O, Addolorato G, Ammirati E, Baddour L.M, Barengo N.C, Beaton A.Z, Benjamin E.J, Benziger C.P, Bonny A, Brauer M, Brodmann M, Cahill T.J, Carapetis J, Catapano A.L, Chung S.S, Cooper L.T, Coresh J, Criqui M, DeCleene N, Eagle K.A, Emmons-Bell S, Feigin V.L, Fernández-Solà J, Fowkes G, Gakidou E, Grundy S.M, He F.J, Howard G, Hu F, Inker L, Karthikeyan G, Kassebaum N, Koroshetz W, Lavie C, Lloyd-Jones D, Lu H.S, Mirijello A, Temesgen A.M, Mokdad A, Moran A.E, Muntner P, Narula J, Neal B, Ntsekhe M, Moraes de Oliveira G, Otto C, Owolabi M, Pratt M, Rajagopalan S, Reitsma M, Ribeiro A.N.P, Rigotti N, Rodgers A, Sable C, Shakil S, Sliwa-Hahnle K, Stark B, Sundström J, Timpel P, Tleyjeh I.M, Valgimigli M, Vos T, Whelton P.K, Yacoub M, Zuhlke L, Murray C, Fuster V. (2020) Global Burden of Cardiovascular Disease and Risk Factors, 1990-2019: Update From the GBD 2019 Study. *J Am Coll Cardiol.,* 76(25):2982-3021.

4) Anand S, Bradshaw C, Prabhakaran D. (2020). Prevention and management of CVD in LMICs: why do ethnicity, culture, and context matter? *BMC Med*., 18(1)7.

5) Powell-Wiley T.M, Poirier P, Burke L.E, Després J-P, Gordon-Larsen P,Lavie C.J, Lear S.A, Ndumele C.E, Neeland I.J, Sanders P, St-Onge M-P. (2021). Obesity and Cardiovascular Disease: A Scientific Statement From the American Heart Association. *Circulation,* 143(21):e983-e1010.

6) Dai S, Bancej C, Bienek A, et al. (2009). Report summary: tracking heart disease and stroke in Canada, 2009. *Chronic Diseases in Canada*, 29 (4): 192-195.

7) Tran D.T, Palfrey D, Welsh R. (2021). The Healthcare Cost Burden in Adults with High Risk for Cardiovascular Disease. *Pharmacoecon Open*, 5(3):425-435.

8) Namara K.M, Alzubaidi H, Jackson J.K. (2019). Cardiovascular disease as a leading cause of death: how are pharmacists getting involved?. *Integr Pharm Res Pract.*, 8:1-11.

9) Dua S, Bhuker M, Sharma P, Dhall M, Kapoor S. (2014) Body mass index relates to blood pressure among adults. *N Am J Med Sci.*, 6(2):89-95.

10) Swarup, S (2021). *Metabolic* syndrome. StatPearl.

11) Tune J.D, Goodwill A.G, Sassoon D.J, Mather K.J. (2017). Cardiovascular consequences of metabolic syndrome. *Transl Res.*,183:57-70.

12) Li X, Zhai Y, Zhao J, He H, Li Y, Liu Y, Feng A, Li L, Huang T, Xu A, Lyu J. (2021). Impact of Metabolic Syndrome and Its Components on Prognosis in Patients With Cardiovascular Diseases: A Meta-Analysis. *Front Cardiovasc Med.*, 8:704145.

13) Dong Z.M, Brown A.A, Wagner D.D. (2000). Prominent role of P-selectin in the development of advanced atherosclerosis in ApoE-deficient mice. *Circulation,*; 101(19):2290-5.

14) Qiao Q, Gao W, Zhang L, Nyamdorj R, Tuomilehto J. (2007). Metabolic syndrome and cardiovascular disease. *Metabolilc syndrome and cardiovascular disease,*44(Pt3):232-63

15) Rippe J.M. (2018). Lifestyle Strategies for Risk Factor Reduction, Prevention, and Treatment of Cardiovascular Disease. *Am J Lifestyle Med.*, 13(2):204-212

16) Sanchis-Gomar F, Perez-Quilis C, Leischik R, Lucia A. (2016). Epidemiology of coronary heart disease and acute coronary syndrome. *Ann Transl Med.*, 4(13):256.

17) Barquera S, Pedroza-Tobías A, Medina C, Hernández-Barrwea L, Bibbins-Domingo K, Lozano R, Moran A.E. (2015). Global Overview of the Epidemiology of Atherosclerotic Cardiovascular Disease. *Arch Med Res.,* 46(5):328-38.

18) Pant S, Deshmukh A, Gurumurthy G.S, Pothineni N.V., Watts T.E., Romeo F, Mehta J.L. (2014). Inflammation and atherosclerosis-revisited. *J Cardiovasc Pharmacol Ther.*, 19(2):170-8.

19) Deaton C, Froelicher E.S., Wu L.H, Ho C, Shishani K, Jaarsma T. (2011) The global burden of cardiovascular disease. *Eur J Cardiovasc Nurs.,* 10 Suppl 2:S5-13.

20) Vakhtangadze T, Tak R.S., Singh U, Baig M.S, Bezsonov E. (2021). Gender Differences in Atherosclerotic Vascular Disease: From Lipids to Clinical Outcomes. *Front Cardiovasc Med.*, 8:707889.

21) Lusis A.J. (2000). Atherosclerosis. *Nature*, 407(6801):233-41.

22) Milutinović A, Šuput D, Zorc-Pleskovič R. (2020). Pathogenesis of atherosclerosis in the tunica intima, media, and adventitia of coronary arteries: An updated review. *Bosn J Basic Med Sci.*, 20(1):21-30.

23) Gimbrone Jr M.A, García-Cardeña G. (2016). Endothelial Cell Dysfunction and the Pathobiology of Atherosclerosis. *Circ Res.*, 118(4):620-36.

24) Bobryshev Y.V. (2006). Monocyte recruitment and foam cell formation in atherosclerosis. *Micron.*, 37(3): 208-22

25) Gui Y, Zheng H, Cao R.Y. (2022). Foam Cells in Atherosclerosis: Novel Insights Into Its Origins, Consequences, and Molecular Mechanisms. *Front Cardiovasc Med.*, 9:845942.

26) Zaman A.G., Helft G, Worthley S.G., Badimon J.J. (2000). The role of plaque rupture and thrombosis in coronary artery disease. *Atherosclerosis,* 149(2):251-66.

27) Sumpio B.E., Riley J.T., Dardik A. (2022). Cells in focus: endothelial cell. *Int J Biochem Cell Biol.*, 34(12):1508-12.

28) Theodorou K, Boon R.A. (2018). Endothelial Cell Metabolism in Atherosclerosis. *Front Cell Dev Biol.*, 6:82.

29) Davignon J, Ganz P. (2004). Role of endothelial dysfunction in atherosclerosis. *Circulation*, 109(23 Suppl 1):III27-32.

30) Krüger-Genge A, Blocki A, Franke R-P, Jung F. (2019). Vascular Endothelial Cell Biology: An Update. *Int J Mol Sci.*, 20(18):411.

31) Bonetti P.P, Lerman L.O, Lerman A. (2003). Endothelial dysfunction: a marker of atherosclerotic risk. *Arterioscler Thromb Vasc Biol.*, 23(2):168-75.

32) Peng Z, Shu B, Zhang Y, Wang M. (2019). Endothelial Response to Pathophysiological Stress. *Arterioscler Thromb Vasc Biol.*, 39(11):e233-e243.

33) Kawashima S, Yokoyama M. (2004). Dysfunction of endothelial nitric oxide synthase and atherosclerosis. *Arterioscler Thromb Vasc Biol.,* 24(6):998-1005.

34) de Winther M.P.J., Kanters E, Kraal G, Hofker M.H. (2005). Nuclear factor KappaB signalling in atherosclerosis. *Arterioscler Thromb Vasc Biol.,* 25(5): 904-14.

35) Liu T, Zhang L, Joo D, Sun S-C. (2017). Nf-κB signalling in inflammation. *Signal Transduct Target Ther.*, 2:17023.

36) Mäkimattila S, Virkamäki A, Groop P.H., Cockcroft J, Utriainen T, Fagerudd J, Yki-Järvinen H. (1996). Chronic hyperglycemia impairs endothelial function and insulin sensitivity via different mechanisms in insulin-dependent diabetes mellitus. *Circulation,* 94(6): 1276-82.

37) Virdis A, Bacca A, Colucci R, Duranti E, Fornai M, Materazzi G, Ippolito C, Bernardini N, Blandizzi C, Bernini G, Taddei S. (2013). Endothelial

dysfunction in small arteries of essential hypertensive patients: role of cyclooxygenase-2 in oxidative stress generation. *Hypertension,* 62(2): 337-44.

38) Steinberg H.O., Bayazeed B, Hook G, Johnson A, Cronin J, Baron A.D. (1997). Endothelial dysfunction is associated with cholesterol levels in the high normal range in humans. *Circulation,* 96(10): 3287-93.

39) Schlager O, Willfort-Ehringer A, Hammer A, Steiner S, Dritsch M, Giurgea A, Margeta C, Lilaj I, Zehetmayer S, Widhalm K, Koppensteiner R, Gschwandtner M.E. (2011). Microvascular function is impaired in children with morbid obesity. *Vasc Med.,* 16(2): 97-102.

40) Xia P, Gamble J.R., Rye K.A, Wang L, Hii C.S, Cockerill P, Khew-Goodall Y, Bert A.g., Barter P.J., Vadas M.A. (1998). Tumor necrosis factor-alpha induces adhesion molecule expression through the sphingosine kinase pathway. *Proc Natl Acad Sci U S A.,* 95(24):14196-201.

41) O’Carroll S.J., Kho D.T, Wiltshire R, Nelson V, Rotimi O, Johnson R, Angel C.E, Graham E.S. (2015). Pro-inflammatory TNFα and IL-1β differentially regulate the inflammatory phenotype of brain microvascular endothelial cells. *J Neuroinflammation.,* 12:131.

42) Josephs S.F., Ichim T.E, Prince S.M, Kesari S, Marincola F.M, Escobedo A.R., Jafri A. (2018). Unleashing endogenous TNF-alpha as a cancer immunotherapeutic. *J Transl Med.,* 31; 16(1): 242.

43) Zelová H, Hošek J. (2013). TNF-α signalling and inflammation: interactions between old acquaintances. *Inflamm Res.,* 62(7): 641-51.

44) Hahne M, Jäger U, Isenmann I, Hallmann R, Vestweber D. (1993). Five tumor necrosis factor factor-inducible cell adhesion mechanisms on the surface of mouse endothelioma cells mediate the binding of leukocytes. *J Cell Biol.*, 121(3):655-64.

45) Ferri C, Desideri G, Valenti M, Bellini C, Pasin M, Santucci A, De Mattia G. (1999). Early upregulation of endothelial adhesion molecules in obese hypertensive men. *Hypertension,* 34(4 Pt 1):568-73.

46) Bourdillon M-C, Randon J, Barek L, Zibara K, Covacho C, Poston R.N, Chignier E, McGregor J.L. (2006). Reduced atherosclerotic lesion size in P-selectin deficient apolipoprotein E-knockout mice fed a chow but not a fat diet. *J Biomed Biotechnol.*, 2006(2):49193.

47) Subramaniam M, Koedam J.A., Wagner D.D. (1993). Divergent fates of P-and E-selectins after their expression on the plasma membrane. *Mol Biol Cell.*, 4(8): 791-801.

48) Valentijn K.M., Sadler J.E, Valentijn J.A, Voorberg J, Eikenboom J. (2011). Functional architecture of Weibel-Palade bodies. *Blood,* 117(19):5033-43.

49) Gupta G.S. (2012). Selectins and Associated Adhesion Proteins in Inflammatory disorders. *Animal Lectins: Form, Function and Clinical Applications.*, 991-1026.

50) Martins P.d.C, García-Vallejo J-J, van Thienen J.V., Fernandez-Borja M, van Gils J.M., Horrevoets A.J, Hordijk P.L, Zwaginga J-J. (2007). P-selectin glycoprotein ligand-1 is expressed on endothelial cells and mediates monocyte adhesion to activated endothelium. *Arterioscler Thromb Vasc Biol.*, 27(5):1023-9.

51) Johnson R.C, Chapman S.M., Dong Z.M., Ordovas J.M., Mayadas T.N., Herz J, Haynes R.O., Schaefer E.J., Wagner D.D. (1997). Absence of P-selectin delays fatty streak formation in mice. *J Clin Invest.*, 99(5):1037-1043.

52) Pircher J, Merkle M, Wörnle M, Ribeiro A, Czermak T, Stampnik Y, Mannel H, Niemeyer M, Vielhauer V, Krötz. (2012). Prothrombotic effects of tumor necrosis factor alpha in vivo are amplified by the absence of TNF-alpha receptor subtype 1 and require TNF-alpha receptor subtype 2. *Arthritis Res Ther.,* 14(5):R225.

53) Bischoff J, Brasel C. (1995). Regulation of P-selectin by tumor necrosis factor-alpha. *Biochem Biophys Res Commun*., 210(1): 174-80.

54) Wenzel K, Felix S, Kleber F.X., Brachold R, Menke T, Schattke S, Schulte K.L., Gläser C, Rohde K, Baumann G. (1994). E-selectin polymorphism and atherosclerosis: an association study. *Hum Mol Genet.*, 3(11):1935-7.

55) Zarbock A, Ley K, McEver R.P, Hidalgo A. (2011). Leukocyte ligands for endothelial selectins: specialized glycoconjugates that mediate rolling and signaling under flow. *Blood,* 118(26):6743-6751.

56) Silva M, Fung R.K.F., Donnelly C.B., Videira P.A., Sackstein R. (2017). Cell-specific Variation in E-Selectin Ligand Expression among Human Peripheral Blood Mononuclear Cells: Implications for Immunosurveillance and Pathobiology. *J Immunol.*, 198(9):3576-3587.

57) Collins R.G, Velji R, Guevara N.V., Hicks M.J., Chan L, Beaudet A.L. (2000). P-selectin or intracellular adhesion molecule (ICAM)-1 deficiency substantially protects against atherosclerosis in apolipoprotein E-deficient mice. *J Exp Med.,* 191(1):189-94.

58) Dong Z.M., Chapman S.M., Brown A.A., Frenette P.S., Hynes R.O., Wagner D.D. (1998). The combined role of P- and E-selectin in atherosclerosis. *J Cin Invest.,* 102(1):145-52.

59) Wyble C.W., Hynes K.L., Kuchibhotla J, Marcus B.C., Hallahan D, Gewertz B.L. (1997). TNF-alpha and IL-1 upregulate membrane-bound and soluble E-selectin through a common pathway. *J Surg Res.*, 73(2):107-12.

60) Ley K, Huo Y. (2001). VCAM-1 is critical in atherosclerosis. *J Clin Invest.*, 107(10):1209-1210.

61) Cook-Mills J.M., Marchese M.E., Abdala-Valencia H. (2011). Vascular cell adhesion molecule-1 expression and signaling during disease: regulation by reactive oxygen species and antioxidants. *Antioxid Redox Signal.,* 15(6):1607-38.

62) Gerhardt T, Ley K. (2015). Monocyte trafficking across the vessel wall. *Cardiovasc Res.*, 107(3): 321-30.

63) Kong D-H, Kim Y.K., Kim M.R., Jang J.H., Lee S. (2018). Emerging Roles of Vascular Cell Adhesion Molecule-1 (VCAM-1) in immunological Disorders and Cancer. *Int J Mol Sci.,* 19(4): 1057.

64) Cybulsky M.I., Iiyama K, Li H, Zhu S, Chen M, Iiyama M, Davis V, Gutierrez-Ramos J-C., Connelly P.W., Milestone D.S. (2001). A major role for VCAM-1, but not ICAM-1, in early atherosclerosis. *J Clin Invest.*, 105(10): 1255-1262

65) Sawa Y, Sugimoto Y, Ueki T, Ishikawa H, Sato A, Nagato T, Yoshida S. (2007). Effects of TNF-alpha on leukocyte adhesion molecule expressions in cultured human lymphatic endothelium. *J Histochem Cytochem.*, 55(7): 721-33.

66) Bui T.M., Wiesolek H.L., Sumagin R. (2020). ICAM-1: A master regulator of cellular responses in inflammation, injury resolution, and tumorigenesis. *J Leukoc Biol.*, 108(3):787-799.

67) Lawson C, Wolf S. (2009). ICAM-1 signaling in endothelial cells. *Pharmacol Rep.*, 61(1): 22-32.

68) Watanabe T, Fan J. (1998). Atherosclerosis and inflammation mononuclear cell recruitment and adhesion molecules with reference to the implication of ICAM-1/LFA-1 pathway in atherogenesis. *Int J Cardiol.*, 66 Suppl 1: S45-53.

69) Burke-Gaffney A, Hellewell P.G. (1996). Tumour necrosis factor-alpha-induced ICAM-1 expression in human vascular endothelial and lung epithelial cells: modulation by tyrosine kinase inhibitors. *Br J Pharmacol.*, 199(6):1149-58.

70) Reglero-Real N, Colom B, Bodkin J.V. (2016). Nourshargh S: Endothelial Cell Junctional Adhesion Molecules: Role and Regulation of Expression in Inflammation. *Arterioscler Thromb Vasc Biol.*, 36(10):2048-2057.

71) Lertkiatmongkol P, Liao D, Mei H, Hu Y, Newman P.J. (2016). Endothelial functions of platelet/endothelial cell adhesion molecule-1 (CD31). *Curr Opin Hematol.*, 23(3):253-9.

72) Muller W.A, Weigl S.A, Deng X, Phillips D.M. (1993). PECAM-1 Is Required for Transendothelial Migration of Leukocytes. *J Exp Med.*, 178(2): 449-460.

73) Vestweber D. (2008). VE-cadherin: the major endothelial adhesion molecule controlling cellular junctions and blood vessel formation. *Arterioscler Thromb Vasc Biol.*, 28(2):223-32.

74) Park K-H, Park W.J. (2015). Endothelial Dysfunction: Clinical Implications in Cardiovascular Disease and Therapeutic Approaches. *J Korean Med Sci.*, 30(9): 1213-25.

75) Rajendran P, Rengarajan T, Thangavel J, Nishigaki Y, Sakthisekaran D, Sethi G, Nishigaki I. (2013). The Vascular Endothelium and Human Diseases. *Int J Biol Sci.*, 9(10): 1057-1069.

76) Hemanthakumar K.A., Fang S, Anisimov A, Mäyränpää M.I., Mervaala E, Kivelä R. (2021). Cardiovascular disease risk factors induce mesenchymal features and senescence in mouse cardiac endothelial cells. *Elife.*, 10:e62678.

77) Cai H, Harrison D.G. (2000). Endothelial dysfunction in cardiovascular diseases: the role of oxidant stress. *Circ Res.*, 87(10):840-4.

78) Mulhem A, Moulla Y, Klöting N, Ebert T, Tönjes A, Fasshauer M, Dietrich A, Schön M.R., Stumvoll M, Richter V, Blüher M. (2021). Circulating cell adhesion molecules in metabolically healthy obesity. *Int J Obes (Lond).*, 45(2): 331-336.

79) Yin L, Bai J, Yu W-J, Liu Y, Li H-H, Lin Q-Y. (2022). Blocking VCAM-1 Prevents Angiotensin II-Induced Hypertension and Vascular Remodeling in Mice. *Front Pharmacol.*, 13:825459.

80) Thakar S, Katakia Y.T., Ramakrishnan S.K., Thakkar N.P., Majumder S. (2021). Intermittent High Glucose Elevated Nuclear Localization of EZH2 to Cause H3K27me3-Dependent Repression of KLF2 Leading to Endothelial Inflammation. *Cells.*, 10(10):2548.

81) Kado S, Wakatsuki T, Yamamoto M, Nagata N. (2001). Expression of intracellular adhesion molecule-1 induced by high glucose concentrations in human aortic endothelial cells. *Life Sci.*, 68(7):727-37.

82) Srinivasan S, Yeh M, Danziger E.C., Hatley M.E., Riggan A.E., Leitinger N, Berliner J.A., Hedrick C.C. (2003). Glucose regulates monocyte adhesion through endothelial production of interleukin-8. *Circ Res.*, 92(4): 371-7.

83) Song Y, Manson J.E., Tinker L, Rifai N, Cook N.R., Hu F.B., Hotamisligil G.S., Ridker P.M., Rodriguez B.L., Margolis K.L., Oberman A, Liu S. (2007). Circulating levels of endothelial adhesion molecules and risk of diabetes in an ethnically diverse cohort of women. *Diabetes*, 56(7):1898-904.

84) Beriault D.R., Sharma S, Shi Y, Khan M.I., Werstuck G.H. (2011). Glucosamine-supplementation promotes endoplasmic reticulum stress, hepatic steatosis and accelerated atherogenesis in ApoE$^{-/-}$ mice. *Atherosclerosis,* 219(1):134-40.

85) Beriault D.R., Werstuck G.H. (2012). The role of glucosamine-induced ER stress in siabetic atherogenesis. *Exp Diabetes Res.*, 2012:187018.

86) Werstuck G.H., Khan M.I., Femia G, Kim A.J., Tedesco V, Trigatti B, Shi Y. (2006). Glucosamine-induced endoplasmic reticulum dysfunction is associated with accelerated atherosclerosis in a hyperglycemic mouse model. *Diabetes,* 55(1):93-101.

87) Yuan M, Gong M, Zhang Z, Meng L, Tse G, Zhao Y, Bao Q, Zhang Y, Yuan M, Liu X, Li G, Liu T. (2020). Hyperglycemia Induces Endoplasmic Reticulum Stress in Atrial Cardiomyocytes, and Mitofusin-2 Downregulation Prevents Mitochondrial Dysfunction and Subsequent Cell Death. *Oxid Med Cell Longev.*, 2020:6569728.

88) Sheikh-Ali M, Sultan S, Alamir A-R., Hass M.J., Mooradian A.D. (2010). Hyperglycemia-induced endoplasmic reticulum stress in endothelial cells. *Nutrition,* 26(11-12):1146-50.

89) Schröder M. (2008). Endoplasmic reticulum stress response. *Cell Mol Life Sci.*, 65(6):862-94.

90) Choi J-A, Song C-H. (2019). Insights Into the Role of Endoplasmic Reticulum Stress in Infectious Disease. *Front Immunol.*, 10:3147.

91) Malhotra J.D., Kaufman R.J. (2007). The endoplasmic reticulum and the unfolded protein response. *Semin Cell Dev Biol.*, 18(6):716-31.

92) Minamino T, Komuro I, Kitakaze M. (2010). Endoplasmic reticulum stress as a therapeutic target in cardiovascular disease. *Circ Res.,* 107:1071-82.

93) van der Kallen C.J.H., van Greevenbroek M.M.J., Stehouwer C.D.A, Schalkwijk C.G. (2009). Endoplasmic reticulum stress-induced apoptosis in the development of diabetes: is there a role for adipose tissue and liver?. *Apoptosis*, 14(12): 1424-1434.

94) Wang B-C., Zhang S-T, Chen G. (2020). Research Progress of the UPR Mechanism and its Effect on Improving Foreign Protein Expression. *Protein Pept Lett.*, 27(9): 831-840.

95) Hertz C, Zhang K, Kaufman R.J. (2020). Mechanisms, regulation and functions of the unfolded protein response. *Nat Rev Mol Cell Biol.*, 21(8):421-438.

96) Sano R, Reed J.C. (2013). ER stress-induced cell death mechanisms. *Biochim Biophys Acta.*, 1833(12):3460-3470.

97) Zhou J, Lhoták S, Hilditch B.A., Austin R.C. (2005). Activation of the unfolded protein response occurs at all stages of atherosclerotic lesion development in apolipoprotein E-deficient mice. *Circulation*, 111(14):1814-21.

98) Read A, Schröder M. (2021). The unfolded Protein Response: An Overview. *Biology (Basel),* 10(5):384.

99) Di Conza G, Ho P-C. (2020). ER Stress Responses: An Emerging Modulator for Innate Immunity. *Cells.*, 9(3): 695.

100) Chen Y, Brandizzi F. (2013). IRE1: ER stress sensor and cell fate executor. *Trends Cell Biol.*, 23(11): 547-55.

101) Adams C.J., Kopp M.C., Larburu N, Nowak P.R., Ali M.M.U. (2019). Structure and Molecular Mechanism of ER Stress Signaling by the Unfolded Protein Response Signal Activator IRE1. *Front Mol Biosci.*, 6:11.

102) Wu R, Zhang Q-H., Lu Y-J, Ren K, Yi G-H. (2015). Involvement of the IRE1-α-XBP1 pathway and XBP1s- dependent transcriptional reprogramming in metabolic disease. *DNA Cell Biol.*, 34(1):6-18.

103) Hotamisligil G.S. (2010). Endoplasmic reticulum stress and the inflammatory basis of metabolic disease. *Cell.*, 140(6): 900-17.

104) Moncan M, Mnich K, Blomme A, Almanza A, Samali A, Gorman A.M. (2021). Regulation of lipid metabolism by the unfolded protein response. *J Cell Mol Med.,* 25(3):1359-1370.

105) Hillary R.F., FitzGerald U. (2018). A lifetime of stress: ATF6 in development and homeostasis. *J Biomed Sci.*, 25(1):48.

106) Humeau J, Leduc M, Cerrato G, Loos F, Keep O, Kroemer G. (2020). Phosphorylation of eukaryotic initiation factor-2α (eIF2α) in autophagy. *Cell Death Dis.*, 11(6): 433.

107) Masuda M, Miyazaki-Anzai S, Levi M, Ting T.C., Miyazaki M. (2013). PERK-eIF2α-ATF4-CHOP signaling contributes to TNFα-induced vascular calcification. *J Am Heart Assoc.*, 2(5): e000238.

108) Sozen E, Ozer N.K. (2017). Impact of high cholesterol and endoplasmic reticulum stress on metabolic diseases: An updated mini-review. *Redox Biol.*, 12:456-461.

109) Gargalovic P.S., Gharavi N.M., Clark M.C., Pagnon J, Yang W-P, He A, Truong A, Baruch-Oren T, Berliner J.A., Kirchgessner T.G., Lusis A.J.

(2006). The unfolded protein response is an important regulator of inflammatory genes in endothelial cells. *Arterioscler Thromb Vasc Biol.*, 26(11): 2490-6.

110) Chattopadhyay A, Kwartler C.S., Kaw K, Li Y, Kaw A, Chen J, LeMaire S.A., Shen Y.H., Milewicz D.M. (2021). Cholesterol-Induced Phenotypic Modulation of Smooth Muscle Cells to Macrophage/Fibroblast-like Cells Is Driven by an Unfolded Protein Response. *Arterioscler Thromb Vasc Biol.*, 41(1): 302-316.

111) Green C.D., Olson L.K. (2011). Modulation of palmitate-induced endoplasmic reticulum stress and apoptosis in pancreatic β-cells by stearoyl-CoA desaturase and Elovl6. *Am J Physiol Endocrinol Metab.,* 300(4): E640-9.

112) Lu Y, Chend J, Chen L, Li C, Chen G, Gui L, Shen B, Zhang Q. (2015). Endoplasmic reticulum stress involved in high-fat diet and palmitic acid-induced vascular damages and fenofibrate intervention. *Biochem Biophys Res Commun.*, 458(1):1-7.

113) Lu J, Wang Q, Huang L, Dong H, Lin L, Lin N, Zheng F, Tan J. (2012). Palmitate causes endoplasmic reticulum stress and apoptosis in human mesenchymal stem cells: prevention by AMPK activator. *Endocrinology.*, 153(11):5275-84.

114) Raghaven S, Vassy J.L., Ho Y-L, Song R.J., Gagnon D.R., Cho K, Wilson P.W.F., Phillips L.S. (2019). Diabetes Mellitus-Related All-Cause and Cardiovascular Mortality in a National Cohort of Adults. *J Am Heart Assoc.*, 8(4):e011295.

115) Chiaradonna F, Ricciardiello F, Palorini R. (2018). The Nutrient-Sensing Hexosamine Biosynthetic Pathway as the Hub of Cancer Metabolic Rewiring. *Cells.*, 7(6): 53.

116) Xu C, Ng D.T.W. (2015). Glycosylation-directed quality control of protein folding. *Nat Rev Mol Cell Biol.*, 16(12): 742-52.

117) Beriault D.R., Dang V.T, Zhong L.H., Petlura C.I., McAlpine C.S., Shi Y, Werstuck G.H. (2017). Glucosamine induces ER stress by disrupting lipid-linked oligosaccharide biosynthesis and N-linked protein glycosylation. *Am J Physiol Endocrinol Metab.*, 312(1): E48-E57.

118) Sage A.T., Walter L.A, Shi Y, Khan M.I, Kaneto H, Capretta A, Werstuck G.H. (2010). Hexosamine biosynthesis pathway flux promotes endoplasmic reticulum stress, lipid accumulation, and inflammatory gene expression in hepatic cells. *Am J Physiol Endocrinol Metab.*, 298(3): E499-511.

119) Raciti G.A.., Iadicicco C, Ulianich L, Vind B.F., Gaster M, Andreozzi F, Longo M, Teperino R, Ungaro P, Jeso B.D., Formisano P, Beguinot F, Miele C. (2010). Glucosamine-induced endoplasmic reticulum stress affects GLUT4 expression via activating transcription factor 6 in rat and human skeletal muscle cells. *Diabetologia.*, 53(5):955-65.

120) Fiorentino T.V., Procopio T, Mancuso E, Arcidiacono G.P., Andreozzi F, Arturi F, Sciacqua A, Perticone F, Hribal M.L., Sesti G. (2015). SRT1720 counteracts glucosamine-induced endoplasmic reticulum stress and endoplasmic dysfunction. *Cardiovasc Res.*, 107(2): 295-306.

121) Stacchiotti A, Favero G, Rezzani R. (2013). Endoplasmic Reticulum Stress in the Endothelium: A Contribution to Athero-susceptibility. Current Trends in atherogenesis. *INTECH.*

122) Wang G, Liu K, Li Y, Yi W, Yang Y, Zhao D, Fan C, Yang H, Geng T, Zing J, Zhang Y, Tan S, Yi D. (2014). Endoplasmic reticulum stress mediates the anti-inflammatory effect of ethyl pyruvate in endothelial cells. *PLoS One.*, 9(12): e113983.

123) Cai X, Bao L, Ding Y, Dai X, Zhang Z, Li Y. (2017). Quercetin alleviates cell apoptosis and inflammation via the ER stress pathway in vascular endothelial cells cultured in high concentrations of glucosamine. *Mol Med Rep.*, 15(2): 825-832.

124) Zhao R, Xie X, Le K, Li W, Moghadasian M.H., Beta T, Shen G.X. (2015). Endoplasmic reticulum stress in diabetic mouse or glycated

LDL-treated endothelial cells: protective effect of saskatoon berry powder and cyanidin glycans. *J Nutr Biochem.*, 26(11):1248-58.

125) Cimellaro A, Perticone M, Fiorentino T.V., Sciacqua A, Hribal M.L. (2016). Role of endoplasmic reticulum stress in endothelial dysfunction. *Nutr Metab Cardiovasc Dis.*, 26(10): 863-71.

126) Nair M.M., Zhao R, Xie X, Shen G.X. (2016). Impact of glycated LDL on endothelial nitric oxide synthase in vascular endothelial cells: involvement of transmembrane signaling and endoplasmic reticulum stress.*J Diabetes Complications.*, 30(3): 391-7.

127) McAlpine C.S., Huang A, Emdin A, Banko N.S., Beriault D.R., Shi Y, Werstuck G.H. (2015). Deletion of myeloid GSK3α Attenuates Atherosclerosis and Promotes an M2 Macrophage Phenotype. *Arterioscler Thromb Vasc Biol.*, 35(5): 1113-22.

128) Doble B.W., Woodgett J.R. (2003). GSK-3: tricks of the trade for a multi-tasking kinase. *J Cell Sci.,* 116(Pt7): 1175-86.

129) Kaidanovich-Beilin O, Woodgett J.R. (2011). GSK-3: Functional Insights from Cell Biology and Animal Models. *Front Mol Neurosci.*, 4:40.

130) Grassilli E, Ianzano L, Bonomo S, Missaglia C, Cerrito M.G., Giovannoni R, Masiero L, Lavitrano M. (2014). GSK3A is Redundant with GSK3B in Modulating Drug Resistance and Chemotherapy-Induced Necroptosis. *PLoS One.,* 9(7): e100947.

131) Huang A, Patel S, McAlpine C.S., Werstuck G.H. (2018). The Role of Endoplasmic Reticulum Stress-Glycogen Synthase-3 Signaling in Atherogenesis. *Int J Mol Sci.*, 19(6):1607.

132) McAlpine C.S., Bowes A.J, Khan M.I., Shi Y, Werstuck G.H. (2012). Endoplasmic reticulum stress and glycogen synthase kinase-3β activation in apolipoprotein E-deficient mouse models of accelerated atherosclerosis. *Arterioscler Thromb Vasc Biol.*, 32(1): 82-91.

133) Meares G.P., Jope R.S. (2007). Resolution of the nuclear localization mechanism of glycogen synthase kinase-3: functional effects in apoptosis. *J Biol Chem.*, 282(23):16989-7001.

134) Beurel E, Grieco S.F., Jope R.S. (2015). Glycogen synthase Kinase-3 (GSK3): regulation, actions, and disease. *Pharmacol Ther.*, 148:114-31.

135) Tsend A-S, Rngel F.B., Keating M.T. (2006). The GSK-3 inhibitor BIO promotes proliferation in mammalian cardiomyocytes. *Chem Biol.*, 13(9):957-63.

136) Jope R.S., Yuskaitis C.J, Beurel E. (2007). Glycogen synthase kinase-3 (GSK3): inflammation, disease, and therapeutics. *Neurochem Res.*, 32(4-5): 577-95.

137) Doble B.W., Woodgett J.R. (2003). GSK-3: tricks of the trade for a multi-tasking kinase. *J Cell Sci.*, 116(pt7): 1175-86.

138) Thornton T.M., Pedraza-Alva G, Beng B, Wood C.D, Aronshtam A, Clements J.L, Sabio G, Davis R.J., Matthews D.E., Doble B, Rincon M. (2008). Phosphorylation by p38 MAPK as an alternative pathway for GSK3beta inactivation. *Science.*, 320(5876): 667-70.

139) Fang X, Yu S.X., Lu Y, Bast Jr R.C., Woodgett J.R., Mills G.B. (2000). Phosphorylation and inactivation of glycogen synthase kinase 3 by protein kinase A. *Proc Natl Acad Sci U S A.,* 97(22): 11960-5.

140) Cole A, Frame S, Cohen P. (2004). Further evidence that the tyrosine phosphorylation of glycogen synthase kinase-3 (GSK3) in mammalian cells iis an autophosphorylation event. *Biochem J.*, 377(Pt 1): 249-255.

141) Bijur G.N., Jope R.S. (2001). Proapoptotic stimuli induce nuclear accumulation of glycogen sythase kinase-3 beta. *J Biol Chem.*, 276(40): 37436-42.

142) He L, Endress J, Cho S, Li Z, Zheng Y, Asara J.M., Blenis J. (2022). Suppression of nuclear GSK3 signalling promotes serine/one-carbon

metabolism and confers metabolic vulnerability in lung cancer. *Sci Adv.*, 8(20): eabm8786.

143) Nikoulina S.E., Ciaraldi T.P Mudaliar S, Mohideen P, Carter L, Henry R.R. (2000). Potential role of glycogen synthase kinase-3 in skeletal muscle insulin resistance of type 2 diabetes. *Diabetes.*, 49(2): 263-71.

144) Banko N.S., McAlpine C.S, Venegas-Pino D.E, Raja P, Shi Y, Khan M.I., Werstuck G.H. (2014). Glycogen sythase kinase 3α deficiency attenuates atherosclerosis and hepatic steatosis in high fat diet-fed low density lipoprotein receptor-deficient mice. *Am J Pathol.*, 184(12):3394-404.

145) Phiel C.J., Wilson C.A., Lee V. M-Y, Klein P.S. (2003). GSK-3alpha regulates production of Alzeimer's disease amyloid-beta peptides. *Nature.*, 423(6938):435-9.

146) Klein P.S., Melton D.A. (1996). A molecular mechanism for the effect of lithium on development. *Proc Natl Acad Sci U S A.*, 93(16): 8455-9.

147) Lee J, Kim M-S. (2007). The role of GSK2 in glucose homeostasis and the development of insulin resistance. *Diabetes Res Clin Pract.*, 77 Suppl 1: S49-57.

148) Patel S, Werstuck G.H. (2021). Macrophage Function and the role of GSK3. *Int J Mol Sci.*, 22(4): 2206.

149) Komiya Y, Habas R. (2008). Wnt Signal transduction pathways. *Oranogenesis.*, 4(2): 68-75.

150) Clevers H. (2006). Wnt/beta-catenin signaling in development and disease. *Cell.*, 127(3):469-80.

151) MacDonald B.T., Tamai K, He X. (2009). Wnt/β-catenin signaling: components, mechanisms, and disease. *Dev Cell.*, 17(1): 9-26.

152) Valenta T, Hausmann G, Basler K. (2012). The many faces and functions of β-catenin. *EMBO J.,* 31(12): 2714-36.

153) Zhang W, Liu H.T. (2002). MAPK signal pathways in the regulation of cell proliferation in mammalian cells. *Cell Res.,* 12(1): 9-18.

154) Piazzi M, Bavelloni A, Faenza I, Blalock W. (2020). Glycogen synthase kinase (GSK)-3 and the double strand RNA-dependent kinase, PKR: When two kinases for the common good turn bad. *Biochem Biophys Acta Mol Cell Res.*, 1867(10):118769.

155) Goode N, Hughes K, Woodgett J.R., Parker P.H. (1992). Differential regulation of glycogen synthase kinase-3 beta by protein kinase C isotypes. *J Biol Chem.*, 267(24):16878-82.

156) Stambolic V, Woodgett J.R. (1994). Mitogen inactivation of glycogen synthase kinase-3 beta in intact cells via serine 9 phosphorylation. *Biochem.*, 303(Pt3):701-4.

157) Yoshida H. (2007). ER stress and disease. *FEBS J.*, 274(3):630-58.

158) Ren J, Bi Y, Sowers J.R., Hertz C, Zhang Y. (2021). Endoplasmic reticulum stress and unfolded protein response in cardiovascular disease. *Nat Rev Cardiol.*, 18(7):499-521

159) Werstuck G.H., Khan M.I., Femia G, Kim A.J., Tedesco V, Trigatti B, Shi Y. (2006). Glucosamine-induced endoplasmic reticulum dysfunction is associated with accelerated atherosclerosis in a hyperglycemic mouse model. *Diabetes*., 55(1): 93-101.

160) Falck-Hansen M, Kassiteridi C, Monaco C. (2013). Toll-like receptors in atherosclerosis. *Int J Mol Sci.*, 14(7):14008-23.

161) Martin M, Rehani K, Jope R.S., Michalek S.M. (2005). Toll-like receptor-mediated cytokine production is differentially regulated by glycogen synthase kinase 3. *Nat immunol*., 6(8): 777-84.

162) Hoeflich K.P., Luo J, Rubie E.A., Tsao M.S., Kin O, Woodgett J.R. (2000). Requirement for glycogen synthase kinase-3beta in cell survival and NF-kappaB activation. *Nature*., 406(6791):86-90.

163) Zhang J-S, Herreros-Villanueva M, Koenig A, Deng Z, de Narvajas A.A-M, Gomes T.S., Meng X, Bujanda L, Ellenrieder V, Li X.K., Kaufmann S.H., Billadeau D.D. (2014). Differential activity of GSK-3 isoforms regulates NF-κB and TRAIL-or TNFα induced apoptosis in pancreatic cancer cells. *Cell Death Dis.*, 5(3):e1142.

164) Choi S-E, Juang H-J, Kang Y, Jung J.G, Han S.J., Kim H.J., Kim D.J., Lee K-W. (2010). Atherosclerosis induced by a high-fat diet is alleviated by lithium chloride via reduction of VCAM expression in ApoE-deficient mice. *Vascul Pharmacol.*, 53(5-6):264-72.

165) Patel S, Mastrogiacomo L, Fulmer M, Shi Y, Werstuck G.H. (2022). Deletion of Macrophage-Specific Glycogen Synthase Kinase (GSK)-3α Promotes Atherosclerotic Regression in LDLR$^{-/-}$ Mice. *Int J Mol Sci.*, 23(16):9293.

166) Stump B, Shrestha S, Lamattina A.M, Louis P.H, Cho W, Perrella M.A, Ai X, Rosas I.O, Wagner F.F, Priolo C, Astin J, El-Chemaly S. (2019). Glycogen synthase kinase 3-β inhibition induces lymphangigenesis through β-catenin-dependent and mTOR-independent pathways. *PLos One.*, 14(4):e0213831.

167) Ramirez S.H, Fan S, Zhang M, Papugani A, Reichenbach N, Dykstra H, Mercer A.J., Tuma R.F, Persidsky Y. (2010). Inhibition of glycogen synthase kinase 3 beta (GSK3beta) decreases inflammatory responses in brain endothelial cells. *Am J Pathol.*, 176(2):881-92.

168) Weikel K.A, Cacicedo J.M, Ruderman N.B, Ido Y. (2016). Knockdown of GKS3β increases basal autophagy and AMPK signalling in nutrient-laden human aortic endothelial cells. *Biosci Rep.*, 36(5):e00382.

169) Frostegård J. (2013). Immunity, atherosclerosis and cardiovascular disease. *BMC Med.,* 11:117.

170) Herrington W, Lacey B, Sherliker P, Armitage J, Lewington S. (2016). Epidemiology of Atherosclerosis and the Potential to Reduce the Global Burden of Atherothrombotic Disease. *Circ Res.,* 118(4): 535-46.

171) Yusuf S, Hawken S, Ounpuu S, Dans T, Avezum A, Lanas F, McQueen M, Budaj A, Pais P, Varigos J, Lisheng L. (2004). INTERHEART Study Investigators: Effects of potentially modifiable risk factors associated with myocardial infraction in 52 countries (the INTERHEART study): case-control study. *Lancet.*, 364(9438):937-52.

172) Bursill C.A., Smith N.J., Palpant N, Tan I, Sunde M, Harvey R.P., Lewis B, Figtree G.A., Vandenberg J.I. (2022). Australian Cardiovascular Alliance: Don’t Turn Off the Tap! The Importance of Discovery Science to the Australian Cardiovascular Sector and Improving Clinical Outcomes Into the Future. *Heart Lung Circ.,* 31(10):1321-1332.

173) Funk S.D., Yurdagul Jr A., Orr A.W. (2012). Hyperglycemia and endothelial dysfunction in atherosclerosis: lessons from type 1 diabetes. *Int J Vasc Med.*, 2012:569654.

174) American Diabetes Association. (2009). Diagnosis and classification of diabetes mellitus. *Diabetes Care*., 32 Suppl 1(Suppl 1):S62-7.

175) Levitan E.B., Song Y, Ford E.S., Liu S. (2004). Is nondiabetic hyperglycemia a risk factor for cardiovascular disease? A meta-analysis of prospective studies.*Arch Intern Med.*, 164(19):2147-55.

176) Ciccone M.M., Cortese F, Gesualdo M, Donvito I, Carbonara S, De Pergola G. (2016). A Glycemic Threshold of 90 mg/dl Promotes Early Signs of Atherosclerosis in Apparetly Healthy Overweight/Obese Subjects. *Endocr Metab Immune Disord Drug Targets.*, 16(4): 288-295.

177) Wilson P.W., Cupples L.A., Kannel W.B. (1991). Is hyperglycemia associated with cardiovascular disease? The Framingham Study. *Am Heart J.*, 121(2Pt 1): 586-90.

178) Venegas-Pino D.E., Wang P-W, Stoute H.K., Singh-Pickersgill N.A., Hong B.Y., Khan M.I., Shi Y, Werstuck G.H. (2016). Sex-Specific Differences in an ApoE (-/-):Ins2(+/Akita) Mouse Model of Accelerated Atherosclerosis. *Am J Pathol.*, 186(1):67-77.

179) Gao Y, Parker G.J., Hart G.W. (2000). Streptozotocin-induced beta-cell death is independent of its inhibition of O-GlcNAcase in pancreatic Min6 cells. *Arch Biochem Biophys.*, 383(2):296-302.

180) Park L, Raman K.G., Lee K.J., Ferran Jr L.J., Chow W.S., Stern D, Schmidt A.M. (1998). Suppression of accelerated diabetic atherosclerosis by the solouble receptor for advanced glycation endproducts. *Nat Med.,* 4(9):1025-31.

181) Veerman K.J., Venegas-Pino D.E., Shi Y, Khan M.I., Gerstein H.C., Werstuck G.H. (2013). Hyperglycemia is associated with impaired vasa vasorum neovascularization and accelerated atherosclerosis in apolipoprotein-E deficient mice. *Atherosclerosis.*, 227(2):250-8.

182) Bowes A.J., Khan M.I., Shi Y, Robertson L, Werstuck G.H. (2009). Valporate attenuates accelerated atherosclerosis in hyperglycemic apoE-deficient mice: evidence in support of a role for endoplasmic reticulum stress and glycogen synthase kinase-3 in lesion development and hepatic steatosis. *Am J Pathol.,* 174(1):330-42.

183) Järvisalo M.J., Raitakari M, Toikka J.O., Putto-Laurila A, Rontu R, Laine S, Lehtimäki T, Rönnemaa, Viikari J, Raitakari O.T. (2004). Endothelial dysfunction and increased arterial intima-media thickness in children with type 1 diabetes. *Circulation.*, 109(14):1750-5.

184) McGill Jr H.C., McMahan C.A., Zieske A.W., Malcolm G.T., Tracy R.E., Strong J.P. (2001). Effects of nonlipid risk factors on atherosclerosis in youth with a favorable lipoprotein profile.*Circulation*., 103(11):1546-50.

185) Collins R.G., Velji R., Guevara N.V., Hicks M.J., Chan L, Beaudet A.L. (2000). P-Selectin or intercellular adhesion molecule (ICAM)-1 deficiency substantially protects against atherosclerosis in apolipoprotein E-deficient mice. *J Exp Med.,* 191(1):189-94.

186) Gurtner G.C., Davis V, Li H, McCoy M.J., Sharpe A, Cybulsky M.I. (1995). Targeted disruption of the murine VCAM1 gene: essential role of VCAM-1 in chorioallantoic fusion and placentation. *Genes Dev.,* 9(1):1-14.

187) Kwee L, Baldwin H.S., Shen H.M., Stewart C.L., Buck C, Buck C.A., Labow M.A. (1995). Defective development of the embryonic and extraembryonic circulatory systems in vascular cell adhesion molecule (VCAM-1) deficient mice. *Development*., 121(2):489-503.

188) Kato E.T., Silverman M.G., Mosenzon O, Zelniker T.A., Cahn A, Furtado R.H.M., Kuder J, Murphy S.A., Bhatt D.L., Leiter L.A., McGuire D.K., Wilding J.P.H., Bonaca M.P., Ruff C.T., Desai A.S., Goto S, Johansson P.A., Gause-Nilsson I, Johanson P, Langkilde A.M., Raz I, Sabatine M.S., Wiviott S.D. (2019). Effect of Dapagliflozin on Heart Failure and Mortality in Type 2 Diabetes Mellitus. *Circulation.*, 139(22):2528-2536.

189) Buse J.B, Wexler D.J., Tsapas A, Rossing P, Mingrone G, Mathieu C, D'Alessio D.A., Davis M.J. (2020). 2019 Update to: Management of Hyperglycemia in Type 2 Diabetes, 2018. A Consensus Report by the American Association (ADA) and the European Association for the study of diabetes (EASD). *Diabetes Care*., 43(2):487-493.

190) Padda I.S., Mahtani A.U., Parmar M. (2022). Sodium-Glucose Transport Protein 2 (SGLT2) Inhibitors. *StatPearls*.

191) Hsia D.S., Grove O, Cefalu W.T. (2018). An Update on SGLT2 Inhibitors for the Treatment of Diabetes Mellitus. *Curr Opin Endocrinol Diabetes Obes.*, 24(1):73-79.

192) Saisho Y. (2020). SGLT2 Inhibitors: The Star in Treatment of Type 2 Diabetes?. *Diseases.*, 8(2):14.

193) Cardoso R, Graffunder F.P., Ternes C.M.P, Fernandes A, Rocha A.V., Fernandes G, Bhatt D.L. (2021). SGLT2 inhibitors decrease cardiovascular death and heart failure hospitalizations in patients with heart failure: A systematic review and meta-analysis. *EClinicalMedicine.*, 36:100933.

194) Lopaschuk G.D, Verma S. (2020). Mechanisms of Cardiovascular Benefits of Sodium Glucose Co-Transporter 2 (SGLT2) Inhibitors: a State-of-the-Art Review. *JACC Basic Transl Sci.*, 5(6): 632-644.

195) Neal B, Perkovic V, Mahaffey K.W, de Zeeuw D, Fulcher G, Erondu N, Shaw W, Law G, Desai M, Matthews D.R. (2017). CANVAS Program Collaborative Group: Canagliflozin and Cardiovascular and Renal Events in Type 2 Diabetes. *N Engl J Med.*, 377(7):644-657.

196) Sugiyama S, Jinnouchi H, Kurinami N, Hieshima K, Yoshida A, Jinnouchi K, Nishimura H, Suzuki T, Miyamoto F, Kajiwara K, Jinnouchi T. (2018). The SGLT2 Inhibitor Dapagliflozin Significantly Improves the Peripheral Microvascular Endothelial Function in Patients with Uncontrolled Type 2 Diabetes Mellitus. *Intern Med.*, 57(15):2147-2156.

197) Mone P, Varzideh F, Jankauskas S.S., Pansini A, Lombardi A, Frullone S, Santulli G. (2022). SGLT2 Inhibition via Empagliflozin Improves Endothelial Function and Reduces Mitochondrial Oxidative Stress: Insights From Frail Hypertensice and Diabetic Patients. *Hypertension.,* 79(8):1633-1643.

198) Wei R, Wang W, Pan Q, Guo L. (2022). Effects of SGLT-2 Inhibitors on Vascular Endothelial Function and Arterial Stiffness in Subjects with Type 2 Diabetes: A Systematic Review and Meta-Analysis of Randomized Controlled Trials. *Front Endocrinol (Lausanne).*, 13:826604.

199) Correale M, Mazzeo P, Mallardi A, Leopizzi A, Tricarico L, Fortunato M, Magnesa M, Tucci S, Maiellaro P, Pastore G, Lamacchia O, Iacoviello M, Di Biase M, Brunetti N.D. (2021). Switch to SGLT2 Inhibitors and Improve Endothelial Function in Diabetic Patients with Chronic Heart Failure. *Cardiovasc Drugs Ther.*

200) Kim A.J., Shi Y, Austin R.C., Werstuck G.H. (2005). Valporate protects cells from ER-stress-induced lipid accumulation and apoptosis by inhibiting glycogen synthase kinase-3. *J Cell Sci., 1*18(Pt 1): 89-99.

201) Mooradian A.D., Haas M.J. (2022). Endoplasmic reticulum stress: A common pharmacologic target of cardioprotective drugs. *Eur J Pahrmacol.*, 931:175221.

202) Thorp E, Li G, Seimon T.A., Kuriakose G, Ron D, Tabas I. (2009). Reduced apoptosis and plaque necrosis in advanced atherosclerotic

lesions of ApoE-/- and LDLR-/- mice lacking CHOP. *Cell Metab.*, 9(5):474-81.

203) Kolb P.S, Ayaub E.A., Zhou W, Yum V, Dickhout J.G., Ask K. (2015). The therapeutic effects of 4-phenylbutyric acid in maintaining proteostasis. *Int J Biochem Cell Biol.*, 61:45-52.

204) Huang A, Young T.L, Dang V, Shi Y, McAlpine C.S., Werstuck G.H. (2017). 4-phenylbutyrate and valporate treatment attenuates the progression of atherosclerosis and stabilizes existing plaques. *Atherosclerosis.*, 266:103-112.

205) Lynn E.G., Lhoták Š, Lebeau P, Byun J.H., Chen J, Platko K, Shi C, O'Brien E.R., Austin R.C. (2019). 4-Phenylbutyrate protects against atherosclerotic lesion growth by increasing the expression of HSP25 in macrophages and in the circulation of Apoe-/- mice. *FASEB J.*, 33(7):8406-8422.

206) Yu W, Liu X, Feng L, Yang H, Yu W, Feng T, Wang S, Wang J, Liu N. (2017). Glycation of paraoxonase 1 by high glucose instigates endoplasmic reticulum stress to induce endothelial dysfunction in vivo. *Sci Rep.*, 7:45827.

207) McAlpine C.S., Werstuck G.H. (2014). Protein kinase R-like endoplasmic reticulum kinase and glycogen synthase kinase-3α/β regulate foam cell formation. *J Lipid Res.*, 55(11):2320-33.

208) Hostiuc S, Perlea P, Marinescu M, Dogaroiu C, Drima E. (2019). GSK-3 Inhibitors and Tooth Repair: An Ethical Analysis. *Front Pharmacol.*, 9:1495.

209) Bahmad H.F., Chalhoub R.M., Harati H, Bou-Ghrios J, Assi S, Ballout F, Monzer A, Msheil H, Araji T, Elajami M.K, Ghanem P, Chamaa F, Kadara H, Abou-Antoun T, Daoud G, Fares Y, Abou-Khier W. (2021). Tideglusib attenuates growth of neuroblastoma cancer stem/progenitor cells in vitro and in vivo by specifically targeting GSK-3β. *Pharmacol Rep.*, 73(1):211-226.

210) Safety and Efficacy of Tideglusib in congenital Myotonic Dystrophy. Clinicaltrials.Gov. 2022 from Https://Clinicaltrials.gov/

211) Martínez-Gonsález L, Gonsalo-Consuegra C, Gómez-Almería M, Porras G, de Lago E, Martín-Requero Á, Martínez A. (2021). Tideglusib, a Non-ATP Competitive Inhibitor of GSK-3β as a Drug Candidate for the Treatment of Amyotrophic Lateral Sclerosis. *Int J Mol Sci*., 22(16):8975.

212) Tideglusib for the Treatment of Amyotrophic Lateral Sclerosis. Clinicaltrials.Gov. 2022 from Https://Clinicaltrials.gov/

213) Weikel K.A, Cacicedo J.M, Ruderman N.B., Iso Y. (2016). Knockdown of GSK3β increases basal autophagy and AMPK signalling in nutrient-laden human aortic endothelial cells. *Biosci Rep.*, 36(5):e00382.

214) Eto M, Kouroedov A, Cosentino F, Lüscher T.F. (2005). Glycogen synthase kinase-3 mediates endothelial cell activation by tumor necrosis factor-alpha. *Circulation.*, 112(9):1316-22.

215) Hoeflich K.P., Luo J, Rubie E.A., Tsao M.S., Jin O, Woodgett J.R. (2000). Requirement for glycogen synthase kinase -3beta in cell survival and NF-kappaB activation. *Nature*., 406(6791):86-90.

216) MacAulay K, Doble B.W, Patel S, Hansotia T, Sinclair E.M, Drucer D.J., Nagy A, Woodgett J.R. (2007). Glycogen synthase kinase 3alpha-specific regulation of murine hepatic glycogen metabolism. *Cell Metab.*, 6(4):329-37.

217) Mamaghani S, Patel S, Hedley D.W. (2009). Glycogen synthase kinase-3 inhibition disrupts nuclear factor-kappaB activity in pancreatic cancer, but fails to sensitize to gemcitabine chemotherapy. *BM Cancer.,* 9:132.

218) Wilson 3rd W, Baldwin A.S. (2008). Maintenance of constitutive IkappaB kinase activity by glycogen synthase kinase-3alpha/beta in pancreatic cancer. *Cancer Res.*, 68(19):8156-63.

219) Hinz M, Scheifereit C. (2014). The IκB kinase complex in NF-κB regulation and beyond.*EMBO Rep.*, 15(1):46-61.

220) Hoeflich K.P., Luo J, Rubie E.A., Tsao M.S., Jin O, Woodgett J.R. (2000). Requirement for glycogen synthase kinase-3beta in cell survival and NF-kappaB activation. *Nature*., 406(6791):86-90.

221) Gareus R, Kotsaki E, Xanthoulea S, van der Made I, Gijbels M.J.J, Kardakaris R, Polykratis A, Kollias G, de Winther M.P.J, Pasparakis M. (2008). Endothelial cell-specific NF-kappaB inhibition protects mice from atherosclerosis. *Cell Metab.*, 8(5):372-83.

222) Liu T, Zhang L, Joo D, Sun S-C. (2017). NF-κB signalling in inflammation. *Signal Transduct Target Ther.*, 2:17023.

223) Collins T, Read M.A., Neish A.S., Whitley M.Z., Thanos D, Maniatis T. (1995). Transcriptional regulation of endothelial cell adhesion molecules: NF-kappa B and cytokine-inducible enhancers. *FASEB J.*, 9(10):899-909.

224) Denk A, Goebeler M, Schmid S, Berberich I, Ritz O, Lindemann D, Ludwig S, Wirth T. (2001). Activation of NF-kappa B via the Ikappa B kinase complex is both essential and sufficient for proinflammatory gene expression in primary endothelial cells. *J Biol Chem.*, 276(30):28451-8.f

225) Rajan S, Ye J, Bai S, Huang F, Guo Y-L. (2008). NF-kappaB, but not p38 MAP kinase, is required for TNF-alpha-induced expression of cell adhesion molecules in endothelial cells. *J Cell Biocehm.*, 105(2):477-86.

226) Wagner F.F, Benajiba L, Campbell A.J., Weïwer M, Sacher J.R, Gale J.P, Ross L, Puissant A, Alexe G, Conway A, Back M, Pikman Y, Galinsky I, DeAngelo D.J., Stone R.M., Kaya T, Shi X, Robers M.B., Machleidt T, Wilkinson J, Hermine O, Kung A, Stein A.J, Lakshminarasimhan D, Hemann M.T., Scolnick E, Zhang Y-L, Pan J.Q., Stegmaier K, Holsen E.B. (2018). Exploiting an Asp-Glu “switch” in glycogen synthase kinase 3 to design paralog-selective inhibitors for use in acute myeloid leukemia. *Sci Transl Med.*, 10(431):eaam8460.

227) Kupetsky E.A., Li Q, Uitto J. (2012). Magnesium reduces carotid intima-media thickness in a mouse model of pseudoxanthoma elasticum: a novel treatment biomarker. *Clin Transl Sci.,* 5(3):259-64.

228) Sandoo A, van Zanten J.J.C.S.V., Metsios G.S., Carroll D, Kitas G.D. (2010). The endothelium and its role in regulating vascular tone. *Open Cardiovasc Med J.*, 302-12.